Observation of the medium intensity inflow into the Baltic Proper in November 2005 and comparison with the model data

Artur Szewczyk

Master Thesis
University of Rostock
Department of Physics

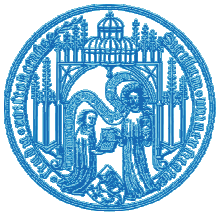

INSTITUT FÜR PHYSIK

Leibniz Institute for Baltic Sea Reasearch
Warnemünde

November 1, 2009

Declaration I hereby assure that I have authored the present thesis by myself with all references specified

November 2009

Contents

Chapter 1

Introduction

The Baltic Sea is the World's largest brackish water system. It is stably stratified for the whole year, which prevents diffusive oxygen transport to its deep waters. The saline inflows from the North Sea are the only mechanisms which provide oxygen for the deep Baltic Sea, therefore studying of these inflows is crucial for understanding the Baltic Sea ecosystem.

Major Baltic Inflows are the only known process for the ventilation of the Baltic Sea deepest basins (Wyrtki, 1954; Matthäus and Franck, 1992; Lass and Matthäus, 1996; Feistel et al., 2006). They occur once a few years and are very well investigated (Matthäus and Franck, 1992). Besides MBIs smaller inflow events, called medium-intensity inflows are of similar importance. In contrast to MBIs they gained awareness just before a few years. These inflows occur several times per year and are vital for the ventilation of intermediate layers in the Bornholm Basin. They enter the Baltic Sea first and most effectively via the Sound and then via the Darss Sill (see fig. 2.1 and 2.2 for coastlines, bathymetry and geographical names) and are caused by barotropic or baroclinic pressure gradient. On their way over the sills, through the Arkona Basin and over the Bornholm Channel the medium-intensity inflows propagate as dense bottom currents, and are subject to entrainment of the overlaying brackish waters which reduce their density and thus decrease the density of the isopycnal surface at which they sandwich into the halocline of the Bornholm Basin.

This master thesis investigates a medium-intensity saline water inflow in November 2005. The inflow was barotropic over the Drogden Sill, and here we focus on this inflow pathway only. This study also compares the observed inflow with model simulations. The main data set analyzed in this master thesis is obtained from Polish Academy of Science ship R/V Oceania. During the November 2005 9 days ship cruise (see sect. 3.1) took place, just after a medium-intensity inflow has started.

During the cruise 18 CTD and ADCP transects were made (fig. 3.5 and 3.6). In the same period two other vessels were observing the inflow. Moreover to estimate the size and the intensity of the inflow, as well as the velocity of the inflow propagation, data from moorings in the Arkona Sea and inside the Sound were analyzed. Data regarding the Sea Surface Height (SSH) were used from the stations in the north of Sound (Viken) and in the south of Sound (Skanoer) (marked crosses on fig. 3.4). The ADCP and CTD data were available for the period of interests from measurement stations at Arkona Basin, Darss Sill, Kriegers Flak South and North as well as from the Drogden Sill (the moorings are marked triangles on the fig. 3.4).

For simulating dynamics of a medium-intensity inflow events the General Estuarine Transport Model (GETM) (Burchard and Bolding, 2002; Burchard et al., 2004; Umlauf and Lemmin, 2005) has been applied. The model results were carried out by Hannes Rennau from Leibniz Institute for Baltic Sea Research in Warnemünde.

The paper is organized as follows: first the theory necessary for understanding of this thesis is explained (chapter 2). Then the field observation of a medium-intensity inflow in November 2005 are described in chapter 3. Next observational data analysis is made (chapter 4) as well as comparison of the observational data with the model (chapter 5). Finally, the results are discussed in chapter 6.

Chapter 2

Theoretical part

2.1 Bathymetry and hydrography of the Baltic Sea

Baltic Sea is a landlocked sea, the only connection with the open ocean takes place through the North Sea. The Baltic Sea is divided into a few deep basins connected by the narrow channels and sills (fig. 2.1). The Baltic Sea is connected with the North Sea via three straits: the Sound, the Little Belt and the Great Belt. The exchange transition area is Kattegat.

The natural oceanographic boundaries between the North Sea and the Baltic Sea are the Darss Sill (0.8 km^2 cross section and 18 m sill depth) and the Drogden Sill (0.1 km^2 cross section; 7 m sill depth). Highly saline water passing the sills is able to flow downward into the central Baltic Sea to replace the water body near or at the bottom. However, the time needed for the advection from the Kattegat into the Baltic Sea depends on the route it takes. The shorter route via the Sound and across the very shallow Drogden Sill (about 100 km) takes 1 to 3 days. The water coming through this pathway is more saline (due to lower mixing) and has lower volume. The longer route through the Great Belt, Fehmarn Belt and Mecklenburg Bight and across the Darss Si11 (about 300 km) seems to be more effective (larger volume), but takes significantly longer time for water to arrive at the Arkona Basin. The water inflowing this pathway is also less saline. It is assumed that highly saline water crossing the Drogden Sill into the Baltic Sea is generally not able to renew the central Baltic Sea deep water significantly. Only the transport of larger volumes of highly saline water across the Darss Sill supported by the inflow across the Drogden Sill is considered to generate the major inflows (Huber et al., 1994).

The first of a chain of a Baltic Sea basins looking from the west is the Arkona Basin (AB). To enter AB water has to pass through the Drogden Sill or through the Darss Sill (see map on fig. 2.2). In the western part of the basin there is a relatively shallow area, Kriegers Flak, with depths from 17 to 40 meters. The inflowing waters normally tend to flow around the Kriegers Flak both along the northern and southern flanks. The AB is 45 meters deep in its deepest place and is connected with the Bornholm Basin (BB) by the Bornholm Channel. The BB has an almost round shape with a diameter of about 80 km and a maximum depth of about 100 m. East of the BB there is a Słupsk Furrow. It is a channel like basin with width of nearly 80 km in the east-west direction and depths of 110 meters in the deepest place. In the northeast direction Supsk Furrow is connected to the Eastern Gotland Basin (EGB). EGB is the largest and the central of all Baltic Sea basins. It is enclosed by a 150 m isobath and has a maximum depth of about 250 meters. In the east of EGB the Gulf of Riga is located. North of EGB the Fearoe Deep continues the chain-like alignments of the basins. In the Western Gotland Basin (WGB), separated from EGB by the island of Gotland there is the Landsort Deep, the deepest place in the Baltic Sea with depths up to 490 meters. The easternmost part of the Baltic Sea is the Gulf of Finland with an east-west extension, whereas northernmost part is the Gulf of Bothnia with north-south extension. The Gulf of Bothnia consist of the Bothnian Sea in the south and the Bay of Bothnia in the North.

Saline inflows from the North Sea produce strong lateral salinity gradients in the Baltic Sea, with salinities in the Kattegat transition area reaching 30 PSU, while in the Gulf of Bothnia salinity is around 5 PSU (Reissman et al., 2009). The Baltic Sea is the worlds largest pool of brackish water. The Baltic Sea low salinity is mostly due to a high precipitation and a big river discharge. The annual river run-off is 436 km^3 (Reissman et al., 2009) mainly due to a big drainage area and humid climate. The annual water budget amounts to 224 km^3 precipitation, 184 km^3 evaporation and 947 km^3 surface water outflow (Brogmus, 1952; HELCOM, 1993) and is compensated by inflow of nearly 500 km^3 of saline water from the North Sea. The water exchange between the Baltic Sea and the North Sea is restricted by the connecting straits and sounds.

In the Baltic Sea a permanent halocline separates the surface water from the water in the deep Baltic Sea basins. In the AB halocline is found from 35 to 40 m depth, in EGB it is significantly deeper: at 70 to 90 m depth (Stigebrandt, 1987a; Elken, 1996). A seasonal thermocline develops during the summer at depths between 10 and 30 m (Matthäus, 1984). The thermocline disappears in winter due to cooling and mixing of the surface water by wind and convection. These processes do not

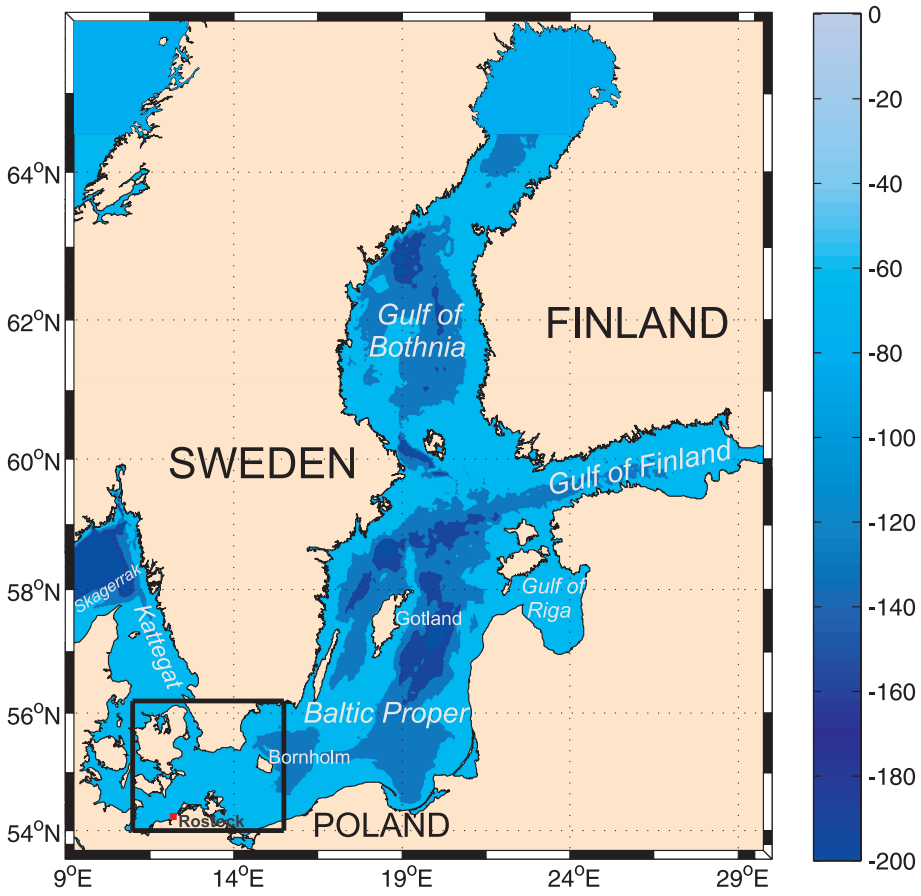

Figure 2.1: Bathymetry of the Baltic Sea. The frame marks the area where the observations discussed in this master thesis were taken. For the area north of the 64th circle of latitude no bathymetry data was available.

affect the deep water which is isolated from the surface water by the halocline. This water can be only replaced by the inflowing water from the North Sea. Because of its high salinity incoming water spreads along the bottom and is subject to a further entrainment of brackish surface water on its way. Therefore, bottom salinities of the deeper basins decrease from west to east. During the stagnation periods (described in sect. 2.6) the oxygen in the Baltic Sea deep waters becomes depleted and hydrogen sulfide may occur.

2.2 Saline water inflows

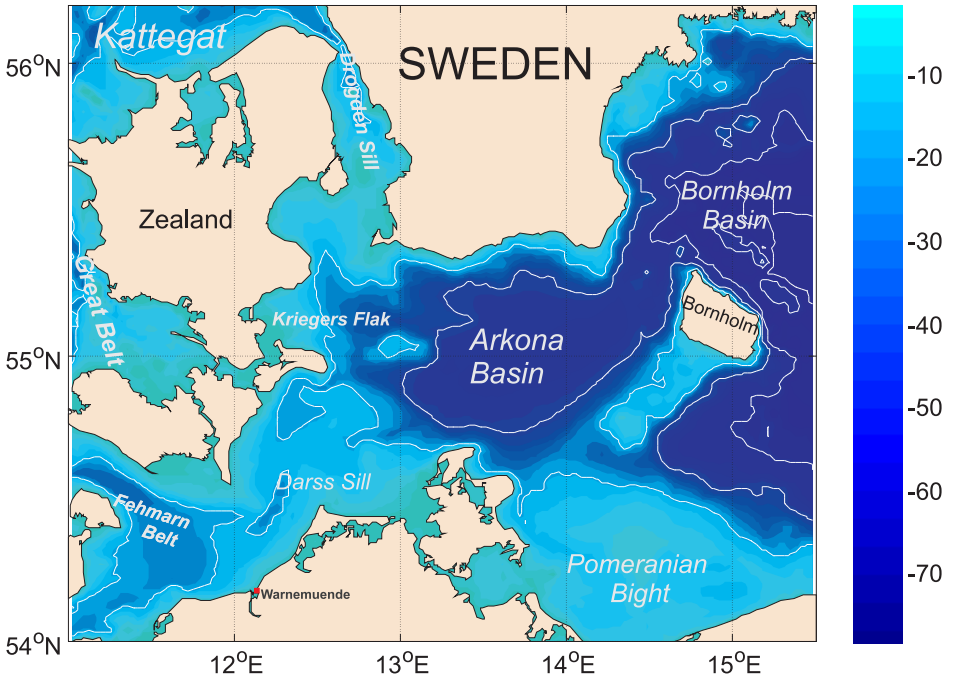

Figure 2.2: The enlarged map of the part of the Baltic Sea where the observational data were acquired.

The Kattegat, which connects the Baltic Sea with the North Sea has a salinities of about 17 PSU in the surface layer and up to 30 PSU in the deep waters. The Baltic Sea as mentioned before is the brackish sea, with salinities in the surface waters up to 10 PSU and strong vertical and lateral gradients. The resulting density differences cause episodic saline water, near-bottom, baroclinic inflow into the Baltic Sea and surface, brackish water outflow from the Baltic Sea, hampered by the narrow and shallow Danish straits, their tidal oscillations and changing wind condition in the westwind belt. Also barotropic inflows occur, caused by sea level differences between the Baltic Proper and the Kattegat.

Only under specific meteorological circumstances significant inflow is possible. When the salty water reaches the Baltic Sea through both the Darss and the Drogden Sill it propagates eastwards along the system of sills and channels and renew the old, bottom water in the deep Baltic Basins, as well as refill the Baltic Sea salt budget. Those inflows occur very irregularly, from repeated events within a

single year, to stagnation periods lasting over a decade or more. The inflows have a significant influence on physical, chemical and biological status of the Baltic Sea, which will be discussed shortly in sect. 2.6.

The inflows into the Baltic Sea can be generally divided into the barotropic-ones and baroclinic-ones. So-called barotropic inflows have been characterized by Franck et al. (1987), Matthäus and Franck (1992), Fisher and Matthäus (1996), Feistel et al. (2003b) and Reissman et al. (2009) as follows:

- They are driven by barotropic pressure gradients, especially sea level differences.
- They appear during persistent westerly gales (mostly in autumn, winter and spring).
- They import salt (typically 2 Gt) into the Baltic Sea along with the water volume transport (typically 200 km^3).
- They import oxygen-saturated water (typically 1 Mt of O_2) if they occur in winter or spring.
- They typically pass through the Sound and the Belt.

In contrast the baroclinic inflows are characterized by Welander (1974), Jakobsen (1980), Feistel et al. (2003a) and Mohrholz et al. (2006):

- They are driven by baroclinic pressure gradients, especially horizontal salinity differences.
- They appear during persistent calm wind condition (usually in late summer).
- They import salt into the Baltic Sea along with the water volume export.
- They import oxygen-deficient water, but ventilate the deep Baltic basins by entrainment of oxygenated surface water.
- They pass only through the Great Belt gateway.

Moreover barotropic inflows can be further divided into Major Barotropic Inflows (MBI's), medium intensity inflows and weak inflows, what will be discussed further in subsections 2.2.1 and 2.2.2.

Winter and spring inflows of either type raise the deep Baltic Sea basins salinities and oxygen, while lowering the temperature. The autumn and summer ones increase salinities and temperature, but carry only little oxygen.

2.2.1 Major Baltic Inflows (MBIs)

The volume of water with a higher salinity crossing the sills during the very frequent but weak inflows (10 - 20 km^3) have little impact on the deep and bottom waters. Such inflows are generally insufficient to displace the bottom waters or significantly change the oceanographic condition in the Baltic Sea deep basins, because their water will be interleaved in or flow just beneath the permanent halocline. Episodic inflows of a larger volume (100 - 250 km^3) of highly saline (17-25 PSU) and oxygen rich water, which penetrates deep into the Baltic, filling each of the deep basin with a fresh water represent the most important mechanism by which the Baltic Sea deep water is replaced and renewed to a significant degree. Such inflows are characteristic basin-scale oceanographic phenomena of the Baltic Sea.

For this process first German names 'Salzeinbruch' (Wyrtki, 1954) and later 'Salzwassereinbruch' (Dickson, 1973) were used. In English written papers most frequently used term is Major Baltic Inflow (MBI) coined by Dickson (1973).

The volume of highly saline water passing into the Baltic Sea across the Drogden Sill is generally thought to be insufficient to renew central the Baltic Sea deep waters significantly. Therefore only the transport of larger volumes of water across the Darss Sill supported by the inflow through the Drogden Sill constitutes a major inflow.

Franck et al. (1987) used the following empirical criteria at Darss Sill to identify the MBIs:

- The stratification coefficient G = 1 - S/S_b, where S is the surface salinity and S_b is the bottom salinity, must be ≤ 0.2 for at least 5 consecutive days.
- The bottom salinity S_b must be higher then 17 PSU.

The total of 96 major inflows were recognized at the Darss Sill during the period from 1897 to 1995, excluding two world wars (Matthäus and Franck, 1992). All inflows occurred between the end of the August and the end of the April. Such events are most frequent between October and February (90 percent) and are less common in August/September and March/April. Major inflows have never occurred between May and mid August. The inflows usually occur in clusters (17 cases), but

some were isolated events (6 cases). A cluster comprise all inflows separated by intervals of less then 1 year. Most clusters last for 2 or 3 seasons, but none lasted more than five (Fischer and Matthäus, 1996). The events were characterized by means of parameter Q, which arranges major events according to their relative intensity. The intensity index is defined as:

$$Q = 50(((k_{GR} - 5)/25) + ((S_{GR} - 17)/7)) \tag{2.1}$$

, where k_{GR} is the duration of the inflow and S_{GR} is the mean salinity of the inflowing water (Fischer and Matthäus, 1996). The intensity index Q varies between 0 ($k_{GR} = 5$ days and $S_{GR} = 17$ PSU) and 100 ($k_{GR} = 30$ days and $S_{GR} = 24$ PSU). Major inflows were classified by their intensity index into weak (Q$\leq$ 15) , moderate ($15 \leq Q \leq 30$), strong ($30 \leq Q \leq 45$) and very strong (Q¿45) . Weak inflows, which are about one half of all major inflows, never last more then eight days and have a maximum salinity of 18.6 PSU. Intensity index Q has a seasonal variation with the highest intensities from November to January (Fischer and Matthäus, 1996). The intensity of the inflows from period 1897-1939 is given on fig. 2.3

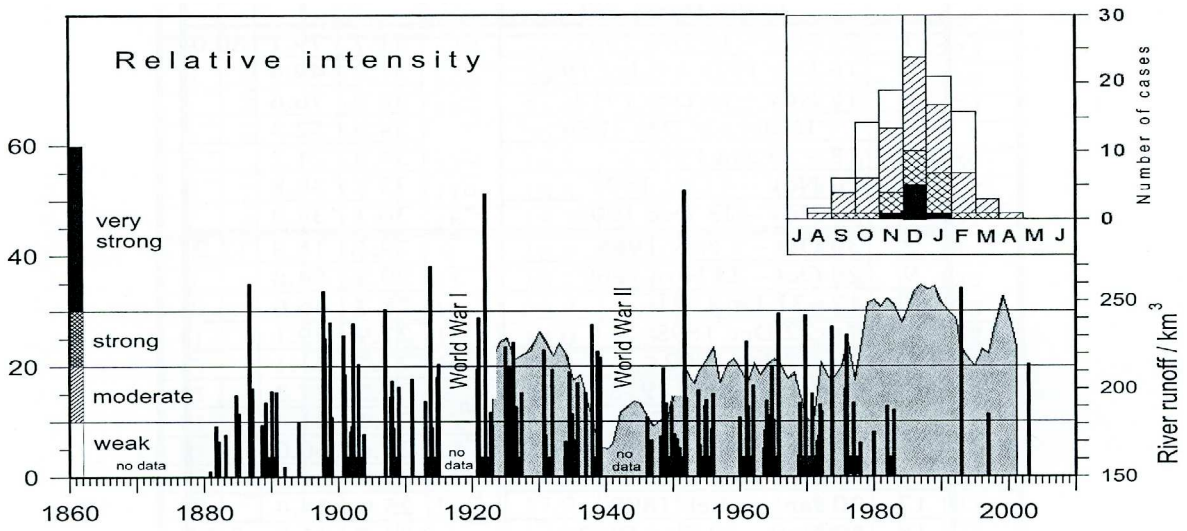

Figure 2.3: Major Baltic Inflows between 1880 and 2005 and their seasonal evolution (upper right) shown in terms of their relative intensity Q and a five year running means of river runoff to the Baltic Sea (inside the entrance sills) averaged from september to march (shaded). Black boxes on the time axis: MBIs arranged in clusters (Matthäus, 2006).

2.2.2 Small and medium intensity inflows

Besides the Major Baltic Inflows which take place with a small frequency, there exist also medium-intensity inflows taking time several times per year. They transport smaller amount of saline water into the Baltic Sea and therefore are not as efficient in renewing the Baltic Sea deep waters. However mixing of these water masses with ambient water in the Arkona Basin results in density anomaly between 7 and 8 PSU in the Bornholm Channel (Burchard et al., 2005). Water of this density has the capability to continue to flow into the intermediate layers of the Bornholm Basin (which is at times subject to oxygen depletion) and maybe even further into the Eastern Gotland Basin. As the Arkona Sea is known to significantly reduce the density of such inflowing water by means of turbulent mixing, quantification of relevant water mass transformations in this area is essential for understanding of the sensitivity of the Baltic Sea to climate change and human impact. The importance of salt water inflows into the Baltic Sea drives throughgoing research of exchange mechanisms and the assessment of enhanced mixing by man-made obstructions (Sellschopp et al., 2006).

2.2.3 Dense water pathways

The inflow event over the Darss Sill in the west of the Arkona Basin typically occurs a few days after the inflow through the Drogden Sill such that the latter can be investigated separately. Saline water propagating over the Drogden Sill propagates southward and branches into two plumes. The northern plume flows downhill into a trench at the northern rim of Kriegers Flak (fig. 2.4), whereas the southern plume follows the isobath and passes through the gap between Kriegers Flak and Møn Island. The further motion of the latter plume is a spiral along the western and southern rim into center of Arkona Basin, where it contributes to the dense bottom plume water (Lass and Mohrholz, 2003a; Burchard et al., 2005). The main inflow pathways can be seen on the fig. 2.4. Numerical simulations show that the core of the northern plume has both higher salinity and higher eastward velocity compared with the southern plume (Pacanowski and Griffies, 1999; Lass et al., 2005). Another plume passing the Darss Sill flows onto a wedge-shaped submarine terrace from the sill to Cap Arkona where it joined the Western Drogden Sill plume associated with mixing and eddy shedding (Meier et al., 2006).

2.2.4 Forcing mechanisms

Inside of the medium-intensity inflows 'warm summer inflows' can be distinguished. Most of these inflows are driven by baroclinic pressure gradients during calm wind conditions in the Belt Sea and in the Arkona Sea. Some of them

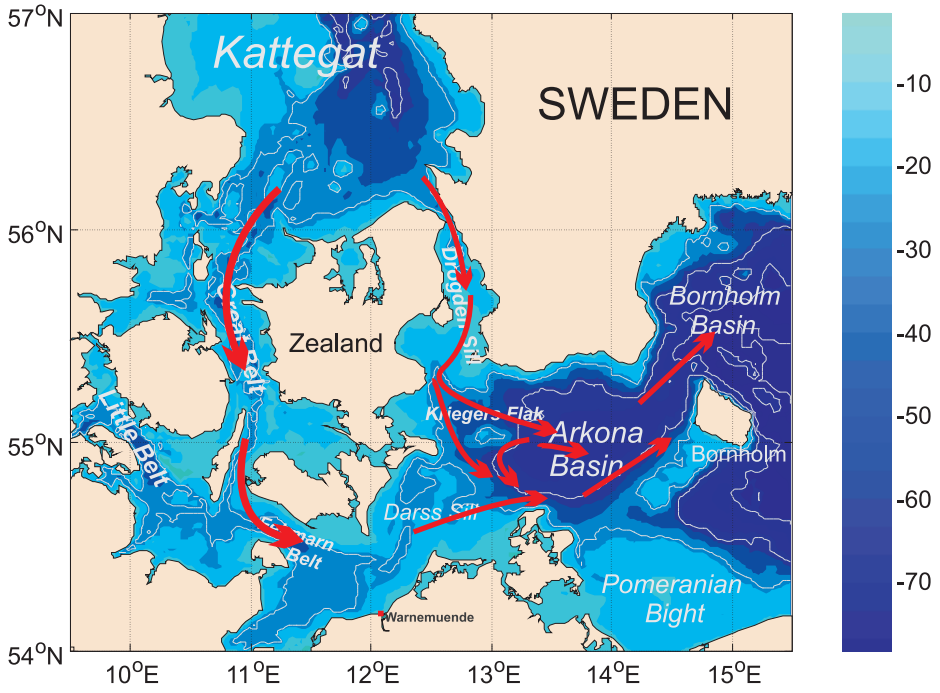

Figure 2.4: Main pathways of the saline inflows into the Baltic Sea.

are baroclinic events, like the warm inflows in 1997 and 2001 (Hagen and Feistel, 2001; Feistel et al., 2003a) and the one described in this thesis. The forcing of the barotropic medium-intensity inflow is similar to the major barotropic inflows. In general barotropic pressure gradients, mainly sea level differences are needed. To obtain those gradients persistent easterly wind should occur for at least few days, which cause the Baltic Sea mean surface elevation to reach its temporal minimum. If afterwards a longer period with prevailing westerly wind occurs, the mean surface elevation will raise causing an inflow from the Kattegat into the Baltic Sea. The comparison of the wind direction over the western Baltic Sea Area with the cumulated water flux through the Drogden Sill into the Baltic Sea is given on 2.5.

2.2.5 Dense water pool in the Arkona Basin

Water spilling over the Darss Sill and Drogden Sill into the Arkona Sea are basically spiralling cyclonically along the rims of the Arkona Basin dragged by some frictional effects into the core of Arkona Basin (Mohrholz et al., 2006). This process feeds

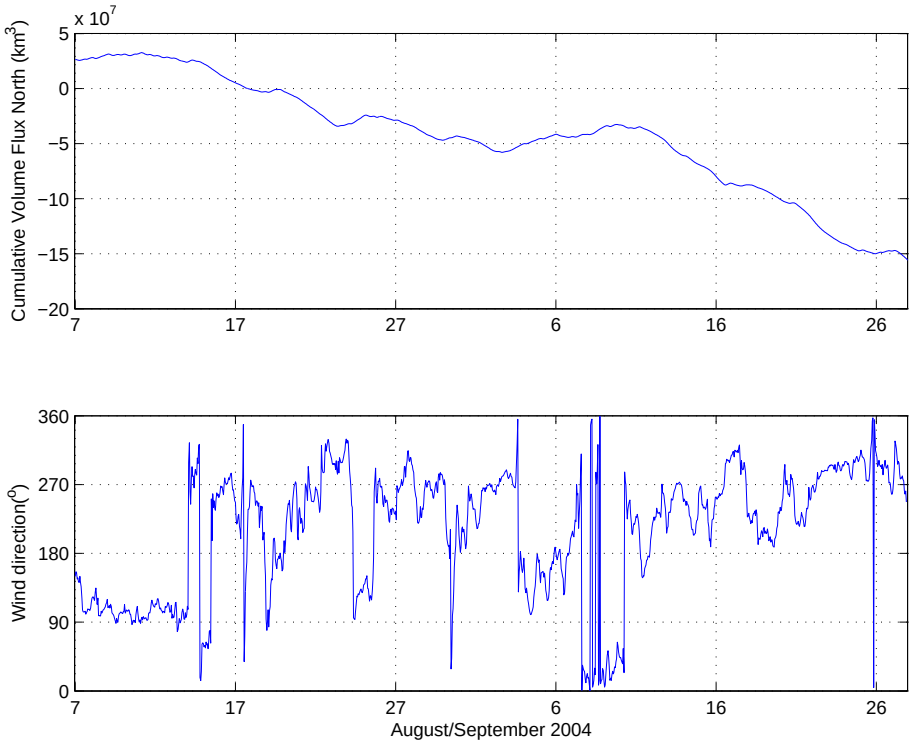

Figure 2.5: The comparison of the wind direction (0 are northerly winds, 90 - easterly and so on) over the western Baltic Sea area with the cumulated water flux through the Drogden Sill. The cumulative volume flux is simply the amount of the water outflowing through the Drogden Sill from the Baltic Sea. On this plot positive values indicate the outflow from the Baltic Sea, whereas the negative indicate inflow into the Baltic Sea. It can be noticed that for periods with prevailing westerly winds the flux decreases (inflow) and for prevailing easterly winds flux increases (outflow).

episodically into an up to 15 m thick bottom pool of dense water resting in the relatively plain eastern part of the Arkona Sea generating a Kelvin-wave type of cyclonic circulation pattern (Lass and Mohrholz, 2003a). This dense water is separated by a halocline from the water of the Baltic Sea origin (Liljebladh and Stigebrandt, 1996). Repeated observation of medium-intensity salt water inflows shows that the residence time of the salt water pool is less then three months (Lass et al., 2005) and is reduced by permanent water leakage through the Bornholm Channel (Walin, 1981). Assuming that the gap in the pool is controlled by Kelvin-wave dynamics (Lass et al., 2005) found that baroclinic Kelvin waves circumnavigate through the Arkona Basin within 4 days and that the time to reduce the initial volume of salt water pool by one half amounts to one month.

In contrast to MBIs which are well investigated and described, there are only a few papers describing medium-intensity inflows as far. During the past two decades, the frequency of large barotropic inflows (mainly in winter) has decreased and the frequency of medium-intensity baroclinic inflows (observed in summer) has increased. As a result of entrainment of ambient oxygen-rich water, summer inflows became more important for the deep water ventilation.

2.2.6 Inflow periods

The MBIs characterized by three significant periods:

- *precursory period* - this period is defined as the time from the minimum Baltic Sea mean elevation preceding a major event to the start of that event at the Darss Sill. Minimum sea mean elevation, which are always below the normal Baltic Sea elevation, precede each inflow of highly saline water. During this period, water with a relatively low salinity (below 17 PSU) flows across the Darss Sill into the Baltic, and highly saline water (partly above 20 PSU) may already be moving across the Drogden Sill. The most important part of the precursory period is called pre-inflow period and starts typically 15 days before the start of the event. However negative Baltic levels in the pre-inflow periods are not necessary for the inflow.

- *main inflow period* is characterized by the inflow of highly saline water through both Drogden and Darss Sills.

- *post inflow period* starts with strong outflow due to weakening of the west wind and the above-normal sea mean elevation in Baltic. The main period of the inflow are shown on the fig. 2.6

2.2.7 Inflows time scales

The ventilation of the Baltic Sea deep water is characterized by various time scales. The advective time scale is rather short. For instance, the salt water of the Major Baltic Inflow in January 2003 arrived at the Bornholm Deep on January 25th, 12 days after the start of the event at the sills (Feistel et al., 2003a; Piechura and Beszczyska-Möller, 2003). A spreading time of 12 days between the Drogden Sill and the Bornholm Channel was also found for the small and medium-strength inflows in November and December 1998 (Lass and Mohrholz, 2003b) and August/September 2002 (Mohrholz et al., 2006). The residence time of the salt water pool in the Arkona Basin was estimated to be 1 month (Lass et al., 2005). After about 3 months the first signs of the inflowing water were observed in the Gotland Deep (Feistel et al., 2003a).

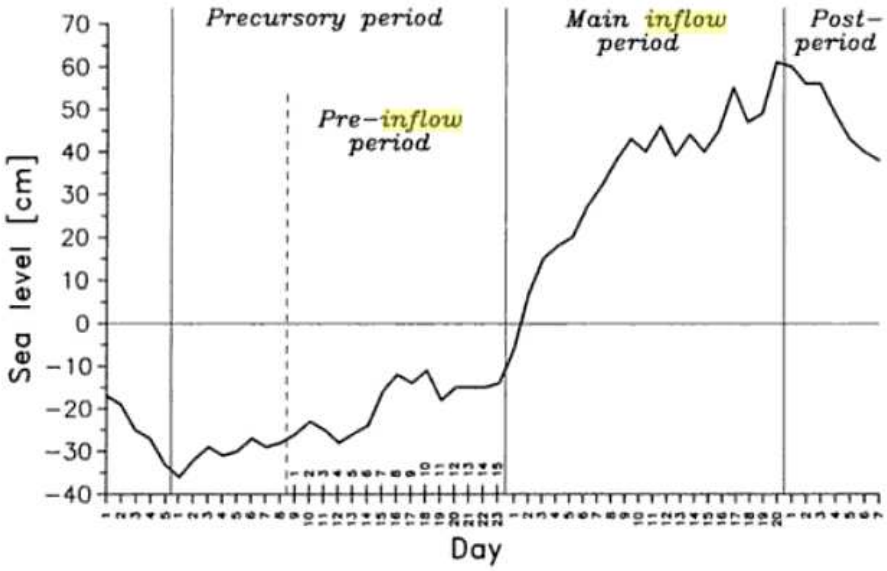

Figure 2.6: Main inflow periods and related changes in sea level. After Matthäus and Franck (1992)

In contrast to the relatively short advective time scale, the diffusive time scale is much longer, for the inflow it takes not more then 20 days to arrive in the Bornholm Channel, but vertical mixing with the ambient water takes significantly more time (Meier et al., 2006).

2.3 Entrainment

On the way from a sub-basin to a sub-basin, the salinity of the inflowing water decreases due to entrainment of the ambient, less saline water, whereas the volume flow increases (Meier et al., 2006). The dense bottom flow carries the intruding sea water and drives the vertical circulation of the Baltic Sea (Stigebrandt, 1987a; Reissman et al., 2009). Using measurements from the period from 1970 to 1990 Kouts and Omstedt (1993) identified three main mixing zones: the Belt Sea and the Sound, the Arkona Sea, and the Słupsk Furrow.

This data analysis located the regions of increased mixing of inflows into the Baltic Sea, but did not discuss the processes causing the mixing. In a more detailed investigation Lass and Mohrholz (2003a) identified three major mixing mechanisms:

- wind mixing in the vicinity of sills,

- differential advection in the head region of the dense bottom currents, which increase mixing by shearing denser water over less dense water,
- shear-induced entrainment of ambient water into dense bottom currents.

The wind related mixing, however, can only be effective at relatively shallow depths (e.g. the Drogden Sill), whereas in the deeper Bornholm Channel the dense bottom currents are mostly protected against wind mixing by an overlaying stratified layer.

The entrainment across the pycnocline on top of the dense bottom current due to interfacial shear has been investigated in much detail since several decades (Arneborg et al., 2007; Reissman et al., 2009). This generally results in a dependence of the entrainment parameter, defined here for the non-divergent plumes as $E = w_E/U$ (with the entrainment velocity w_E representing the rising velocity of the pycnocline and the mean downslope velocity U) on the Froude number, defined here as (Reissman et al., 2009):

$$Fr = U/(g'H)^{1/2} \tag{2.2}$$

(with the reduced gravity g' and the plume thickness H), which is of the form

$$E = cF_r^a$$

with the positive non-dimensional parameters a and c.

Observations of the gravity currents with Froude numbers close to one indicate a dependency for the Froude number of the form (Wahlin and Cenedese, 2006)

$$w_E/U = 10^{-3}Fr^8 \tag{2.3}$$

Recent laboratory experiments of gravity currents on rotating gentle slopes indicate a somewhat weaker dependency (Cenedese et al., 2004)

$$w_E/U = 4 \cdot 10^{-4}Fr^{3.5} \tag{2.4}$$

with the entrainment being caused by the breaking of roller waves on the interface. An alternative expression based on the along-flow slope rather than on the Froude number has been shown to work well for weak slopes and subcritical flows (Pedersen, 1980; Stigebrandt, 1987b; Arneborg et al., 2004),

$$w_E/U = 0.07s \tag{2.5}$$

where s is the bottom slope in the along-flow direction.

For a steady current, the entrainment can be derived by observations of the increase of volume flux or decrease in density or salinity in the flow direction. In the data analyzed in this master thesis the volume flux budgets are unclear, but we will look for the entrainment effects in the salinity data. The salinity decreases in the flow direction as

$$\frac{\partial S}{\partial x} = \frac{(S - S_0)Bw_E}{Q} \tag{2.6}$$

(Sellschopp et al., 2006)

where S_0 is the salinity outside the gravity current, B is width of gravity current, and Q is the volume flux.

Recent observation made by Arneborg et al. (2007) and Umlauf and Arneborg (2009) suggest that entrainment is affected by the Ekman number E_k as well as by the Froude number. They suggested that variations of E_k are an important factor controlling the entrainment process, which is supported by the generally strong correlation between E and E_k.

2.4 Dynamics of the currents passing through a channel

Theoretical works on rotating bottom gravity currents show the importance of bottom friction for the downward steering of dense waters along submarine canyons (Wahlin, 2002, 2004) and ridges (Darelius and Wahlin, 2007; Darelius, 2008). These authors suggested a simple model based on the ideas that the flow along the corrugation is geostrophically balanced, and that frictional control adjusts the speed exactly such that the bottom stress balances the interfacial pressure-gradient along the corrugation.

An interesting constraint was pointed by Wahlin (2002), who showed that topographic downward-steering along a channel or a ridge implies that the transverse Ekman transport and the transverse geostrophic transport due to the down-channel tilt of the interface exactly cancel.

Last work by Umlauf and Arneborg (2009) suggest that the transverse transport of fluid inside the interface have a profound impact on the development of the transverse density structure in the gravity current. This transport is marked on the fig. 2.7 as q_i.

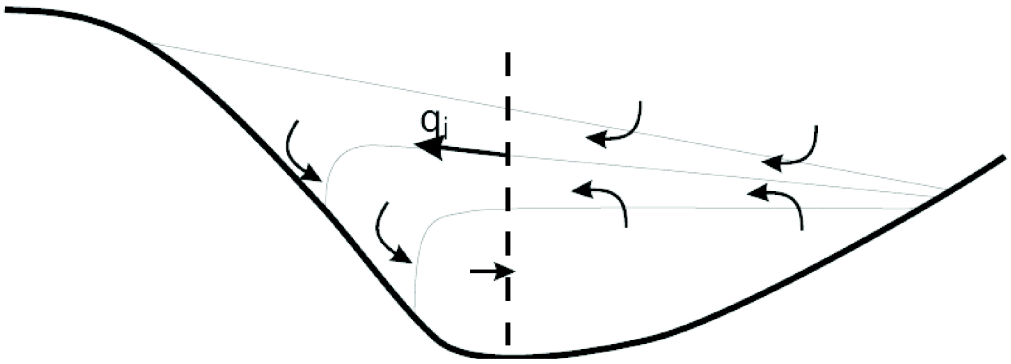

Figure 2.7: Schematic view of the entrainment process and the effect of the interfacial jet. The down-channel flow is directed out of the page. After Umlauf and Arneborg (2009).

If interfacial fluid is involved in the transverse recirculation, the transverse transport inside the interface must be balanced by a motion of isopycnals, due to diapycnal mixing or to transverse advection of the density field. The transverse interfacial jet advects water of intermediary buoyancy from the northern side of the gravity current towards the southern side, increasing buoyancy in the southern part by both transverse advection of interfacial water and local entrainment of ambient water. The advected, buoyant fluid is mixed down by strong turbulence on the southern slope in a process that requires further clarification, and is then advected back towards the center of the channel with the transverse return current in the interior (again fig. 2.7). This process of entrainment around the corner also creates the characteristic lateral buoyancy gradient in the interior and the wedge-shaped interface, which can be observed as:

- draining the interface in the northern part
- spreading the isopycnals on the southern side

(Umlauf and Arneborg, 2009)

These characteristic interfaces have been reported for laboratory experiments, numerical simulations and numerous oceanic observations. Also the bending of

isopycnals at the downwelling-favorable side is evident from investigations of some shallow, channelized gravity currents in the ocean and from idealized numerical simulations. A likely consequence of this type of communication between interfacial and interior fluid is an increase of entrainment, consistent with the recent observation of Wahlin et al. (2008) that topographic steering in laboratory experiments results in stronger net entrainment.

Previous investigations have looked for an explanation of the interfacial deformation in terms of the interfacial Ekman transport, and its interaction with the bottom Ekman layer (Johnson and Sanford, 1992). In contrast to these ideas, Umlauf and Arneborg (2009) suggested that the geostrophically balanced part of the transverse transport in the interface, a process so far ignored in this context, plays the key role in shaping the interface and generating lateral stratification in the interior of the gravity current. Umlauf and Arneborg (2009) showed that transverse transport q_i has a geostrophically balanced contribution, directed towards the right of the down-channel flow, and an oppositely directed contribution due to entrainment

2.5 Mesoscale eddies

The mesoscale eddies in the Baltic Sea (also called Beddies) are found at various depths from the surface to the bottom, some of them cover the whole water column. Most of Beddies are observed in the region of the permanent halocline and show no surface signature. They diameters varies from 10 to 20 km and their thickness ranges between a few meters and the entire water depth. The Beddies drift with velocities of a few cm/s and spin with maximum rotational speeds between 20 cm/s and 30 cm/s. They seem to be almost in geostrophic balance (Reissman, 2002). The cyclonic eddy is called a cold-core eddy or ring and the anti-cyclonic eddy is called a warm-core eddy or ring.

The number of Beddies coexisting in each region varies from about 15 in the Arkona Basin, the Bornholm Basin and the Słupsk Furrow up to 30 in the Eastern Gotland Basin (Reissman et al., 2009). Most of the Beddies are found in or above the regional main pycnocline. This is certainly a consequence of the smaller volume available for the Beddies at the bottom due to the basin shape in each region and does not mean that there are no Beddies below the main pycnocline. Also very interesting is the fact that all Beddies in each region occupy a constant fraction of about 12% of the investigated basin volume (Reissman et al., 2009). Taking into account the respective number of Beddies this corresponds to mean volumes of the Beddies ranging from about 1.5 km^3 in the Arkona Basin over values of around 2 km^3 in the Bornholm Basin to more than 3 km^3 in the Eastern Gotland Basin. This

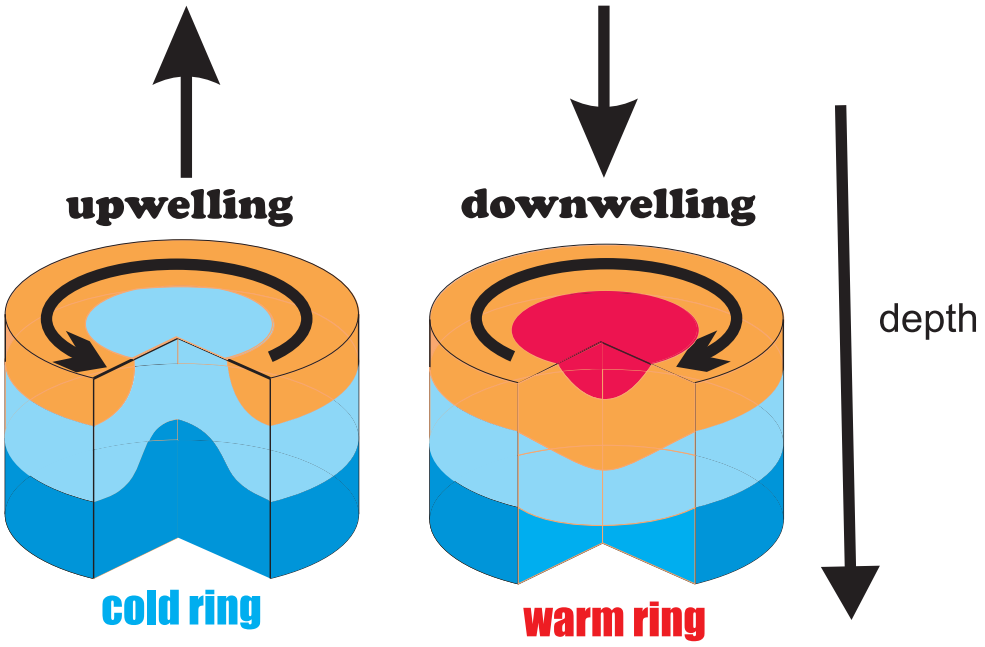

Figure 2.8: A scheme of cold-core and warm-core eddies. The arrows on top of the eddies mark water movement direction, cyclonic for cold-core eddies and anti-cyclonic for warm-core eddies.

increase of the mean volume is accompanied by an increase of the mean thickness of the Beddies from around 13 m in the Arkona Basin up to 23 m in the Eastern Gotland Basin, while their mean horizontal cross-sectional area varies only little within the range corresponding to radii between 4 km and 5 km for the different regions (Reissman, 2002) .

The formation mechanisms and the life histories of eddies remain the subject of oceanographic research. There are several different conditions giving rise to their formation just as there are for their atmospheric counterparts, the low and high pressure eddies. For example, currents like the Gulf Stream meander in a rather wave-like fashion and become unstable. These flow instabilities lead to pinching off relatively warm or cool waters that act as seeds for eddies. Also flow over seamounts can cause eddies. Also, under suitable divergent conditions, cool, nutrient-rich waters can upwell from deeper waters to act as a seed for the formation of a cold-core eddy . Likewise, warmer, nutrient-poor waters may converge, be downwelled, and a warm-core eddy can be formed (fig. 2.8).

2.6 Stagnation periods and anoxic condition

Stagnation periods have a significant impact on the Baltic Sea ecosystem. The Baltic Sea is too fresh for most marine species and too salty for most freshwater species and most species experience physiological stress. Changes in salinity and oxygen concentrations may have a considerable impact on species distributions, food webs and life-histories (Meier et al., 2006).

The eutrophic Baltic Sea produces large amounts of organic matter, which sinks into the deeper water, mineralizes there and lowers the oxygen concentration. Major Baltic Inflows (MBIs), see sect. 2.2.1, occurring on the decadal time scale are the main process which ventilates these depleted deeper water. During the stagnation periods between two MBIs the near-bottom water of the deeper basins typically becomes anoxic with the consequence that large amounts of phosphate are released from the sediments.

Also the nutrient conditions in the deep basins of the Baltic Sea are strongly influenced by episodic inflows of larger volumes of highly saline, oxygen-rich water from the North Sea. Owing to their high density and their considerable oxygen content, these inflows are the only mechanism by which the deep water in the central basins can be replaced and significantly renewed. Major Baltic Inflows (MBIs) has the biggest effect on the deep basins water renewal, but also medium-intensity inflows take part of this process. They transport smaller amount of saline water into the Baltic Sea and therefore are not as efficient. However mixing of these water masses with ambient water in the Arkona Basin results in density anomaly between 7 and 8 PSU (Burchard et al., 2005) in the Bornholm Channel. Water of this density has the capability to continue to flow into the intermediate layers of the Bornholm Basin (which is generally subject to oxygen depletion).

2.7 Influence of the wind farms on the inflows

The natural mixing processes in the western Baltic Sea may actually be modified by offshore constructions such as bridges and wind farms. During the planning phase of the Great Belt Link and the Sound Bridge a zero-blocking solution has been postulated, meaning that the bridge constructions must have no influence on the volume flux through the Sound and the Great Belt. Stigebrandt (1992) estimated a flow reduction by the Sound bridge of only 0.6%, with almost no measurable effect for the Baltic Sea hydrography. Møller et al. (1997) carried out laboratory experiments with obstacles dragged through stratified water and found no significant mixing effect. However, observations of currents, stratification, and turbulence

upstream and downstream from the western part of the Great Belt Bridge carried out by Lass et al. (2006) revealed significant effects of the bridge pylons on the vertical flow structure. They observed von Karman straits in the wake of the bridge pylons with the potential to generate internal waves. These may propagate away from the constructions and release their energy into diapycnal mixing remotely.

In recent years extensive off-shore wind farms have been planned in up to 15 places in the western Baltic Sea area. Many of them are located near the coast at shallow depths, where the dense bottom currents do not occur, but it is the intention to locate some of these projected wind farms in overflow areas such as around the Kriegers Flak. Their foundations may act as obstacles for the dense bottom currents with the effect of increased entrainment.

The Quantas-Off project (in frame of which this master thesis is involved) is investigating the influence of the off-shore wind farms on the inflows into the Baltic Sea. The recent conclusions made in the frame of the project is that in the worst case the currently planned wind farms in the western Baltic Sea will reduce the mean monthly salinity at the bottom of the Bornholm Channel by up to 0.2 PSU ((Rennau and Burchard, 2009)). From 15 wind farms planned in the western Baltic Sea area, construction of 13 has been allowed, of which one is currently under construction.

2.8 GETM

For simulating dynamics of a medium-intensity inflow events over Drogden Sill, the GETM (Burchard and Bolding, 2002; Burchard et al., 2004) has been applied. The General Estuarine Transport Model (GETM) is an open source coastal ocean model (available from http://www.getm.eu).

GETM is a three-dimensional free-surface primitive equation model using the Boussinesq and boundary layer approximations. For the discretisation, a high-resolution bathymetry (0.5 n.m. resolution) has been used as well as bottom- and surface-fitted vertical coordinates with 25 vertical layers and a horizontally homogeneous bottom and surface layer thickness , such that the flow can smoothly advect along the bed. The model domain has open boundaries at the northern end of the Sound, towards the West across the Fehmarn Belt and towards the East along 14^o 46'5" E.

The major advantage of bottom fitted vertical coordinates, in comparison to geopotential coordinates with a step-like bottom approximation, is that for bottom-

following flows the advective fluxes across vertical coordinates and thus the associated discretisation errors are minimized . Furthermore, bottom-following coordinates allow high near-bed resolution also in domains with large depth variations (Burchard et al., 2009).

GETM has been successfully applied to several coastal, shelf sea and limnic scenarios, for turbulent flows in the Wadden Sea, for dynamics in the North Sea, for an idealized plume study in the Arkona Basin, for estimating exchange and residence times in the Willapa Bay in Washington State and for a basin-exchange study in the Lake of Geneva (Burchard et al., 2009).

2.8.1 Bathymetry adjustment procedure

High resolution bathymetries for the Western Baltic Sea show a deep and continuous channel pervading like a vein through the Great Belt. In order to partially account for this dynamically relevant topographic feature, the model bathymetry was modified by hand to include this deep channel. This led to an increase of transport of salinity through the Great Belt and hence resulted in improved agreement of timing and salinity for the stations Darss Sill and Arkona Buoy (Burchard et al., 2009).

The unmodified Western Baltic Sea bathymetry is underestimating salinities in the Fehmarn Belt and in the Drogden Sill. This problems in the volume and salinity transports have motivated some further adjustments in the model bathymetry and open boundary conditions. Step-wise bathymetry changes in the Great Belt and the Sound and concurrent model validation with station measurements have resulted in an increase of depth of parts of the Great Belt by up to 35% and in the Sound by up to 15% to obtain reasonable agreement of salinities for the Drogden Sill station and in the Fehmarn Belt. Also the barotropic pressure difference between both open boundaries have been increased (Burchard et al., 2009).

Chapter 3

Ship, on-board devices and moorings

3.1 RV Oceania

The data analyzed in this master thesis come from the cruise done by RV Oceania in November 2005. RV Oceania, or SY Oceania, is a tall ship, owned by the Polish Academy of Sciences, and used as a research vessel. The ship is equipped with laboratories able to provide hydrographic, optic, acoustic, chemical, biological and particulate experiments and observations. In this work CTD and ADCP data obtained during the cruise will be analyzed.

3.1.1 CTD Sensor

RV Oceania is equipped with CTD (conductivity, temperature, depth) sensor, produced by SeaBird Electronics. The model name of the sensor is FastCAT CTD Sensor (SBE 49). Below some important parameters are listed:

Measurement range:

- Temperature: -5 to +35 ^{o} C
- Conductivity: 0 to 9 S/m
- Pressure 0 to 350 meters

Initial accuracy:

- Temperature: 0.002 ^{o} C

- Conductivity: 0.0003S/m
- pressure 0.004 % full scale range

Resolution:

- Temperature: 0.0001 ^{o} C
- Conductivity: 0.00001 S/m (fresh waters)
- pressure 0.002 % full scale range

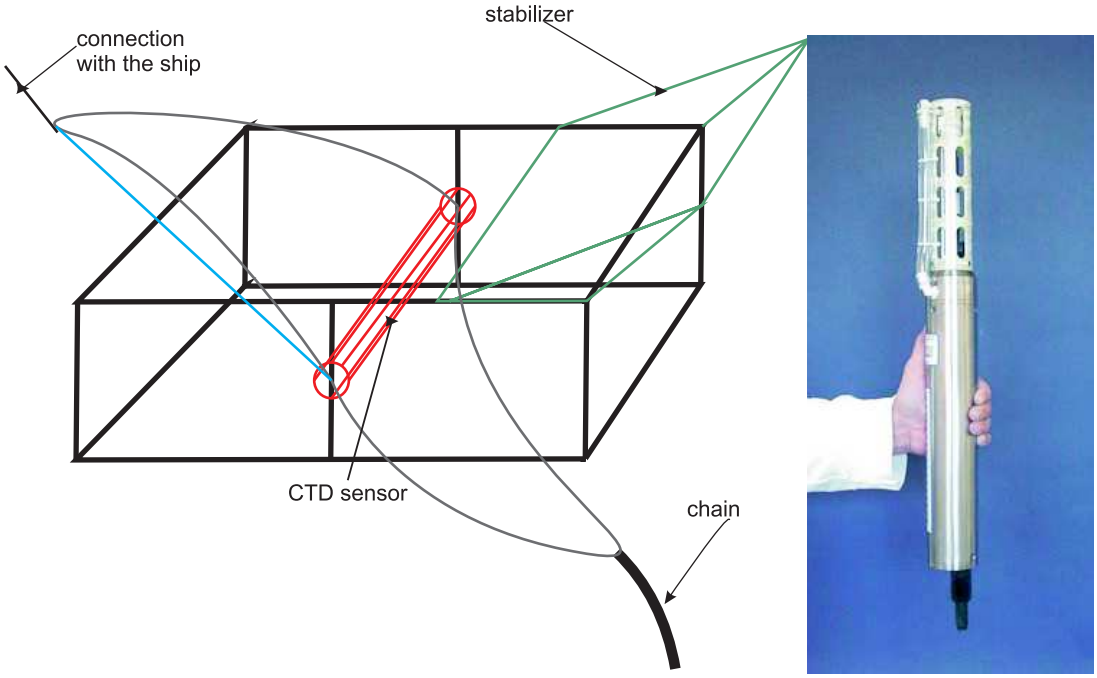

Figure 3.1: The metal framework used with the CTD. On the sides lines connecting the framework to the ship are attached. Underneath the metal chain is visible, and on the one side of the framework there is a stabilizer.

The CTD used on the RV Oceania ship is installed inside of the metal framework (fig. 3.1), parallel to the seabed. From the sides of the framework two lines leading to the ship are attached and as well metal chain is embedded. The main purpose of the chain is to increase the weight, so the CTD probe falls faster, which increases measurements resolution. Also, the chain helps to determine when the CTD sensor is approaching seabed (when the CTD crew inside of the ship observe slowing down of the probe it indicates that the chain has touched the ground).

Not like most of the CTD's, the data on the Oceania's CTD are collected while up- and down-movement of the probe, which gives the better spatial resolution. The down-going velocity is driven by gravity and is generally not depending on the human factor, but the up-going velocity depends on the winch speed. The problem is, that if the CTD up-movement is to fast, the probe and the cage around it causes disturbances of the water around it, and the CTD sensor do not read e.g. the correct water salinity, but the water salinity that is actually deeper (the probe pulls up the water while its up-movement). To correct this error, for the area with the corrupted data, up-going casts were removed and replaced with the down-going casts proceding them. On the fig. 3.2 the salinity data for one part of a transect is shown, before and after removing corrupted up-going casts. The problem exhibits in less then 10% of R/V Oceania data.

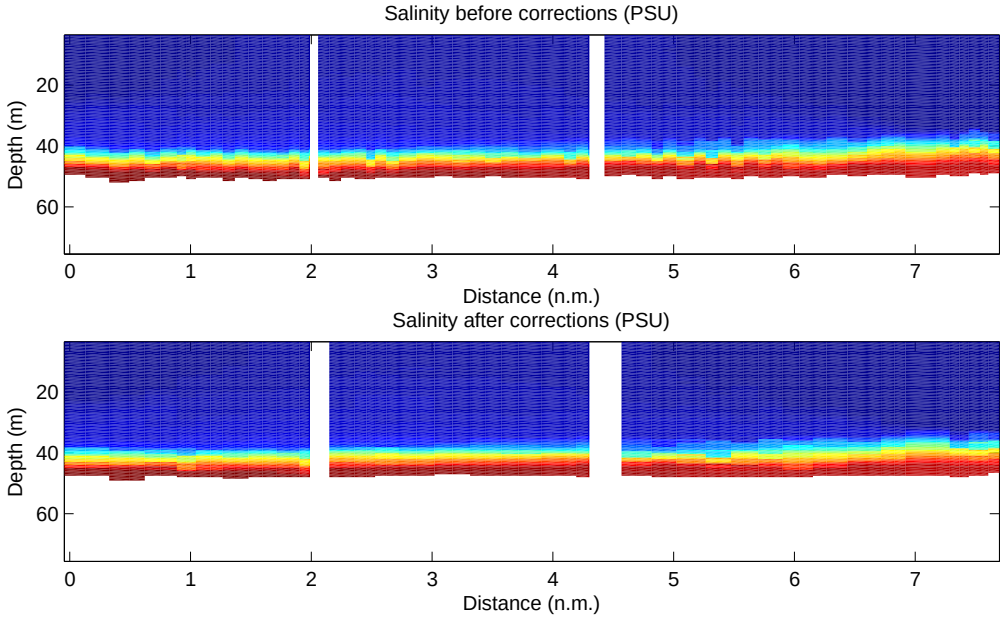

Figure 3.2: The original salinity data (upper panel) and the data after removing up-going casts (lower panel) and replacing them with down-going casts. On the corrected plots no salinity data zigzagging is visible, but it has two times lower resolution.

3.1.2 ADCP profiler

ADCP (Acoustic Doppler Current Profilers) use the Doppler effect by transmitting sound at a fixed frequency and listening to echoes returning from sound scatterers in the water. These sound scatterers are small particles or plankton that

reflect the sound back to the ADCP. Scatterers are everywhere in the ocean. They float in the water and on average they move at the same horizontal velocity as the water. Sound scatters in all directions from scatterers . Most of the sound goes forward, unaffected by the scatterers. The small amount that reflects back is Doppler shifted. When sound scatterers move away from the ADCP, the sound they hear is Doppler-shifted to a lower frequency proportional to the relative velocity between the ADCP and scatterer. The backscattered sound then appears to the ADCP as if the scatterers were the sound source.

When an ADCP uses multiple beams pointed in different directions, it senses different velocity components. For example, if the ADCP points one beam east and another north, it will measure east and north current components. If the ADCP beams point in other directions, trigonometric relations can convert current speed into north and east components. A key point is that one beam is required for each current component. Therefore, to measure three velocity components (e.g. east, north, and up), there must be at least three acoustic beams.

ADCP mounted on RV Oceania is a product of RD Instruments. The measuring frequency is 153.6 kHz and the measuring range is 250 meters, with bottom tracking range up to 400 meters. The accuracy of the profiler is 0.2% of the measured velocity. This ADCP has 4 transducer, each facing different direction. Also, each transducer beam angle is oriented 30^o from vertical. Due to ADCP measurement specifications it is impossible to measure the velocities near the surface and near the bottom (see sect. 3.1.3). Unfortunately the measurement of bottom velocities are of high interest in the frame of this master thesis - the dense bottom currents, ie. the medium-intensity inflows propagate nearby the bottom, as they are denser than the ambient water.

3.1.3 Measurements near the bottom

The echo from a hard surface such as the bottom is so much stronger than the echo from scatterer in the water that it can overwhelm the side lobe suppression of the transducer. One should normally reject data from distances too close to the surface (when looking up) or bottom (when looking down). Fig. 3.3 shows transducer beam angle oriented 30^o from vertical. For the 30^o transducer, the echo through the side lobe facing the bottom returns to the ADCP at the same time as the echo from the main lobe at 85% of the distance to the bottom. This means data from the last 15% of the range to the bottom can be contaminated. The effect is the same for an ADCP at the bottom looking up to the surface.

The equation that governs this is:

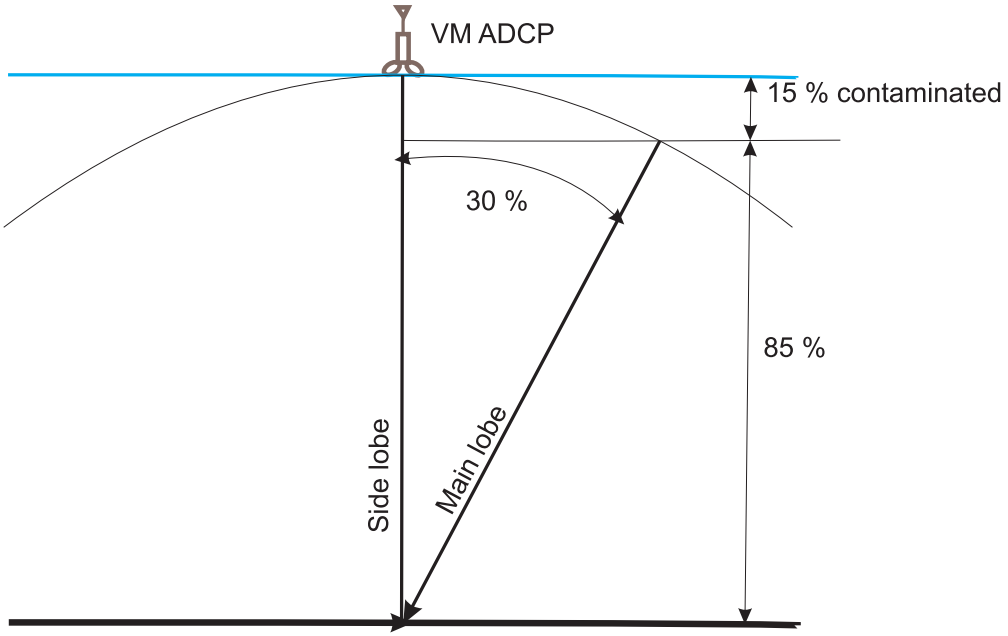

Figure 3.3: The relationship between transducer beam angle and the thickness of the contaminated layer at the surface.

$$R_{max} = Dcos(\Theta) \tag{3.1}$$

Where: R_{max} is the maximum range for acceptable data D is the distance from the ADCP to the surface or bottom (as appropriate) Angle Θ is the angle of the beam relative to vertical (normally 20^o or 30^o) When looking down, contamination from bottom echoes usually biases velocity data toward zero. In a moving vessel, contamination from bottom echoes is less predictable. The velocity of the surface or the bottom is zero on average; it is this zero velocity that biases the measured velocity toward zero.

3.2 Methods.

From 10th to 19th of November 2005 ship cruise with R/V Oceania (see sect. 3.1) from IOPAN in Sopot took place just after a medium intensity inflow has started. During the cruise 18 CTD and ADCP transects were made. Moreover to estimate the size and the intensity of the inflow as well as the velocity of the inflow propagation, data from moorings in the Arkona Sea and inside of the Sound were analyzed. Data regarding the Sea Surface Height (SSH) were used from the stations in the

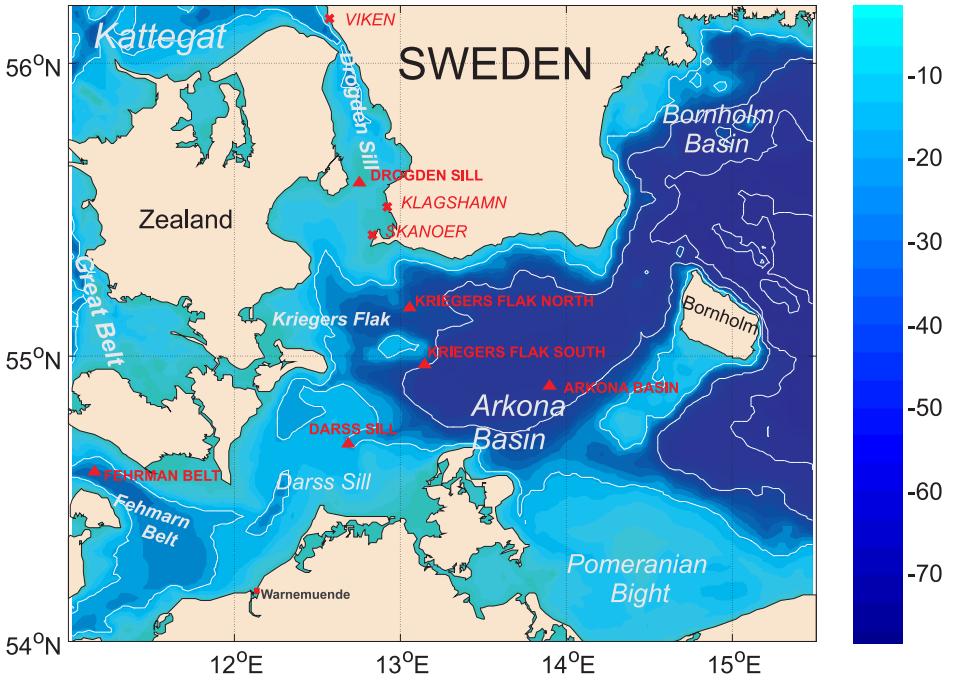

Figure 3.4: Map of the Arkona Basin with bathymetry lines every 20 meters. Sea Surface Height (SSH) measuring station are marked with crosses and moorings with triangles.

north of the Sound (Viken) and in the south of the Sound (Skanör) (marked crosses on the fig. 3.4). This data were used to estimate flux through the Sound. The Arkona Basin (AB) and Darss Sill (DS) measurement buoys wind data were used to find the wind patterns before, during and after the inflow. The ADCP and CTD data were available for the period of interests from measurement stations at Arkona Basin, Darss Sill, Kriegers Flak South (KFS) and North (KFN) as well from the Drogden Sill (all the moorings are marked triangles on the fig. 3.4).

To estimate the propagation of the inflow in the Arkona Basin CTD data from the Drogden Sill, Arkona Basin and Kriegers Flak South and North were used, as well as CTD and ADCP data from the Darss Sill. The inflow through the Sound is traced at stations at Drogden Sill, Kriegers Flak North and further east at Arkona Basin. The inflow through the Belt, which is delayed to the one through the Sound by couple of days is measured at stations at Darss Sill, Kriegers Flak South and Arkona Basin. To calculate the inflow propagation correlation between Darss Sill

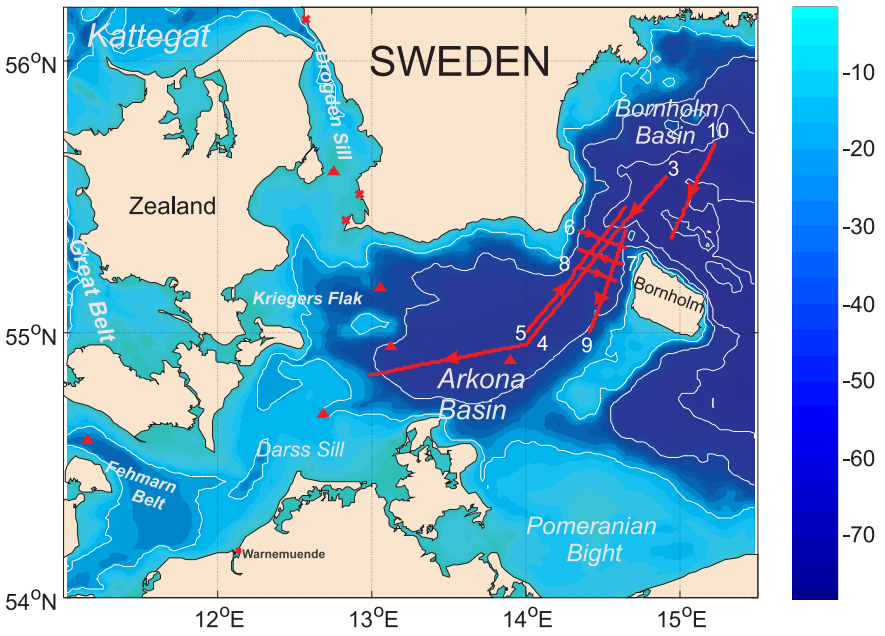

Figure 3.5: Map of the Arkona Basin with bathymetry lines every 20 meters. The first part of transects from R/V Oceania is marked with red lines. Sea Surface Height (SSH) measuring station are marked with crosses and moorings with triangles.

and Arkona Basin were calculated as well between Drogden Sill and Arkona Basin. Unfortunately, station at Kriegers Flak North has no data for the first part of the inflow.

Eighteen transects from R/V Oceania CTD probe and ADCP were taken between 10th (313th day of year 2005) and 19th of November 2005 (323rd day of year 2005). Transects are numbered from 3 to 20. Between transects 10th and 11th the larger time gap (ca. 3 days) occurred. It was caused by a storm (see fig. 4.1 on page 34 for wind velocities), which made measurements impossible (R/V Oceania is a sail boat). The transects made before the gap (3rd to 10th) are shown on fig. 3.5 , the rest, made after the gap are shown on fig. 3.6 . The timelines for all transects can be seen on fig. 3.7.

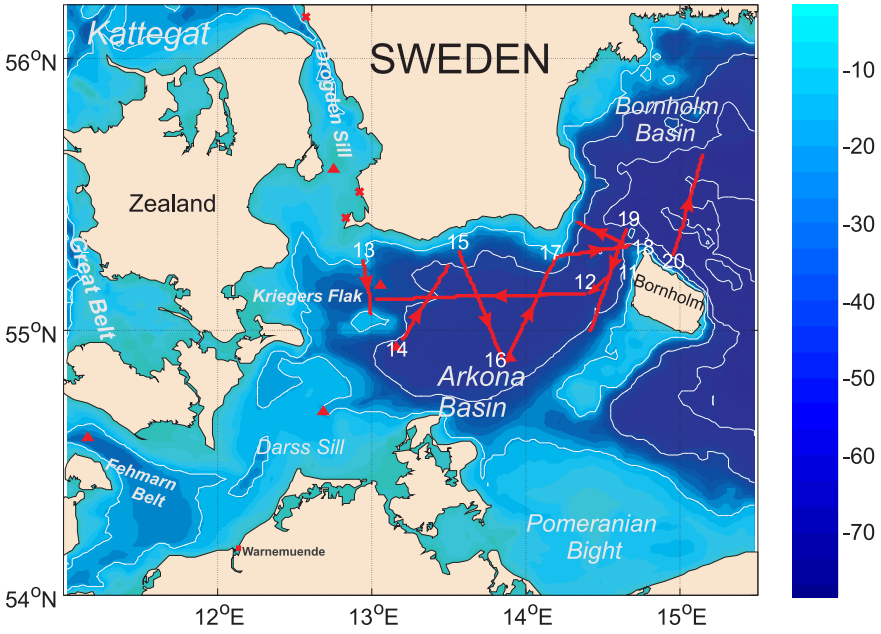

Figure 3.6: Map of the Arkona Basin with the second part of transects from R/V Oceania (red lines). Symbol notation as in the fig. 3.5.

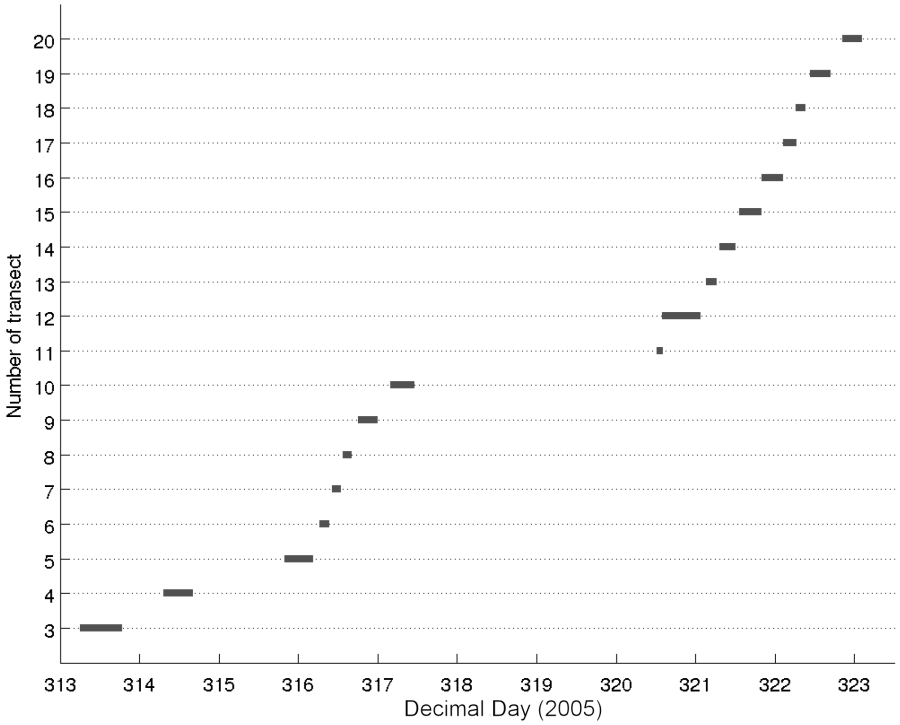

Figure 3.7: Plot of the duration of the each transect vs. the transect number. The time gap between the transects number 10th and 11th can be seen. The date is expressed in days starting from the beginning of the year 2005.

Chapter 4

Observational data analysis

4.1 Cumulated volume flux vs. wind pattern

Medium-intensity inflows through the Sound (section 2.2) are generally well-mixed over the shallowest sill regions. The pressure gradient caused by surface elevation differences is balanced by the bottom friction and forms a drag. The surface elevation differences are caused by regional wind patterns (Gustafsson and Andersson, 2001). Westerly winds tend to raise Kattegat Sea level and to lower Arkona Sea level, thereby causing inflow of fresh, saline water whereas easterly winds tend to cause outflow (Lass and Matthäus, 1994).

Medium-intensity inflow can be reconstructed on the basis of observed sea level data in Viken and Skanoer measuring stations. Several studies (Jakobsen et al., 1997; Green and Stigebrandt, 2002) show that the flow through the Sound is well described by a quadratic friction law of a type:

$$\eta_N - \eta_S = KQ|Q| \tag{4.1}$$

where $\eta_N - \eta_S$ is the total sea level difference from south to north, which is taken to be equal to the water level difference between stations at Skanoer and Viken, Q is the southward volume flux and K is the specific resistance. Jakobsen et al. (1997) estimated the volume fluxes from ADCP (Acoustic Doppler Current Profiler) measurements from the Drogden and Flinten Channels, and used the sea level data from Roedvig and Skanoer to the south and Hornbaek and Viken to the north. They had estimate the parameter $K = 2.26 \times 10^{-10}$ s^2/m^{-5}. This value is used in the present work to calculate the volume fluxes from observed sea level differences between Skanoer and Viken for October and November 2005 (fig. 4.1).

Accumulated volume flux suggest that a significant sequence of inflows started at the end of October and lasted until middle of November. Unfortunately no

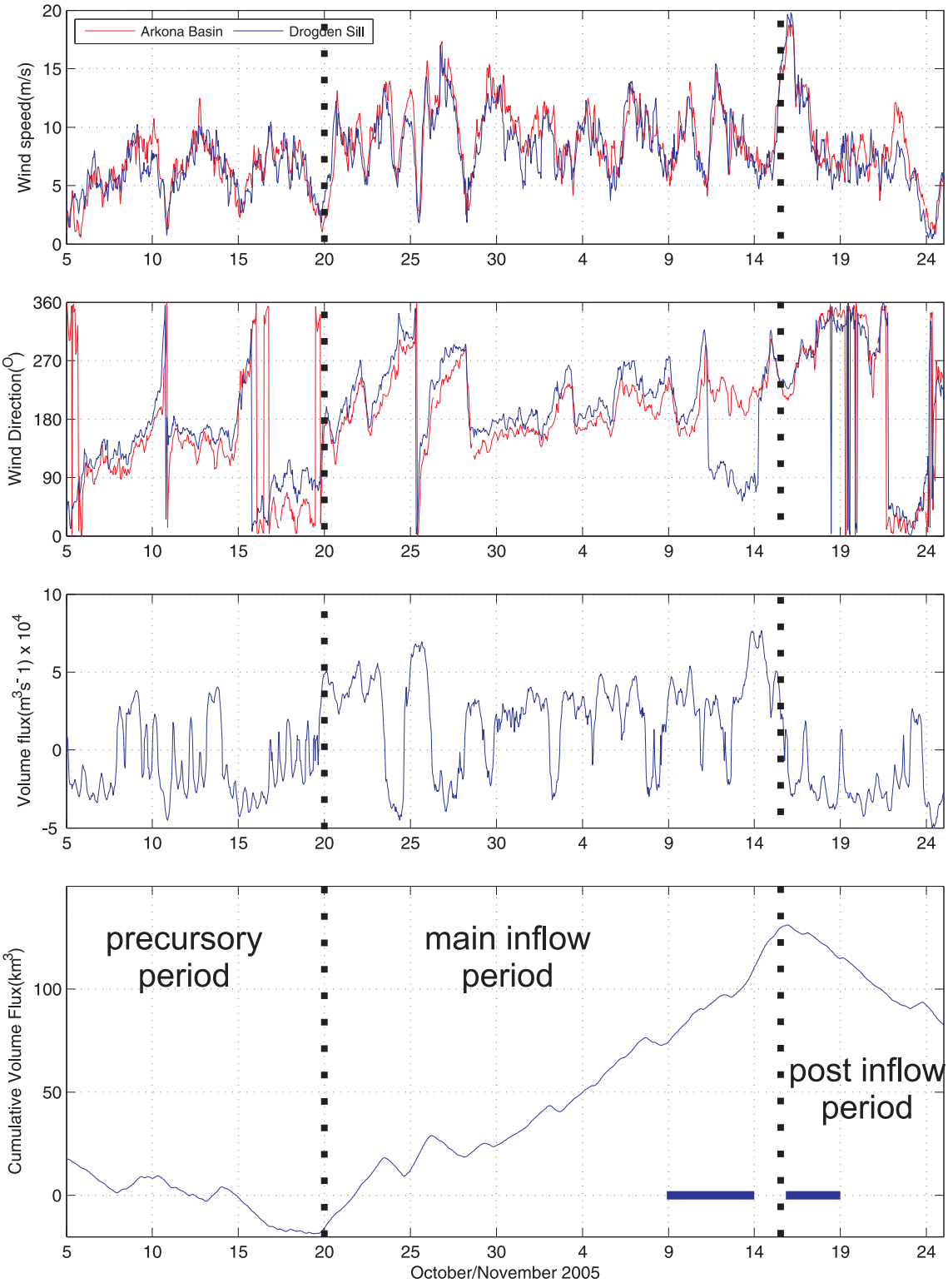

Figure 4.1: In two upper panels time series of the wind speed and the wind direction from the Darss Sill Station (blue) and the Arkona Sea Station (red) during October and November 2005 are shown. On the lower panels southward volume fluxes calculated by the means of equation 4.1 from observed sea levels at Viken and Skanoer and accumulated volume flux obtained by integrating volume flux over time are shown. Horizontal bars at the bottom of the panel indicate two phases of the cruise. On the accumulated volume flux plot division into inflow periods is marked (see section 2.2).

ADCP data are available for this period at the Drogden Sill station to compare with calculated flux. The wind data at the Arkona Sea station and Darss Sill station (fig. 4.1) are strongly correlated during the period of interest, except from 10th to 13th of November. During the period proceeding the inflow (ie. from 5th to 20th of October) main easterly wind with velocity of up to 10 m/s was observed. This wind pattern caused outflow from the Baltic Sea to the Atlantic Ocean and lowered the Baltic Sea level to its temporal minimum. As expected, long period of westerly winds coming directly after period of easterly winds caused inflow. For the period starting from 20th of October until 16th of November winds at both station turned into southerly or westerly with a small period of northerly winds on 23th and 24th of October. The wind speed in the observed period varies from 5 to 15 m/s most of the time. The significant westerly wind peak is observed between 14th and 16th of November causing significant southward volume flux increase. During the period of prevailing westerly and southerly winds small periods of winds from east or south can be observed. This wind causes small disturbances of the inflow and as well backing of the high salinity plume, what is further discussed in the next section. After 16th of November northerly winds prevail, which with the high Baltic Sea level causes an outflow.

Inflow processes within the Baltic Sea can be divided into three significant periods: the precursory period, the main inflow and the post period (Fisher and Matthäus, 1996). On the fig. 4.1 those division is shown for the observed inflow. The precursory period of the inflow lasts from 20th of October up to 2nd of November. The main inflow period lasts from 3rd to 16th of November, when the Baltic Sea level reaches its maximum. With the start of outflow post period begins.

4.2 Propagation of the inflow through the Sound.

On the fig. 4.2 a delay between the inflow start and the salinity increase inside of the Sound can be seen. The flux has been calculated from the Sea Surface Height stations, as in the sect. 4.1, the salinity is observed at the Drogden Sill buoy. The positive flux is equal to the inflow into the Baltic Proper and marked with the red color. The negative flux is the outflow and is marked with the blue color. With the black arrows a typical delay between the inflow start and the salinity increase is marked. This typical delay is due to the fact that water masses in the Kattegat consist of low saline surface waters from the Baltic Proper and the highly saline sub-surface water from the North Sea. When the inflow starts, first the low saline surface water (that originates from the Baltic Proper) enters through the Sound and afterwards the highly saline water (that originates from North Sea). Therefore if the inflow lasts not long enough (e.g. 12 hours) it will not be observed as a salinity

increase inside of the Drogden Sill.

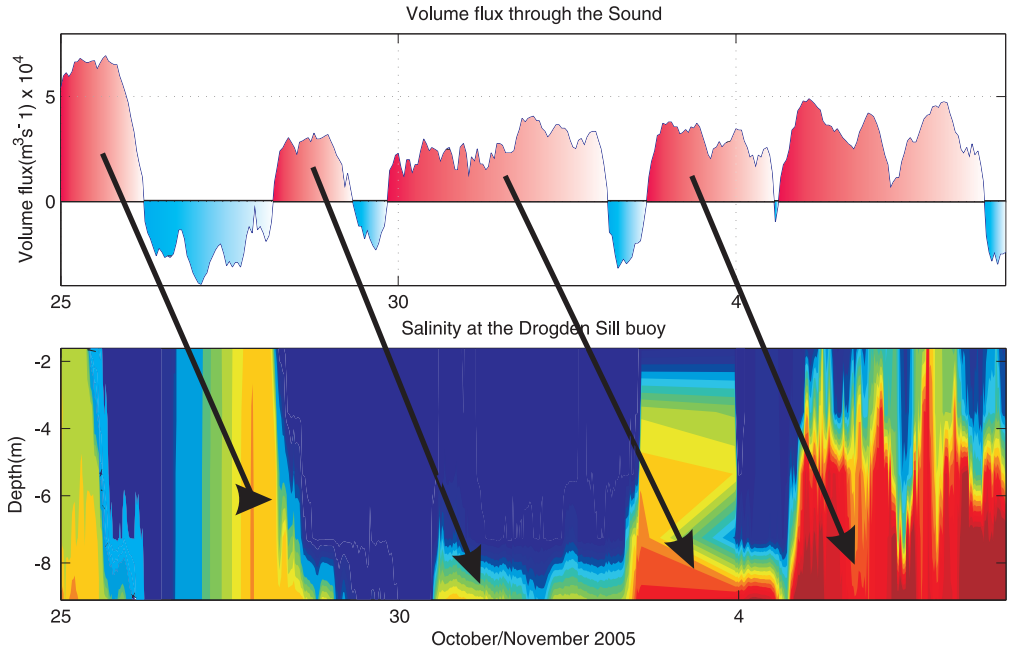

Figure 4.2: Flux through the Sound (upper panel) compared with the salinity measured at the Drogden Sill (lower panel). A typical delay of a few days can be seen between the inflow start and the salinity increase.

To further analyze the inflow the data from the Drogden Sill measuring station were investigated just before and during the inflow. On the fig. 4.3 timeseries of the salinity and the temperature inside the sill during the inflow are shown, as well as the accumulated volume flux, which was already seen on fig. 4.1. The inflow started at the end of October 2005, which can be seen at the cumulative volume flux plot. Unfortunately, the ADCP data for the Drogden Sill were not available for this time period.

Temperature and salinity data for Drogden Sill are available from 25th of October, 5 days after start of the inflow. It can be assumed from the volume flux plot (fig. 4.1) that no major plumes were observed just before this date. Before the inflow the salinity of the water was about 8 PSU for the whole water column which is a typical value for the Baltic Sea surface waters. Two smaller plumes with the salinities of up to 21 PSU are observed about 25th and 27-28th of October. Afterwards no major salinity increase is observed until 3rd of November. From 3rd of November

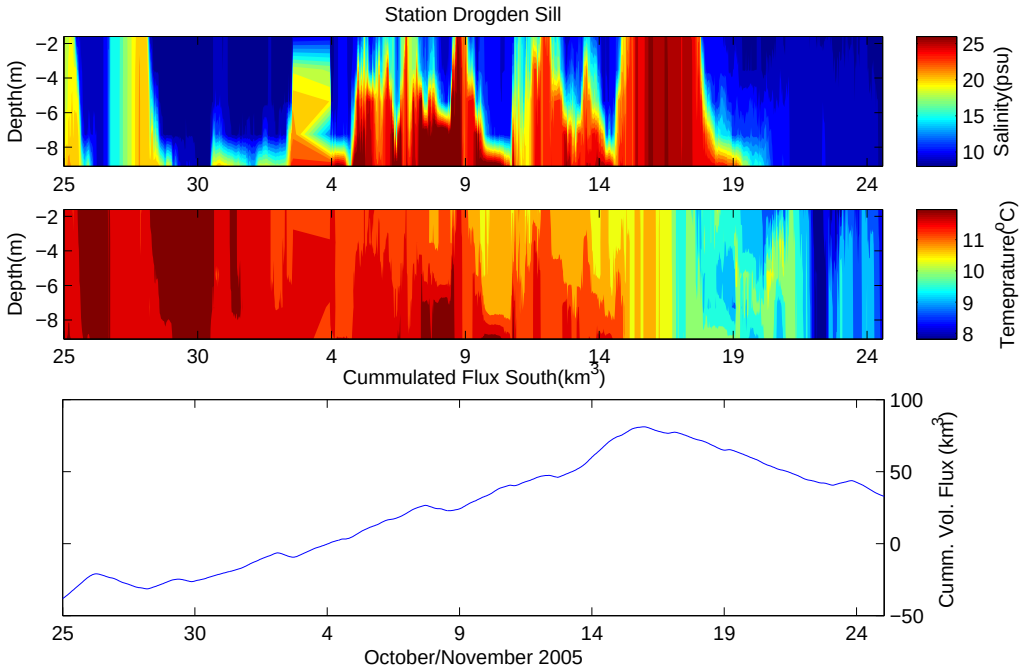

Figure 4.3: Time series of the temperature and salinity for Drogden Sill observed from 25 of October to 25th of November 2005 (two upper panels.) Salinity plot has strange values between 3rd and 4th of November, probably due to a measurement error or equipment malfunction. The lowermost plot shows the accumulated volume flux through the Sound.

the bottom salinity increase up to 23 PSU. Starting from 5th to 10th of November the saline plume is observed in almost whole water column, excluding the surface layer, with salinity up to 26 PSU. Next about one day drop of the salinity to 10 PSU is observed. From 12th to 15th of November increase of water salinity in the bottom layer is observed, and later increase in the whole water column form 15th to 18th of October (up to 26 PSU). After 19th of November salinity drops to 8 PSU. The along bottom salinity stays more saline (over 20 PSU) 2 days more. The reason for this can be that the changing wind pattern over the sill affects first the surface water, the bottom water due to Drogden Sill bathymetry is still inflowing due to gravity forces. The water temperature is fairly mixed through the whole water column and drops from 12 degrees at the end of October through 10 degrees in the middle of November to 8 degrees at the end of November. Drop of temperature of about 3 degrees in just 3 days after 14th of November is caused by the fact that the inflow in this period propagates through the whole water column and through the mixing with the atmosphere temperature is lowered. Due to this rapid temperature decrease, temperature can be used as a tracer of the inflow propagation, alongside

the salinity.

When the inflow takes place, generally most of the saline water from the Kattegat propagates along the bottom. When the inflow reverse the water salinity outflowing through the Sound is about 8 PSU. Heavier, highly saline water is trapped over the Sound and cannot move back because of the low depth of the Sound. The most of the saline water with salinity over 10 PSU, which passed over the sill during the inflow, continues to flow into the Baltic Proper along the bottom.

The major inflow event can be identified by two empirical criteria discussed in the section 2.2: bottom salinity S_b higher the 17 PSU criterion and stratification G criterion (lower the 0.20 for at least 5 consecutive days), both observed in the Darss Sill area. It is clear that described inflow doesn't fulfil these criteria (compare fig. 4.7). This inflow is classified as the medium-intensity inflow.

4.3 Moorings data.

To analyze the inflow propagation in the Arkona Sea the CTD and Advanced Doppler Current Profiler (ADCP) data from several moorings were analyzed, as well as observational data taken during the cruise of R/V Oceania in November 2005. In this work mainly the inflow through the Sound is investigated, as we want to understand better how it is propagating and what mechanisms are driving it. The main pathways of the inflows are shown on the fig. 2.4.

The inflow through the Drogden Sill was discussed in section 2.2. To describe the inflow propagation in the Arkona Sea and further, the CTD data from the stationary moorings were analyzed. Salinity and temperature data for the period of interest were available from buoys at the Arkona Basin (measurements at 5 depths) and Darss Sill (measurements at 6 depths). Moreover ADCP data were available for the period of interest from station at Darss Sill. Unfortunately from the buoys at Kriegers Flak North and Kriegers Flak South data are available only for part of the period of interest. From Kriegers Flak North ADCP and CTD data (for 6 depths) are available after 18th of November, so posterior part of the inflow, and for the station at Kriegers Flak South CTD data at 4 depths for the period before 21st of November are available (first part of the inflow).

As discussed in the section 4.1 the beginning of the inflow was observed about 25th of October 2005 and was followed by the bigger, high salinity plume observed inside the Drogden Sill after about 11 days. The plume with the salinity reaching

26 PSU was observed at the Drogden Sill for about 14 days (fig. 4.3). The plume passing the Sound can be observed first at the station Kriegers Flak North (KFN), later at the station Kriegers Flak South (KFS) and then at the Arkona Basin (AB) station. Entrainment processes can make the plume more extended but less saline (see section 2.3).

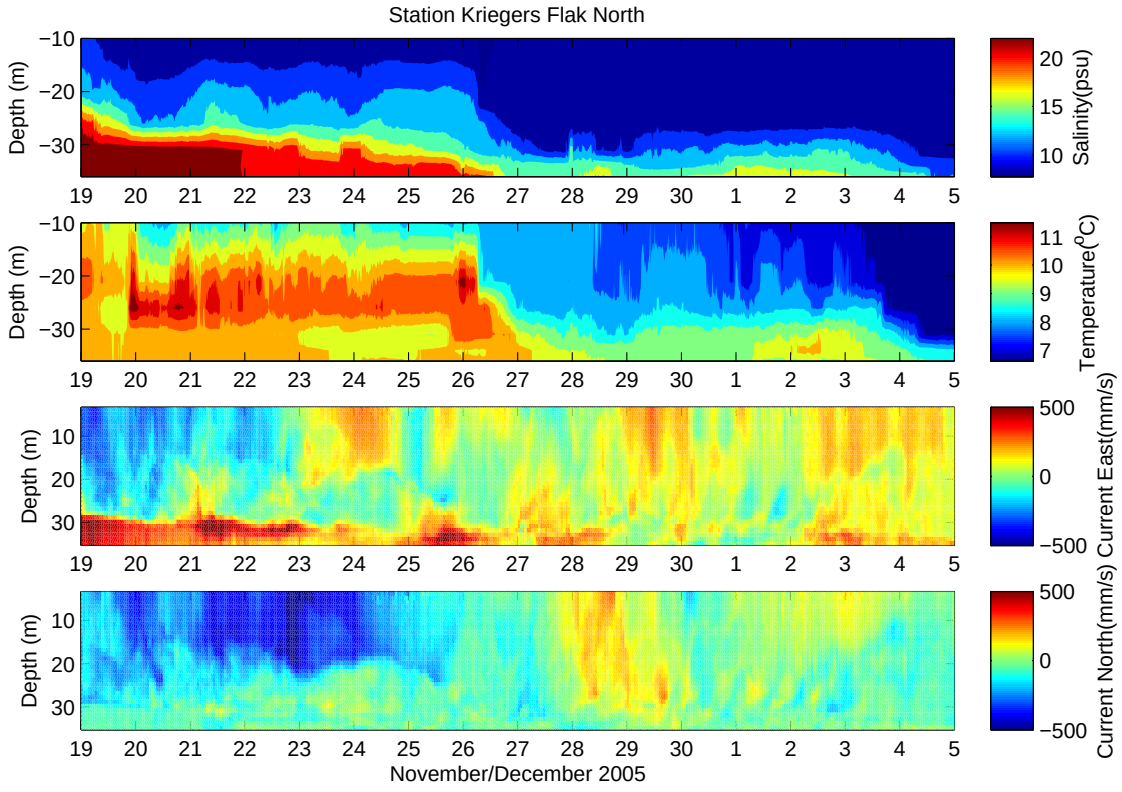

Figure 4.4: CTD (two upper panels) and ADCP (two lower panels) time series from the Kriegers Flak North buoy for the period of November and December 2005.

At the Kriegers Flak North station (fig. 4.4) data for the second part of the inflow are available (starting from 19th of November). Comparing with the data from the Drogden Sill and the data received from the model (see section 5), it can be assumed that maximum salinity of the inflow passed nearby the Kriegers Flak North Station a few days before 19th of November. From the 19th to 22nd of November salinity of the bottom layer is over 22 PSU. Later it drops with time and after 26th of November saline plume is no longer visible at this buoy. The temperature for the period from 19th to 26th of November is unstably stratified, with the surface

temperature of 8 degrees, the bottom temperature of 10 degrees and temperature in between reaching 13 degrees in some periods. The incoming, colder and more dense water is pushing the old, warmer, but lighter water up. The ADCP data show strong eastern current at the bottom layer (about 10 meters) for the period of the inflow.

It is hard to predict how long the high salinity plume is observed on the KFN station due to lack of data, but it can be assumed, from analysis of salinity and water temperature, that the high salinity (20-22 PSU) bottom layer observed at KFN from 19th to 22nd of November originates from the high salinity (24-26 PSU) plume observed at the Drogden Sill from about 16th till 19th of November. The earlier part of the plume at Drogden Sill has lower salinity, which due to entrainment was probably further lowered while progressing into the Arkona Basin. It is hard to say about the inflow propagation from temperature data as they vary to much for the KFN buoy. Besides lowering the salinity the entrainment (see section 2.3) increases the volume flux of the current. The delay of the plume between those two station can be estimated to about 3-4 days, which is in agreement with statistical expectations (see also sect. 4.6 on page 54).

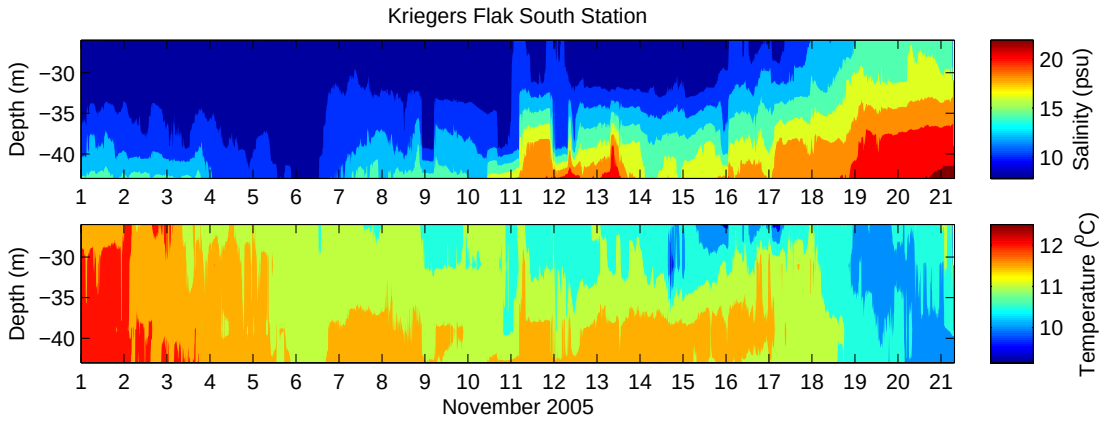

Figure 4.5: CTD time series from the Kriegers Flak South buoy for November 2005.

At Kriegers Flak South (fig. 4.5) temperature and salinity data are available for the first part of the inflow, from 1st to 21st of November. Two separated plumes are visible here: a smaller one from 11th to 14th of November, afterwards the bottom salinity drops for a few days and then a bigger plume is observed from 16th of November. Temperature at the beginning of November reaches 13 degrees,

dropping to ca. 10 degrees around 20th of November. It seems that the plume of the saline water passing south of the Kriegers Flak is thiner and less saline that the plume coming north of the Kriegers Flak, which is in good agreement with calculated volume fluxes (sect. 4.9.2). Moreover it is also delayed by a few days. Specific considerations, however, cannot be done due to lack of data.

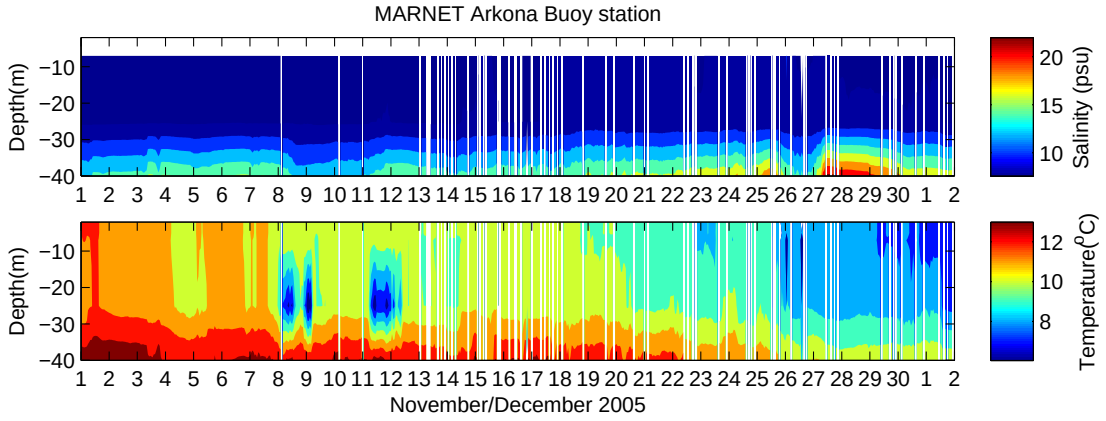

Figure 4.6: CTD time series from the Arkona Basin buoy for November and beginning of December 2005.

Salinity and temperature time series from the Arkona Basin buoy are available for the period from 1st of November until 2nd of December (fig. 4.6). From 22nd to 26th of November a plume with salinity of up to 18 PSU is observed, later salinity drops and a second plume with salinity of up to 22 PSU is observed from 27th to 30th of November. No significant temperature changes are visible for the inflowing water, which is caused by the fact that when the inflow arrive at the Arkona Basin it has the same temperature (10-11 degrees) as the water there. The Arkona Basin buoy is not very adequate where it comes to measuring of the bottom layer salinity. It comes out from the transects taken by the R/V Oceania that the bottom layer salinity is bigger then the one observed at the AB buoy (e.g. the end of transect 3 and beginning of transect 4 were taken nearby the place where AB is placed (see fig. 4.10)). It is due to the fact that the deepest sensors are attached about 5 meters over the seabed, and cannot measure the plume thinner then 5 meters propagating underneath it.

The inflow observed at the Darss Sill station is delayed to the one passing through the Sound by a couple of days according to statistical observations (see sect. 4.6 on the page 54). The salinity, temperature and ADCP data at the Darss Sill buoy are

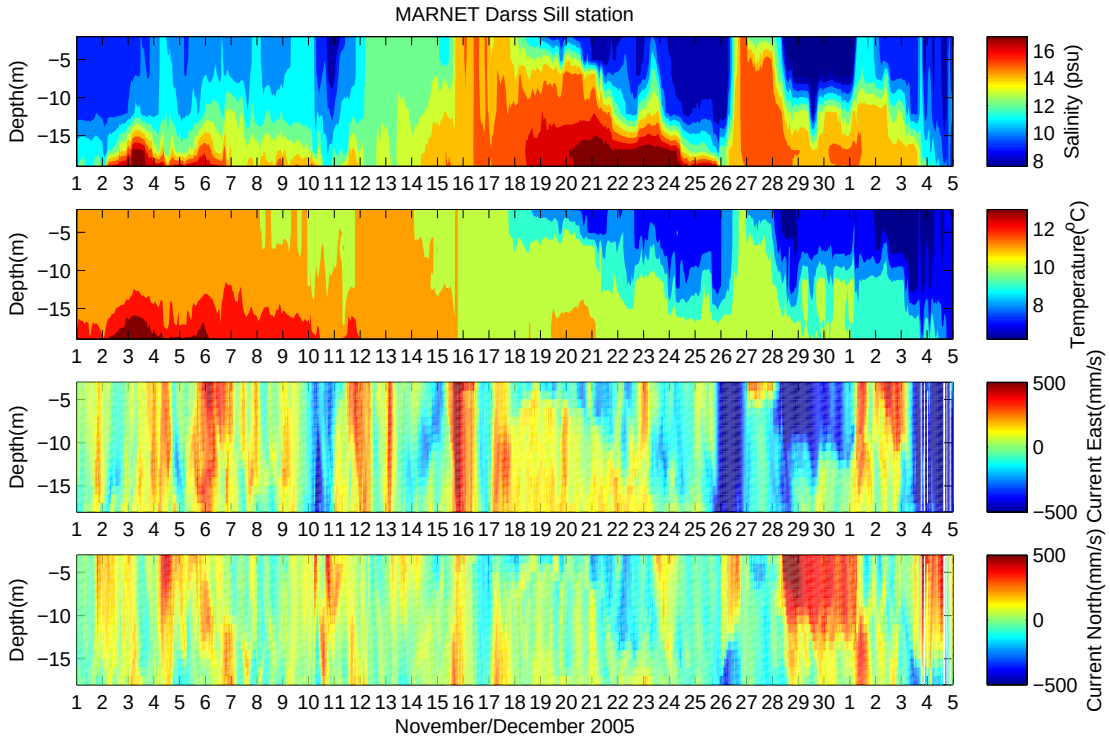

Figure 4.7: CTD and ADCP time series from the Darss Sill buoy for November and beginning of December 2005.

available for the period from the beginning of October 2005 to 5th of December 2005 (see fig. 4.7). The depth underneath the buoy is about 20 meters. A plume of water with salinity up to 16 PSU is visible from 2nd until 7th of November. Then the bottom salinity drops and after 15th of November it raises again reaching 17 PSU from 18th to 26th of November. After 26th there is a one day gap and again an increase of salinity up to 15 PSU lasting for a few days, until 4th of December. The temperature of the plume visible until 12th of the November is about 12 to 13 degrees. The second plume, visible until 26th of November has temperature of 10 to 11 degrees. The last observed plume visible in the end of November has temperature of 10 degrees dropping later to 9 degrees. The ADCP data for the two plumes visible until 26th of November shows mainly northeast currents with velocities up to 50 cm/s. The last plume, observed after 24th of November shows south-west velocity, suggesting that this plume has came from inside of the AB and not from the inflow.

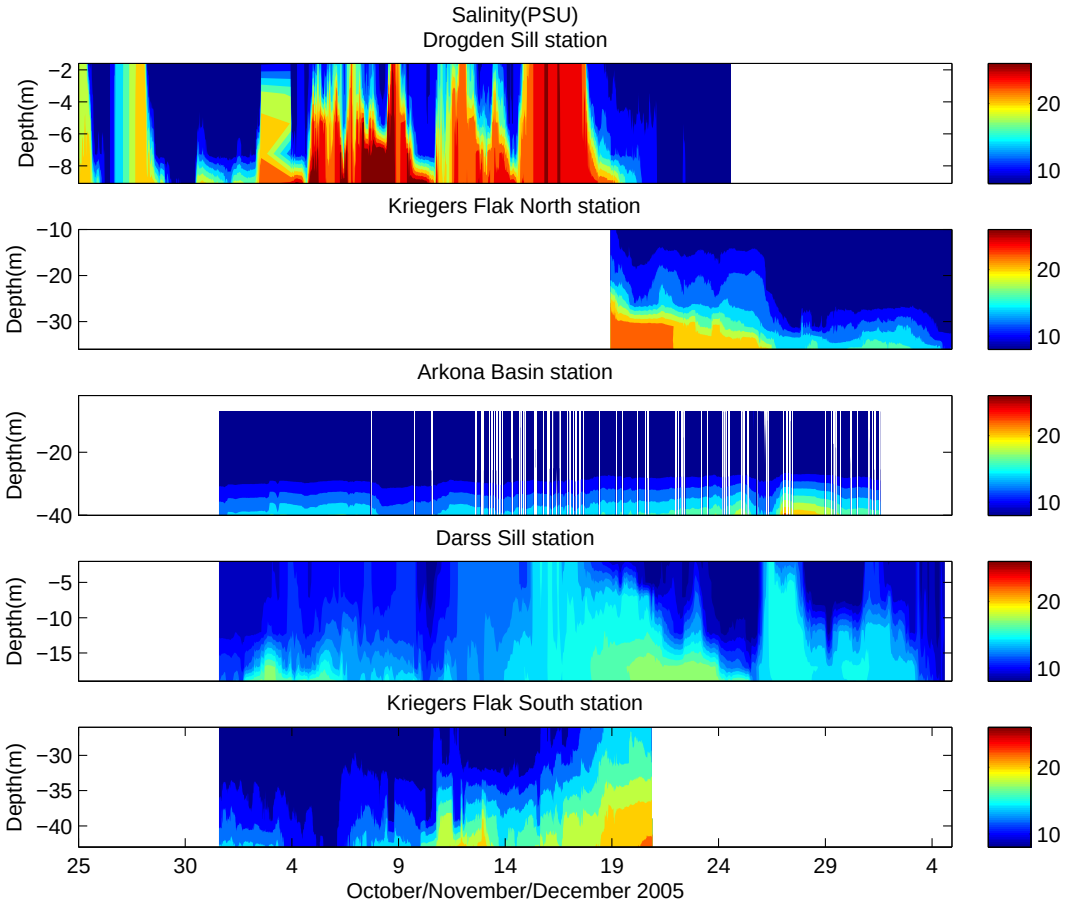

Figure 4.8: Salinity time series for a period from 25th of October to 5th of November for every analyzed buoy. The periods with no data available are filled with the white space.

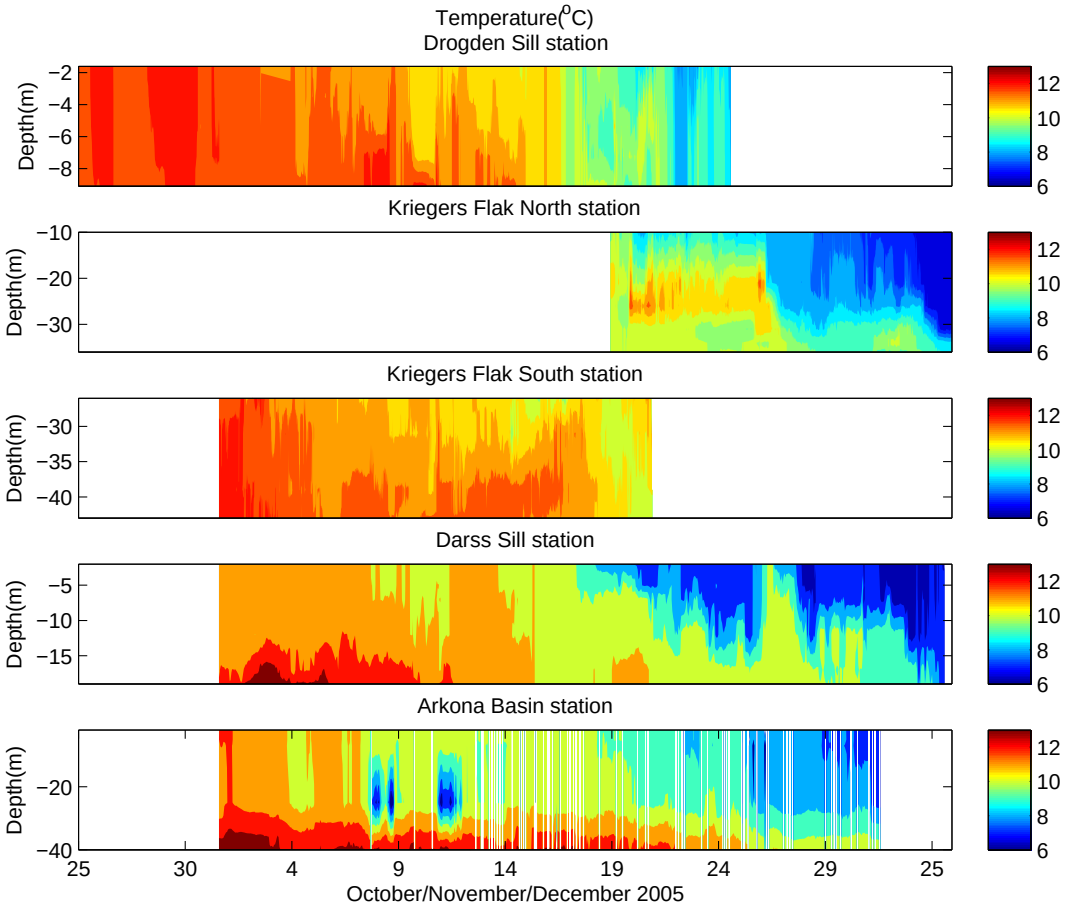

Figure 4.9: Temperature time series for a period from 25th of October to 5th of November for every analyzed buoy. The periods with no data available are filled with the white space.

It is easier to analyze the moorings data when salinity time series and temperature time series for every buoy are displayed on one plot. On the fig. 4.8 salinity time series for five observed buoys for the period from 25th of October 2005 until 5th of December 2005 are shown. On the fig. 4.9 temperature time series are available for the same buoys in the same time period.

At the Drogden Sill inflow reaches salinity of up to 26 PSU from 1st to 20th of April. Depending on the changing wind pattern the salinity varies in time. At KFN station due to lack of data only the last part of the inflow can be observed. The observed part of the inflow (until 26th of November) has salinity of up to 22 PSU with temperatures of about 10 degrees. Judging from the temperature and salinity data, for the inflow it takes no more then a few days to move from the Drogden Sill to the KFN area. More detailed estimation cannot be done due to the lack of data from KFN buoy.

At the KFS buoy two bottom plumes can be observed (starting from 10th of November), with salinities of the second, bigger one up to 22 PSU and temperatures of 11 degrees dropping in time to 10 degrees. The second part of the second plume can not be observed due to lack of data. The plumes observed from the KFS buoy should be the ones propagating through the Sound mainly (see fig. 5.8 on page 81). The observed part of the plume is significantly smaller than the one observed at KFN and shifted in time as well. The second, bigger plume (observed here from about 16th of November) can be the plume observed at the Drogden Sill after 5th of November. If this considerations are correct then the inflow observed at the KFS station can be delayed by about 6 days from the one observed at the Drogden.

At AB buoy saline plume can be seen from 22nd to 29th of November, with salinity of up to 20 PSU and water temperature of about 10 degrees. Estimating from temperature data it could be the part of the plume visible at the Drogden Sill from 15th to 19th of November. This part of the plume was the one which propagated through the whole water column of the Drogden Sill, so theoretically the part which should propagate the furthest. Due to the entrainment the salinity dropped and plume has extended, what is also visible from the data. The plume at the AB buoy has probably about 11 days of delay to the one observed at the Drogden Sill buoy.

The plume visible at the Darss Sill can be the one propagating through the Belt only or be a product of both plumes: the one propagating through the Belt and the one propagating through the Sound. It can be predicted from the GETM model (sect. 5) that the observed plume visible at the Darss Sill is the one propagating

mainly through the Belt. Even if the Darss Sill plumes are not directly correlated with the plumes at Drogden Sill, because of the same wind patterns over whole transition area they are indirectly correlated. It can be assumed that a small plume of salinity of 18 PSU and temperature of 13 degrees observed at Darss Sill station from 2nd to 7th of November are two low salinity pulses seen at the Drogden Sill at the end of October. The rise of salinity observed at the bottom of the Darss Sill from 15th of November to 3rd of December can be in correlation with the inflow visible at the Drogden Sill from 4th to 19th of November. It can be said from the observation that the plume propagating through the Belt was delayed to the one propagating through the Sound by about 7 to 10 days.

4.4 R/V Oceania data.

In the following subsection some of the most important transect for investigating inflow propagation will be discussed. This cruise was taken between 10th and 19th of November 2005 and measurements were divided into 18 transects numbered from 3 to 20 (see sect. 3.2).

From the view of the inflow propagation transects 3 to 8 and 11-12 seem to be most interesting. Transects 3 to 8 were taken from 10th to 13th of November. Inflow of bottom salinity up to 17 PSU can be observed during this period. Transects 11 and 12 were on 17th of November, when bottom salinities reached 25 PSU. Transects were taken in the Arkona Basin (4th and 12th) and the Bornholm Channel (the rest of them).

On the fig. 4.10 transects 3 and 4 can be seen. Transect 3 was made on 10th of November 2005 and transect 4 one day later. There is about a half day gap between them. On transect 3 inflow with salinity of about 17 PSU is observed for the eastern, shallower part of the transect. In the first, deeper part (west of the ridge), the bottom salinity reaches typical Baltic Sea value for deep waters. For transect 4 inflow with salinity of about 17 PSU is observed for the whole transect's length. In temperature data for transect 13 a thermocline at about 40 meters is visible. Inflow observed for transect 3 has a temperature of about 13 degrees. Temperature for the most of transect 4 is fairly mixed with a value of about 11 degrees. For the eastern part of transect 4 and the western part of transect 3 the fresh, denser water pushes the old, less dense water up. The observed part of the inflow could have passed through the Sound after 4th of November. Further observations show that salinity in this area of the Arkona Basin will raise.

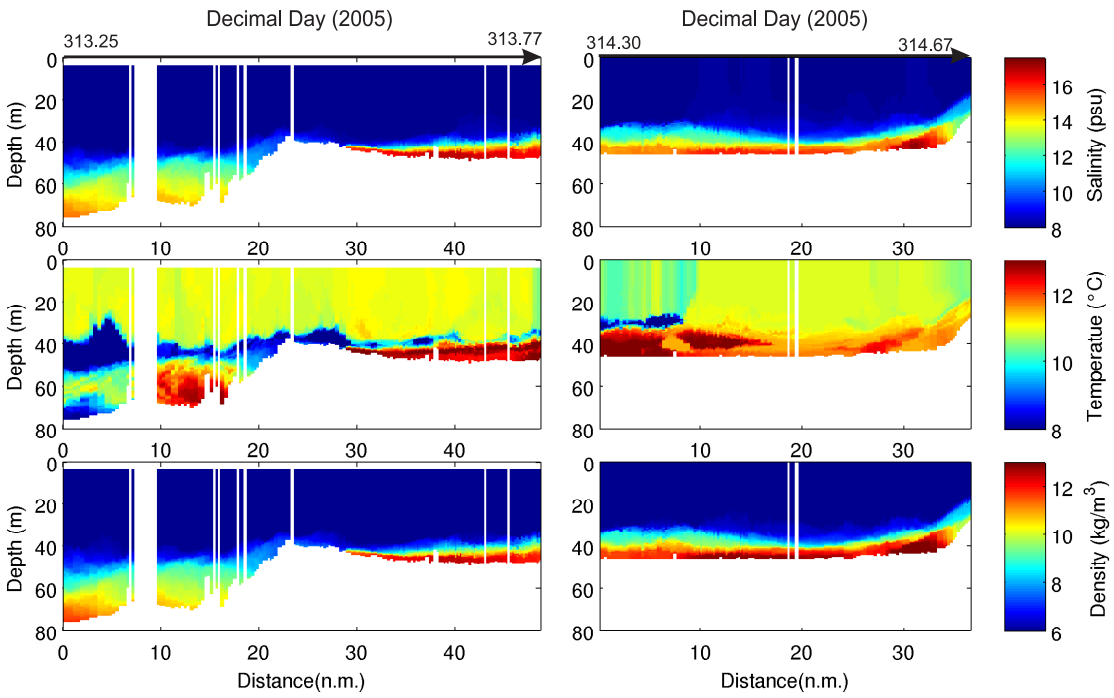

Figure 4.10: CTD data for transects 3 and 4 taken in the Arkona Basin and Bornholm Channel (see the map on fig. 3.5 on the page 29 for the location) on 10th and 11th of November 2005. Time gap between two transects occur. The arrows above the salinity plots show the direction in which the measurements were taken with the numbers being day of the year 2005 for starting and ending transect. White fields on the plots show the area below the seabed or corrupted data.

The inflow observed for these two transects has a slightly higher temperature (not more then 1 degree) and is less saline (about 8-9 PSU) then the inflow observed in the Drogden Sill from 4th of November. Moreover prediction made by Rennau and Burchard (2009) suggest that inflowing water needs 8 to 14 days to travel from the Drogden Sill to the Bornholm Channel. Conclusion can be made that what we see may be the inflow visible in the Drogden Sill from about 4th of November mixed with the deep water of the Arkona Basin which has temperature of about 13 degrees and can have a similar salinity like the inflow because of the waters from the earlier inflows (see sect. 2.2.5). The Arkona Basin buoy, which is placed on the intersection of the transects doesn't show raise of salinity in this days. As was discussed in sect. 4.3 this is due to specifications of this station, which has the lowest salinity sensor 5 meters above the seabed.

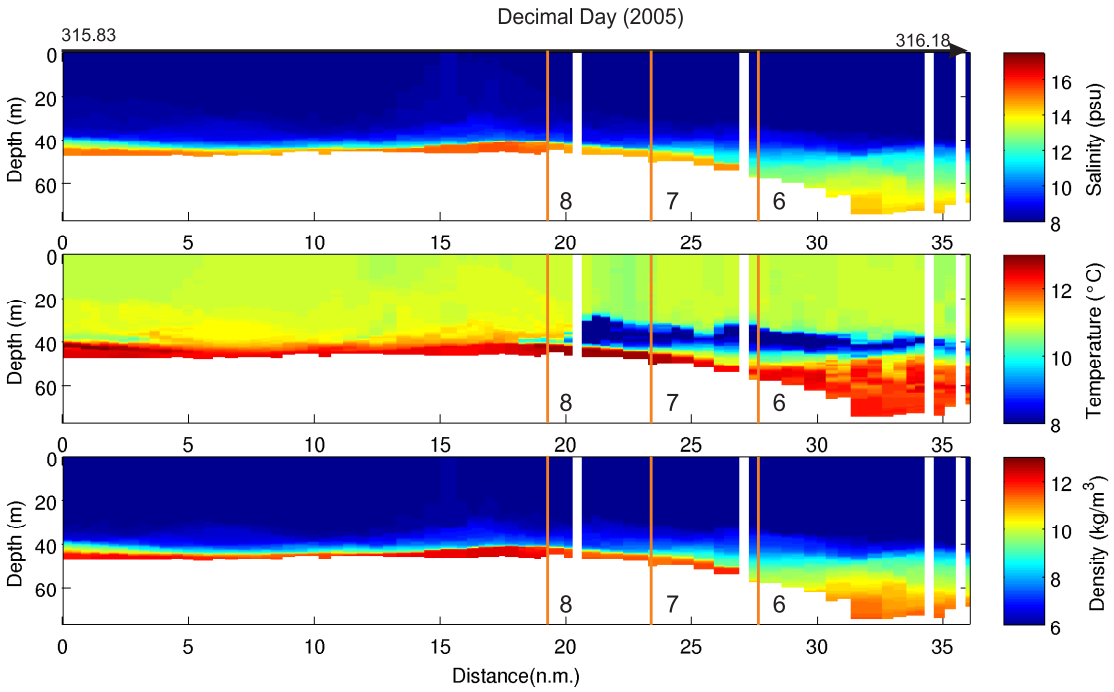

Figure 4.11: CTD data for transect 5 taken in the Bornholm Channel (see the map on fig. 3.5 on the page 29 for the location) on 12th of November 2005. With the orange lines crossings with perpendicular transects 6, 7 and 8 are marked. In the salinity, density and temperature plots white areas are the areas underneath the seabed or corrupted data.

Transect 5 visible on fig. 4.11 taken on the late 12th/early 13th of November shows a plume with a salinity of 17 PSU in the flat part of the seabed under the transect and 14 PSU in the trench at the eastern end of the transect. What is visible, is probably the first part of the plume, mixed with the old bottom waters, reaching the Bornholm Channel. The plume temperature is about 13 degrees. Cold water seen above the bottom layer is the old water which has been pushed up from the bottom by the incoming, heavier plume. The plume is visible until the middle part of the Bornholm Channel with salinities of up to 17 PSU, so it hasn't propagated since it was observed on 10th of November on transect 3.

Transects 6, 7 and 8 were made on 13th of November in the Bornholm Channel, transect 8 is the one closest to the Arkona Basin, whereas transect 6 is the one furthest. Underneath every one of these transects two trenches separated by the ridge are visible (for transect 8th it is not so easy to distinguish the trenches, moreover only part of one of them is visible). In the trenches water with salinity up to 17 PSU and temperature up to 13 degrees is visible. That is probably the inflow from Drogden Sill mixed with the old, warm bottom waters which has propagated

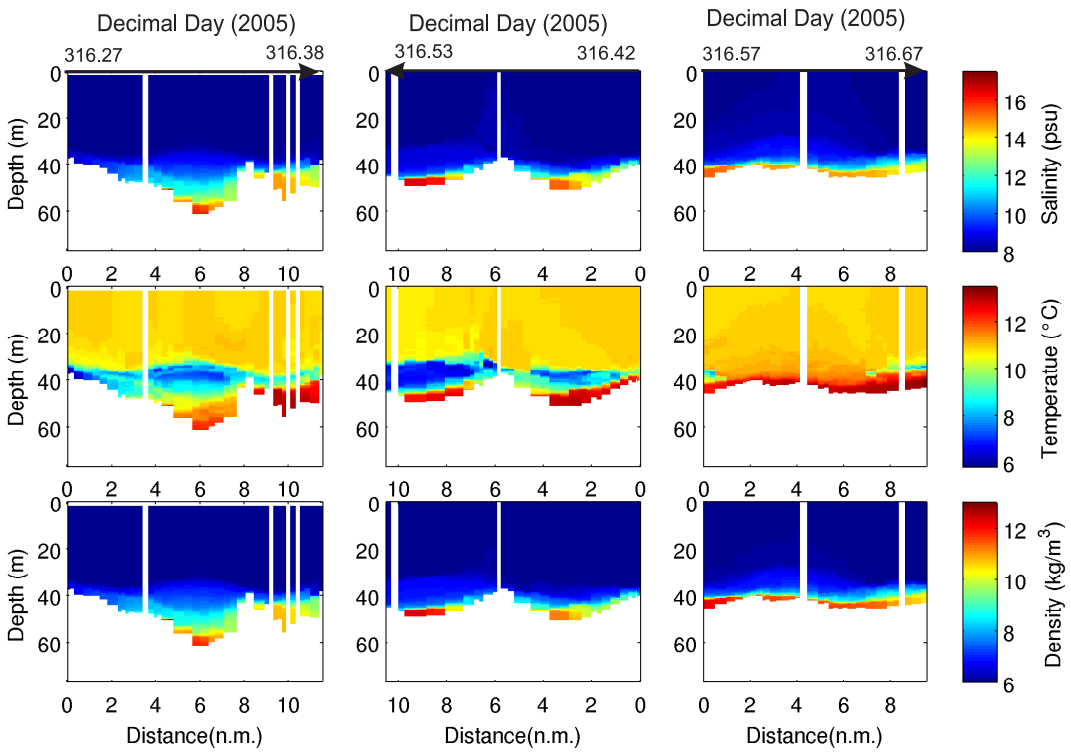

Figure 4.12: CTD data for the transects 6, 7 and 8 taken in the Bornholm Channel (see the map on fig. 3.5 on the page 29 for the location) on 13th of November. With the orange lines crossings with perpendicular transects 5 and 9 are marked. Transect 7 is shown in the opposite direction to the other transects, so they all face in the same direction on this figure.

further east, then according to observations taken one day before. The inflow pushes up the old, colder (about 8 degrees) water up, what is visible for transects 6 and 7. From the density plots the lateral distortion of the interfacial density structure can be visible as a pinching of the interface to the left of the down-channel flow, and a spreading of isopycnals to the right. It is caused by the the transverse transport inside the interface described in the sect. 2.4. The effect of the interfacial jet is better shown for the transect 13 taken in north of the Kriegers Flak on the fig. 4.23 on the page 66.

Transects 11 and 12 seen on the fig. 4.13 were taken a few days later then the transects discussed earlier, on 17th and 18th of November 2005. The inflow's salinity in the eastern end of the 11th transect is about 15 PSU raising gradually to 24 PSU at the western end of 12th transect. The plume thickness in the transect 11 and in

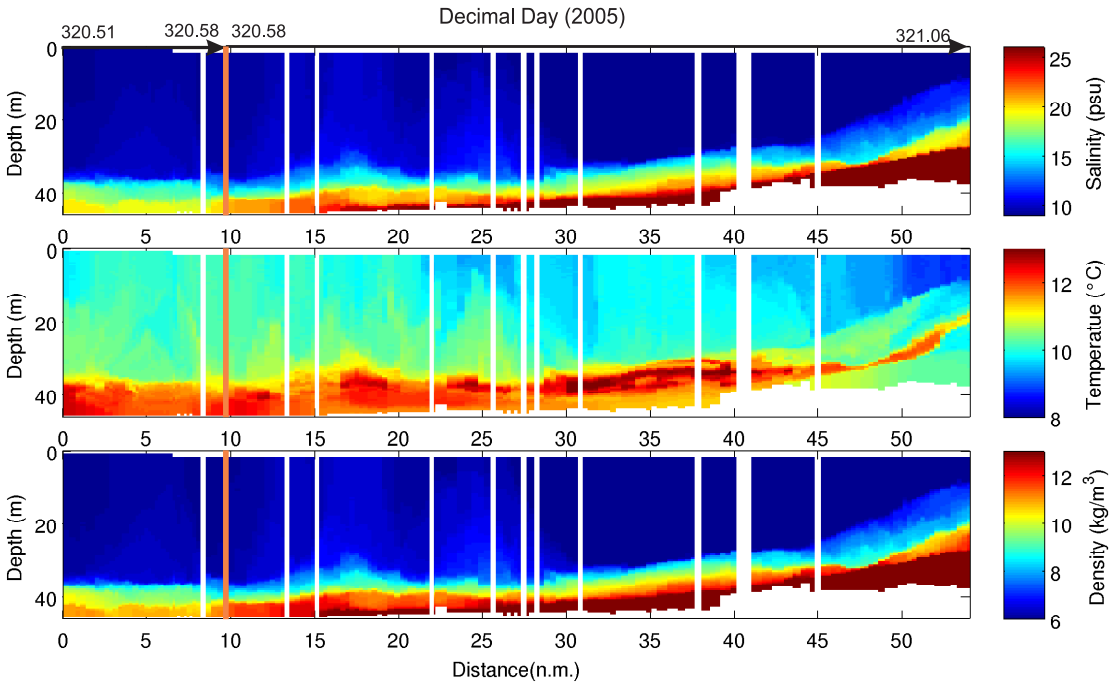

Figure 4.13: CTD data for transects 11 and 12 taken on 17th of November in the Arkona Basin (see the map on fig. 3.5 on the page 29 for the location). Transects were taken next to each other, without a time gap, but with change of direction. The orange line on the plot and the green dot on the map show the the end of the first and the beginning of the second transect. Part of the seabed is at the same level as the x-axis on the CTD plots.

the eastern part of transect 12 is about 10 meters, raising to 20 meters in the western part of transect 12. The bottom temperature is about 13 degrees everywhere but in the western end of transect 12, where the plume increases its thickness. What is interesting here, is the bigger plume of cold (ca. 10-11 degrees), saline water (over 24 PSU) which is observed in the western end of transect 12 (middle part of the Arkona Basin). It pushes up the water which arrived earlier, because it propagates faster due to a bigger salinity gradient with the ambient water and due to lower bottom friction (bigger height). That part of the plume was visible at Drogden Sill after 14th of November. It is significantly colder due to the incoming water's mixing with atmosphere in the Drogden Sill area - the inflow in this period propagates through the whole water column. Bottom ADCP data is missing like in the most of all the other transects, so nothing about the direction of the plume propagation can be told directly. Although from the salinity plot it is easy to say that the more dense water seen on the western end of the transect 12 is clearly faster that the part of the plume with low salinity that procedes it, and propagates in the eastern direction.

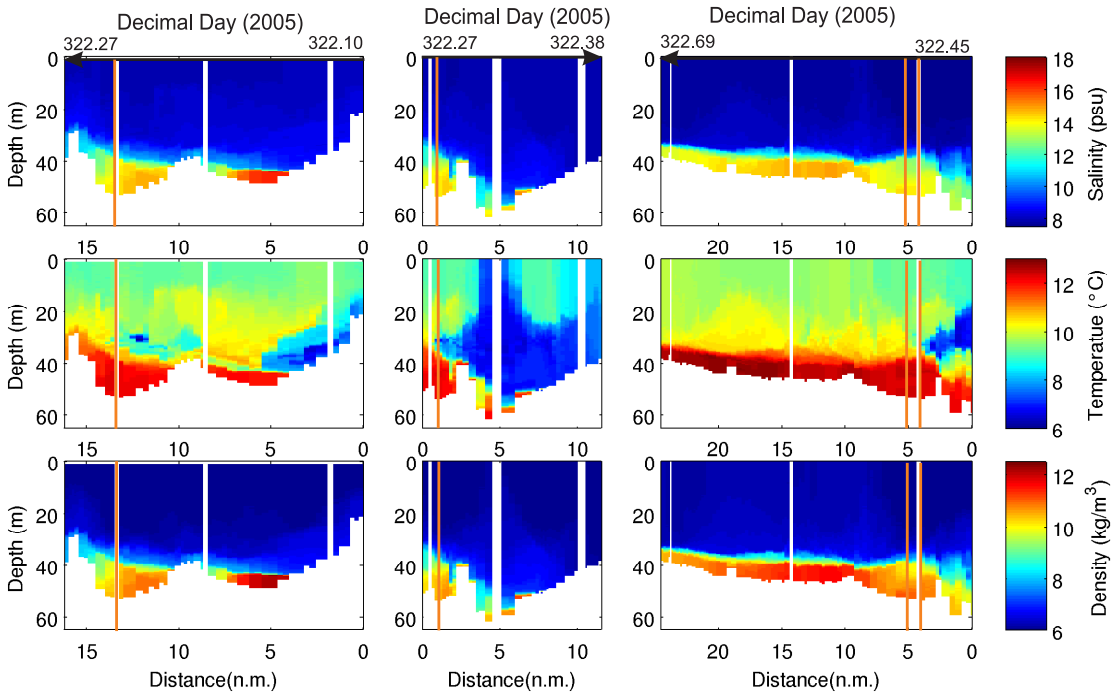

Figure 4.14: Transects 17, 18 and 19 taken on 19th of November in the Bornholm Channel (see the map on fig. 3.5 on the page 29 for the location). Transects 17 and 19 are shown in the other direction then they were made (see the arrows above the salinity plots and map 3.5). Orange lines indicate the places where the transects intersect each other.

On the fig. 4.14 CTD data for transects 17, 18 and 19 made in the Bornholm Channel on 19th of November can be seen. In the eastermost part of the Bornholm Channel salinity drops to 14-15 PSU, with temperatures of about 13 degrees. The colder part of the plume visible on the western part of transect 12 hasn't arrived yet into the Bornholm Channel. The salinity of the inflow drops in comparison to salinity observed in the transects 6, 7 and 8 taken also in the Bornholm Channel (from 17 PSU to about 14-15 PSU). From the density plot for the transect 17 the lateral distortion of the interfacial density structure can be visible as a pinching of the interface to the left of the down-channel flow, and a spreading of isopycnals to the right. It is caused by the the transverse transport inside the interface (interfacial jet - described in sect. 2.4). Transect 17 is one of two transects where the bottom velocities are partially not corrupted. It can be read from the ADCP data that the inflowing water has the north-east velocity of about 25 cm/s. More specific estimations of the inflow velocity can not be done due to lack of ADCP data for the part of the inflowing water.

4.5 General picture of the inflow propagation.

A general plume propagation picture can be told using the ship transects and the moorings' data. The inflow of the water with temperatures of about 12-13 degrees was propagating at the bottom through the Drogden Sill from 3rd to 14th of November, with salinities up to 25 PSU in the lower part of the strait. During the propagation through the Arkona Basin and further entrainment processes will make the plume less saline but more extended. This part of the inflow was observed at the KFS station from about 6th of November (with salinities in this period of about 15 PSU raising later). At the Arkona Basin station bottom salinities on 8th of November were 13.5 PSU, raising to 14 PSU on the 9th of November, 15 PSU on the 10th and 16 PSU on 11th and temperatures for those days of about 13 degrees. The Arkona Basin station cannot observe plumes with thickness smaller then 5 meters. At the Darss Sill station warm inflow arrived on 10th of November with salinities of 15 PSU raising later. It is not clear whether this inflow came through the Sound or through the Belt, probably mainly through the Belt. Then, according to the transects taken by R/V Oceania inflow with salinities of 17 PSU reached middle of the Bornholm Channel and was observed there from 10th to 12th of November, spreading further on 13th of November.

From 15th to 18th of November inflow through the Sound intensified. It was caused by the wind pattern over the transition area (highest wind velocities were observed during this period - see fig. 4.1). The salinities observed during those days were up to 25 PSU in the whole water column passing through the Sound (previously such a high salinities were observed only in the deeper part of the strait). Also temperatures of the inflowing water was lowered from 13 to 10 degrees during those 4 days. It was caused by increased mixing of the inflow with the atmosphere. The cold inflow, with salinities up to 15 PSU and temperature of about 10 degrees was observed by the R/V Oceania in the middle of the Arkona Basin on 17th of November. For transects taken in the eastern part of the Arkona Basin on 18th of November and in the Bornholm Channel on 19th of November warm (13 degrees) bottom water still exhibits - the inflow hasn't propagated further east before these days. After observed Bornholm Channel salinities of about 17 PSU before 13th of November, the salinity in the channel drops to 15 PSU, then probably further increases, dropping again to the level of 15 PSU on 19th of November. The Arkona Basin shows variations of salinity for the whole inflow period.

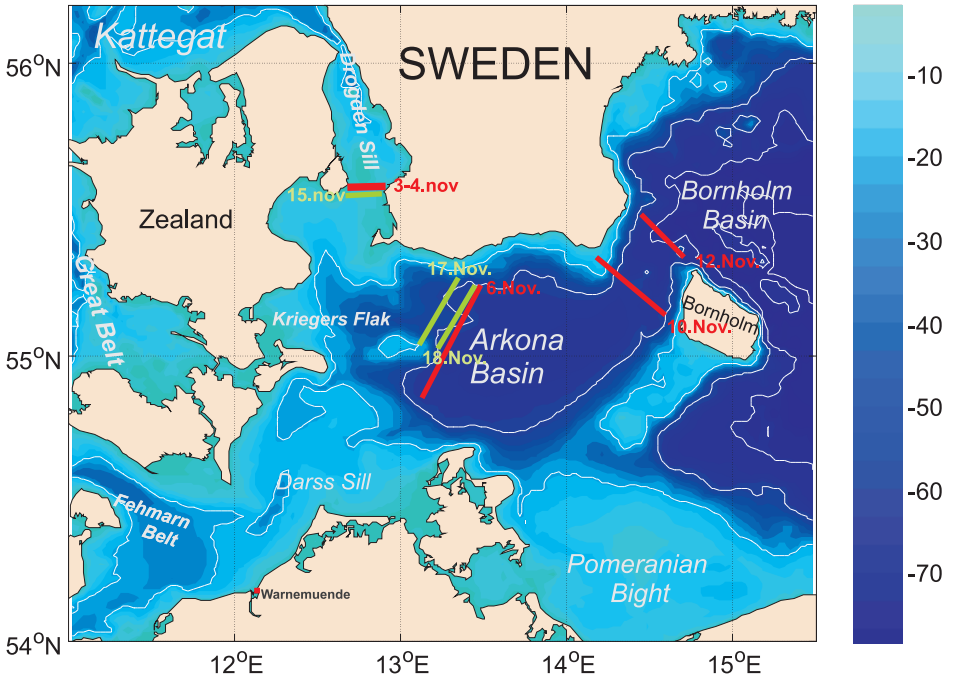

Figure 4.15: Inflow propagation. The red lines mark the approximate propagation of the first part of the inflow with warmer waters (ca 11 degrees). The green lines mark the propagation of the second, colder part of the inflow with temperatures of ca. 9.5 degrees and bigger salinities. Nearby the lines dates of the inflow arrival are marked.

Transects were also taken in the Bornholm Basin on 14th of November (fig. in appendix) and on 20th of November (fig. 4.20). Before 14th of November only warm part of the inflow (with temperatures of about 12-13 degrees in the Bornholm Channel) could be observed in the Bornholm Basin, if any. For the transect taken on 14th of November intrusion of water with temperatures of 13 degrees is visible, but salinities of this water are only 13 PSU at the depth of 60 meters. Moreover the salinity plot shows stable salinity stratification. It is clear that what we see for this transect are leftovers of the previous inflow. Moreover transect taken on 20th of November shows similar bottom salinity and temperature structure as the previous transect - so it can be said that the saline inflow described in this thesis hasn't arrived in the Bornholm Basin until 20th of November. The only difference between those two transect is a doming visible on the salinity and density plots for transect 20. This is caused by a cyclonic eddy (sect. 4.8) visible on the transect's

20th ADCP plots.

On the fig. 4.15 a basic inflow propagation map is shown (what was possible to say from the moorings and ship data). With the red lines the first, warmer part of the inflow, propagating through the Sound from about 3rd of November is marked and with the green line the second, colder part of the inflow with higher salinities (observed in the Sound from 15th of November). Nearby the lines the dates at which each part of the inflow was observed are marked.

4.6 Correlation coefficients.

The correlation of the bottom salinity at buoy at Drogden Sill and KFN for the period from 20th of November 2005 until 10th of July 2006 was made. To eliminate the internal waves influence from the data an averaging over 12 hours for both station was made. The inflow is delayed by a few days, so the bottom salinity data for one of the station were shifted and the biggest correlation was founded to see approximate the inflow delay. The bottom salinity correlation with 4 and 5 days shift between stations is the biggest one and is equal to 0.63. With the shift of three and six days the correlation is 0.58. So judging from the bottom correlation coefficient for the investigated period the typical delay of the inflow between Drogden Sill and KFN is about 3-6 days. Due to lack of data at KFN station exact delay of the observed medium-intensity inflow cannot be estimated. On the fig. 4.16 (upper panel) the delay between the bottom salinity observed at the Drogden Sill and at the position north of Kriegers Flak is marked with the black arrows for some inflow events between 20th of November 2005 and 1st of March 2006.

The correlation of the inflows incoming through the Sound (observed at the Drogden Sill station) and through the Belt (the Darss Sill station) can be made, since both inflows are indirectly correlated by the wind patterns over the whole transition area. Inflows passing through the Belt are delayed by a few days to those passing through the Sound (Burchard et al., 2005). Quite high correlation in the inflows observed at both station can be seen form observations (see fig. 4.8). The calculated correlation for the bottom salinity data shifted by 9 and 10 days is the biggest one and is equal to 0.29. As mentioned, this fairly high correlation is because the part of the inflow propagating through the Belt is indirectly correlated (via the wind pattern) with the part propagating through the Sound. On the fig. 4.16 (lower panel) the delay between the bottom salinity observed at the Drogden Sill and at the Darss Sill between 14th of December 2005 and 26th of February 2006 is shown. Between these two buoys correlation was significantly lower than between the Drogden Sill and the KFN buoys and it is hard to show exactly which plumes visible at both buoys are correlated with each other.

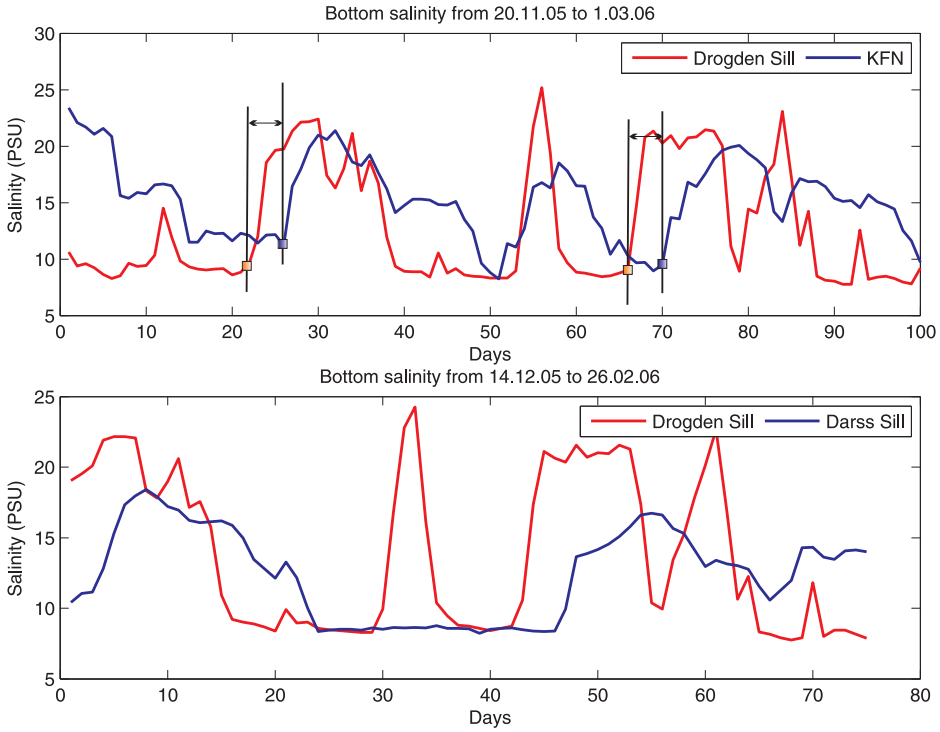

Figure 4.16: Comparison of the bottom salinity from the Drogden Sill buoy and KFN buoy (upper panel) as well as from the Drogden Sill and Darss Sill buoys (lower panel). With black arrows delay for some inflow events was marked in the upper plot. For the lower plot the delay between the inflows is not so easy to find, as the calculated correlation was lower.

4.7 TS diagrams.

Water that originates in a particular region possesses a distinctive salinity and temperature and tends to retain them as it moves. Salt and heat diffuses very slow, therefore these properties can be used as tracers of subsurface waters. Water mass identification is usually done by plotting diagrams of temperature and salinity known as TS diagrams.

In this thesis TS diagrams can be used to compare water masses of transects made in different time periods, but in places nearby to each other (like transects 10 and 20), analyze water masses passing nearby moorings or discuss the inflow propagation.

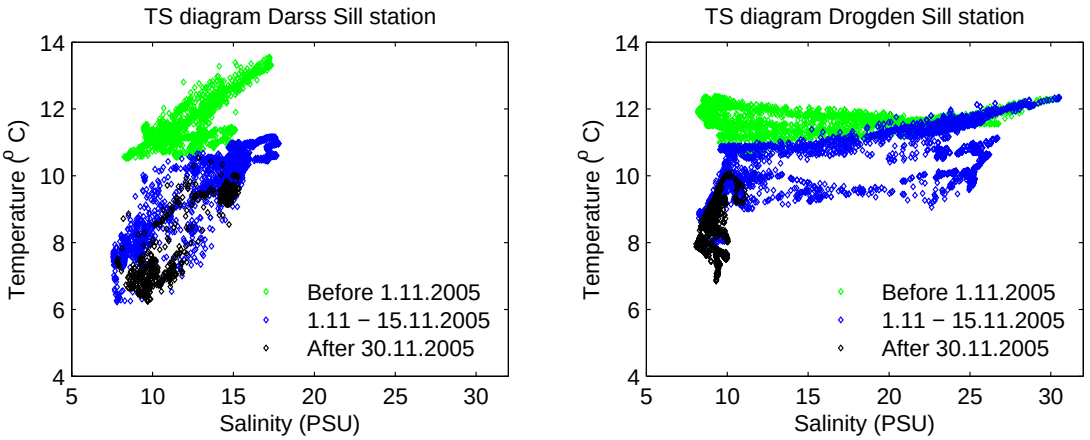

Figure 4.17: TS diagrams for the Drogden Sill station from 28th of October 2005 until 7th of December 2005 (right) and the Darss Sill station from 1st of November 2005 until 4th of December 2005. Data from different time periods were marked with different colors.

The temperature and salinity time series for the Darss Sill measuring station and the Drogden Sill measuring station can be seen on the fig. 4.3 and 4.7 respectively. The data were obtained from end of October, November and beginning of December 2005. The TS diagram for both station can be seen on the fig. 4.17. On both plots with green color data obtained before 15th of November were marked, with blue between 15th and 30th of November and with black color data obtained after 30th of November. Because of the big differences of the water masses passing nearby both stations it is hard to compare them, what can be done is the analysis of the water masses incoming through the Sound (Drogden Sill station) and through the Belt (Darss Sill station).

On the left side of the Drogden Sill TS diagram the water which is not influenced by the inflow can be seen (sill is to shallow to exhibit a halocline - when there is no inflow it will show low salinity in the whole water column). The inflows with high salinities can be observed on the right side of the plot. For the period from 15 to 30 of November inflows with both higher and lower temperature are visible. After 30th of November, but before 7th of December (black plots) no inflow is observed. Branches connecting the brackish waters with the highly saline inflowing waters are visible. It is also clear that the water temperature decreases with time, for the inflowing waters as well as for the typical Drogden Sill waters.

On the right side of the Darss Sill TS diagram two parts of the inflow are visible, first one with higher temperature (earlier part of the inflow) and the second one coming later with lower temperature. This inflowing water masses are connected

with the surface waters via two branches where the mixing takes place. The water masses observed at the Darss Sill station are more entrained then the one observed at the Drogden Sill station due to both longer pathway from the Kattegat as well as bigger depth here than in the Sound. The observed inflow salinities are a lot bigger for water incoming through the Sound. For the observed inflows (right part of the plot) as well as for the normal, brackish water (left side of the plot) it can be seen that the temperature is dropping in time. After 30th of November no inflow events are visible at the Darss Sill buoy.

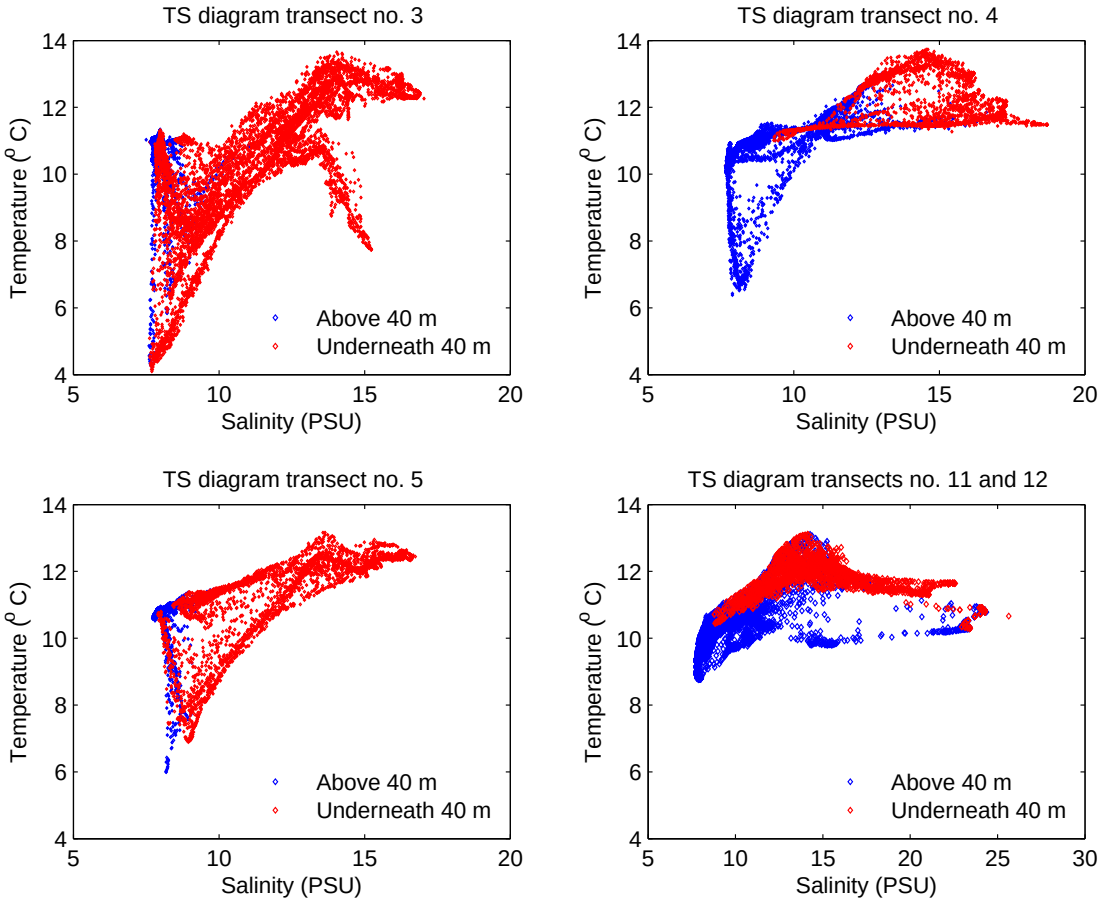

Figure 4.18: TS diagrams for transects: 3 (upper left), 4 (upper right), 5 (lower left) and 11 and 12 (combined, lower right) taken between 10th and 17th of November in the Arkona Basin and Bornholm Channel (see fig. 3.5 and 3.6 on the pages 29 and 30). The water above 35 meters is marked with the blue color and below with the red color.

On the fig. 4.18 TS diagrams for five transect from the Arkona Basin and Bornholm Channel are made. First we compare transect 3 with transect 4 (see fig. 4.10),

first one taken in the Bornholm Channel (and partially in the Bornholm Basin), the second one in the Arkona Basin, on 10th and 11th of November 2005. In both plots surface water with low salinities is visible. The water above 35 meters (typical value at which halocline at the Arkona Basin exhibits) is marked with a blue color, underneath with a red color. For most of the transect 4 water temperature is well mixed. Transect 3 exhibit cold, low salinity water under thermocline which was pushed up by the inflow (lower, left part of the TS diagram). Warm inflow is visible for both transects in the upper, right part of the plots. Salinity for the inflow, as can be seen, is slightly higher for transect 4, which was taken closer to the Danish Straits. All points between the highly saline inflow waters and the low saline surface waters show area of mixing. The mixing is less visible for the transect 4 because the water is already well mixed.

Transect 5 was taken in the Bornholm Channel and Arkona Basin close to the 3rd one, but about 2 days later. Comparing TS diagrams for these two diagrams main difference is the lack of cold, highly saline water for transect 5. This water was observed in the deep Bornholm Basin for transect 3, when the inflow already arrived with warmer water as transect 5 was taken and pushed the old, cold water away. Warm, low salinity water (surface water above the thermocline - left upper part of the diagrams), cold, low salinity water (water below the thermocline - left lower part) and warm, saline water (inflow - right part of the diagrams) form on the diagram a triangle, with branches connecting them being its sides. This branches show mixing area between main water masses exhibiting in this transects. Comparing transect's 3 and transect's 5 TS diagrams it can be said that the warm inflow between 10th and 12th of November 2005 propagated further into the Bornholm Channel removing the older cold water. Also the temperature shows that mixing with the atmosphere took place between these days, mixing the temperature for the whole water depth.

Transects 11 and 12 were taken in the Arkona Basin about 5 days after transect 5. They were taken in the other place than the other transects discussed in this section, but their TS diagram shows some interesting features. For these transects water main masses are: surface waters (left part of the diagram - mainly blue color) and warm, inflowing water (right upper part). Also separated from this two water masses colder, high saline water mass can be seen and the mass with the same temperature, but lower salinity (right lower part). The first one is the cold plume of highly saline coming directly after the warmer one which pushed the warmer water up. The second one is the mass which is over the incoming, colder and denser plume. No bigger mixing is visible between these two water masses and the ambient water. The surface water is warmer than the surface water observed on the other transects.

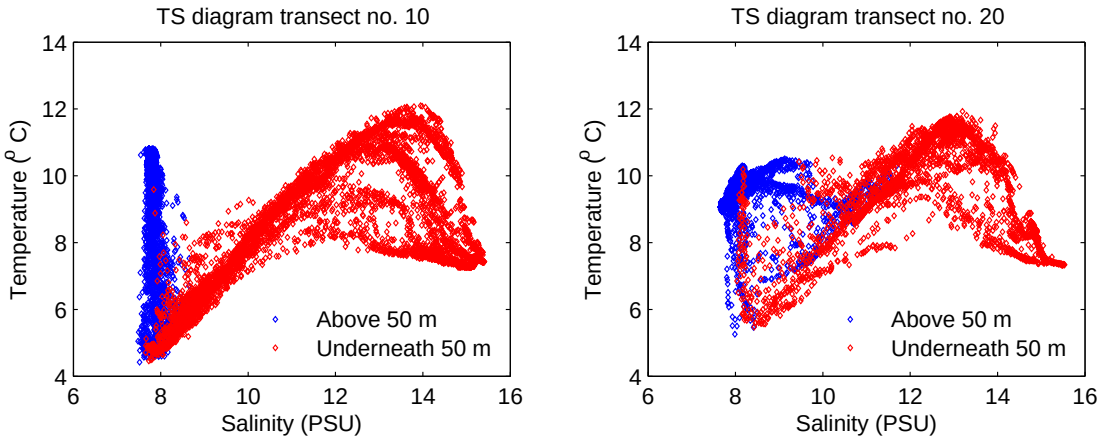

Figure 4.19: TS diagrams for transects 10 (left) and 20 (right) taken on 14th of November (transect 10) and 19th of November (transect 20) in the Bornholm Basin (see fig. 3.5 on the page 29). The water above 40 meters is marked with the blue color and below with the red color.

On the fig. 4.19 TS diagrams for transects 10 and 20 taken in almost the same places in the Bornholm Basin on 14th and 19th of November 2005 can be seen. The water above 40 meters (halocline) was marked with blue color, while the red color marks the water underneath 40 meters. A good distinction between these two waters can be seen on the plots. For the transect 20, two branches of mixed water coming from surface water are visible in the left part of the diagram. Upper one is due to a doming, which can be observed in the southern part of transect 20 (a mesoscale eddy in this region - see fig. 4.20 ob page 4.20). The lower part which also exhibits for transect 10 is the mixing of the surface waters with the deep waters. For the bottom water masses for both transect warm water intrusion (upper right part of the diagrams) is visible. Highly saline bottom water masses are visible for both transects as well (lower right part). Between these water masses four branches (transect 10) or two branches (transect 20) are visible. They mark the places where the mixing between the water masses takes place. Analyzes of the bottom part of these two TS diagrams lead to a conclusion that the water masses hasn't change between 14th and 19th of November 2009. The only difference is due to a doming observed for transect 20. It can be told that the described inflow hasn't arrived in the Bornholm Basin before 19th of November, with is in agreement with our earlier considerations.

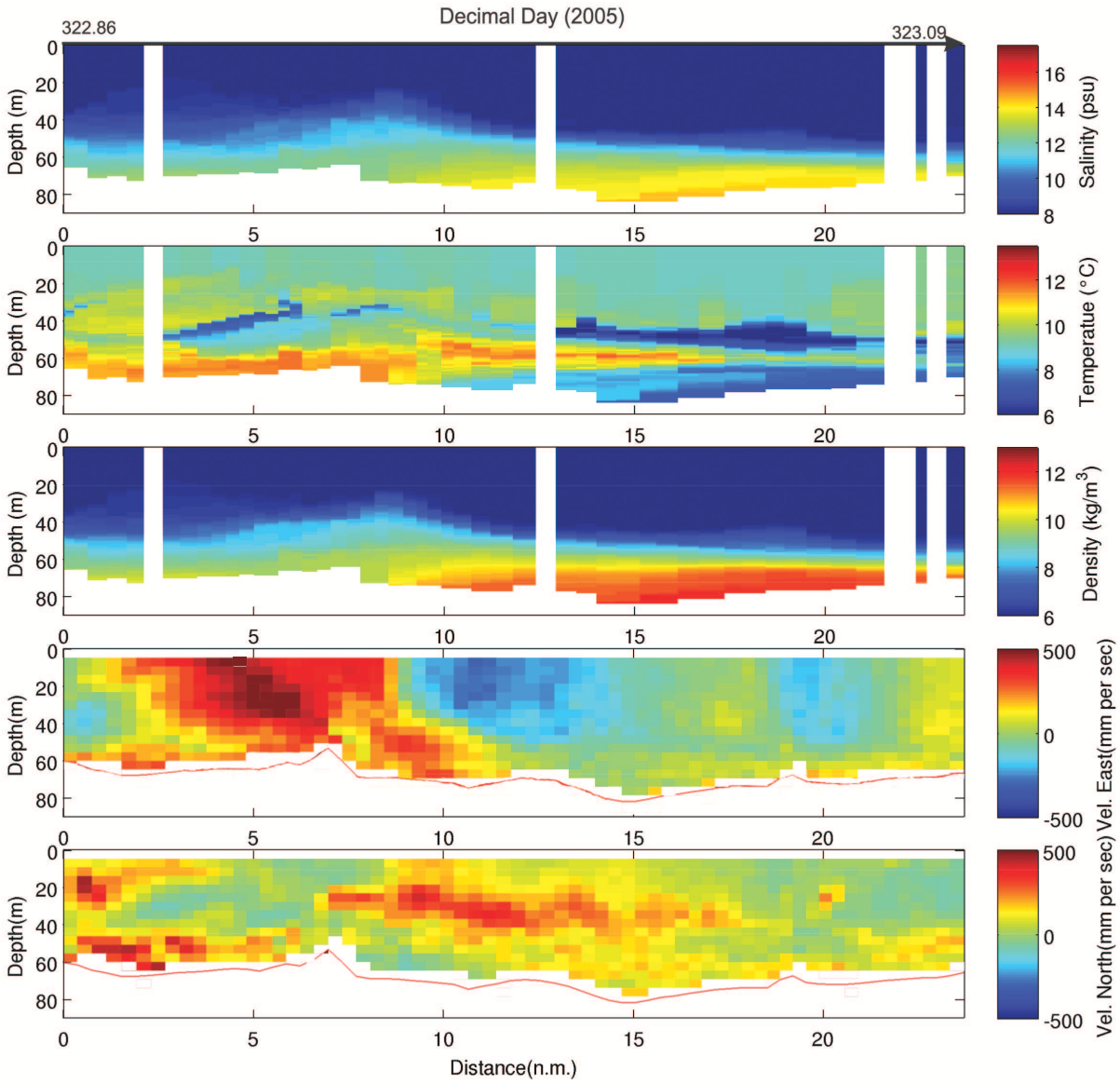

Figure 4.20: CTD and ADCP data for the transect 20, which was taken in the Bornholm Basin on 19th of November. ADCP data shows an anti-cyclonic eddy.

4.8 Mesoscale eddy in the Bornholm Basin.

Transect 20, was taken in the Bornholm Basin, north of the Bornholm Island on 19th of November 2005 (fig. 4.20, map on fig. 3.6 on page 30). The salinity for this transect is stably stratified, reaching 14 PSU at the bottom, with a doming visible in the first part of the transect. In the upper, mixed layer temperature reaches about 10 degrees. Below about 40 meters (thermocline) drop of temperature to 6 degrees is visible with an intrusion of warm (up to 11 degrees) water at the south-west end of the transect. This warm water intrusion is probably a leftover of the earlier, warm inflow.

What is particularly interesting for this transect is a cyclonic eddy of about 22 kilometers in diameter and 45 meters thick, which gives a volume of about 17 km^3. Typical eddies in the BB area has volume of 2 km^3 (Reissman et al. (2009)), therefore observed eddy is a fairly large one. The velocities reaches 50 cm/s east in the south-western part of the eddy and 50 cm/s west in the north-eastern part. The cyclonic eddies are called cold-core eddies or simply cold rings. Under the right divergent conditions, cool waters can upwell from deeper waters to act as a seed for the formation of a cold-core eddy, as described in sect. 2.5. In the core of the eddy a density doming can be observed, which is in order with our predictions (see fig. 2.8 on page 19) - the higher density water in the center was pushed up by the eddy. Southerly and westerly winds were prevailing in the period from the beginning until 15th of November (observed on the station Arkona Basin - see fig. 4.1 on page 34). This wind pattern could cause an upwelling on the eastern coast of the Bornholm Basin, which could produce an cyclonic eddy. It could later moved away from the shore to a place where the transect 20 was made.

4.9 Inflow parameters

4.9.1 Geostrophic vs. observed velocities

The geostrophic eastward velocity can be calculated by integrating thermal wind equation:

$$\frac{\partial U}{\partial z} = \frac{g}{f\rho_0} \cdot \frac{\partial \rho}{\partial y} \tag{4.2}$$

with respect to z. Here the convention that coordinates x and y (with corresponding velocities U and V) point towards the east and north respectively is used. The z-axis points upwards.

For calculating the geostrophic eastward velocities CTD and ADCP data from transects 13 and 17 will be used, first one taken north of the Kriegers Flak on 18th of November 2005 and the second one taken in the Bornholm Channel on 19th of November 2005. The integration has been performed by calculating the horizontal density gradient: in the transect 13 from the two deepest CTD casts in the trench in the southern part of the transect and in the transect 17 from two deepest casts taken in the eastern of two trenches under the transect. The unknown integration constant was determined by fitting the geostrophic velocities to the observed velocities at 15 m depth, i.e. well above the bottom current. The geostrophic velocities are compared with the average eastward ADCP velocities between the two CTD casts on fig. 4.21.

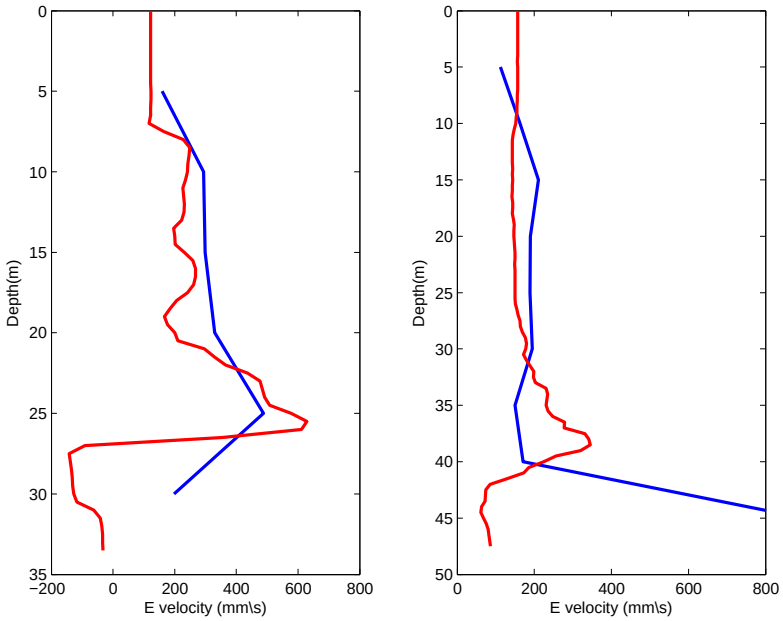

Figure 4.21: Geostrophic (red) and observed (blue) eastward velocities north of the Kriegers Flak on 18th of November 2005 (left) and in the Bornholm Channel on 19th November 2005.

Although the density data were good resolved, the problem with the comparison is the poor resolution of the ADCP data, as well as the missing values of the current velocity nearby the bottom. This is also a reason why a comparison wasn't made for any of the other transects. The correspondence between the geostrophic and observed velocities is high for transect 13, which means that the flow is in geostrophic balance in the cross-stream direction. For the transect 17 ADCP velocities aren't matching the calculated geostrophic velocities, probably due to a bad data resolution and missing bottom data, or to the fact that friction plays an important role here..

One clear feature of the geostrophic velocities, which is also seen in transect's 13 observed velocities, is a decrease in velocity with depth below the interface. This purely inviscid vertical shear in the geostrophic velocities is caused by the transverse density gradient within the current, as already observed by Sellschopp et al. (2006) and Umlauf and Arneborg (2009).

4.9.2 Volume fluxes.

The volume fluxes of saline water are hard to determine due to lack of the bottom ADCP data. However a rough estimate can be done by multiplying a representative velocity, obtained from the transect 13 (the only transect with the bottom ADCP data taken in the KFN area), with the cross-sectional area of the gravity current. This can be done for transects 6, 7, 8 and 17 made in the Bornholm Channel as well as for transect 13 made north of the Kriegers Flak. The cross sectional area below the salinity 10 pycnocline are approximately 14000 m^2, 7000 m^2, 17000 m^2, 35000 m^2 and 26000 m^2 for transects 6, 7, 8, 13 and 17 respectively. The representative velocity obtained from ADCP data for transect 13 is about 0.4 m/s, for the trench north of Kriegers Flak and will be used in calculations in the Bornholm Channel as well. For the area north of the Kriegers Flak (transect 13) it gives the volume flux of approximately 35000 km^3/s, which compared with the flux in the Drogden Sill from 13th to 15th of November being in range of 25000 to 75000 m^3/s (see fig. 4.1) supports findings e.g. by Burchard et al. (2005) and Sellschopp et al. (2006) that the main part of the water entering through the Sound follows a path north of the Kriegers Flak. In the Bornholm Channel the volume fluxes for the transects 6, 7 and 8 made on 13th of November 2005 varies from 7000 to 18000 m^3/s. The transects were taken in the Bornholm Channel, on the same day but in different places. The transect 17 was taken on 19th of November 2005 in the Bornholm Channel and is slightly longer then the previous transects. The volume flux calculated for this transect is about 26000 m^3/s and is bigger then volume flux calculated for the transects taken on 13th of November. It is also visible on the salinity and density plots (plots of all described transects are in the appendix) as increase of the plume thickness.

4.9.3 Entrainment.

For a steady current, the entrainment can be found from the increase of volume flux or decrease in density or salinity in the flow direction. For described inflow the volume flux budgets are too unclear, but it should be possible to see any entrainment

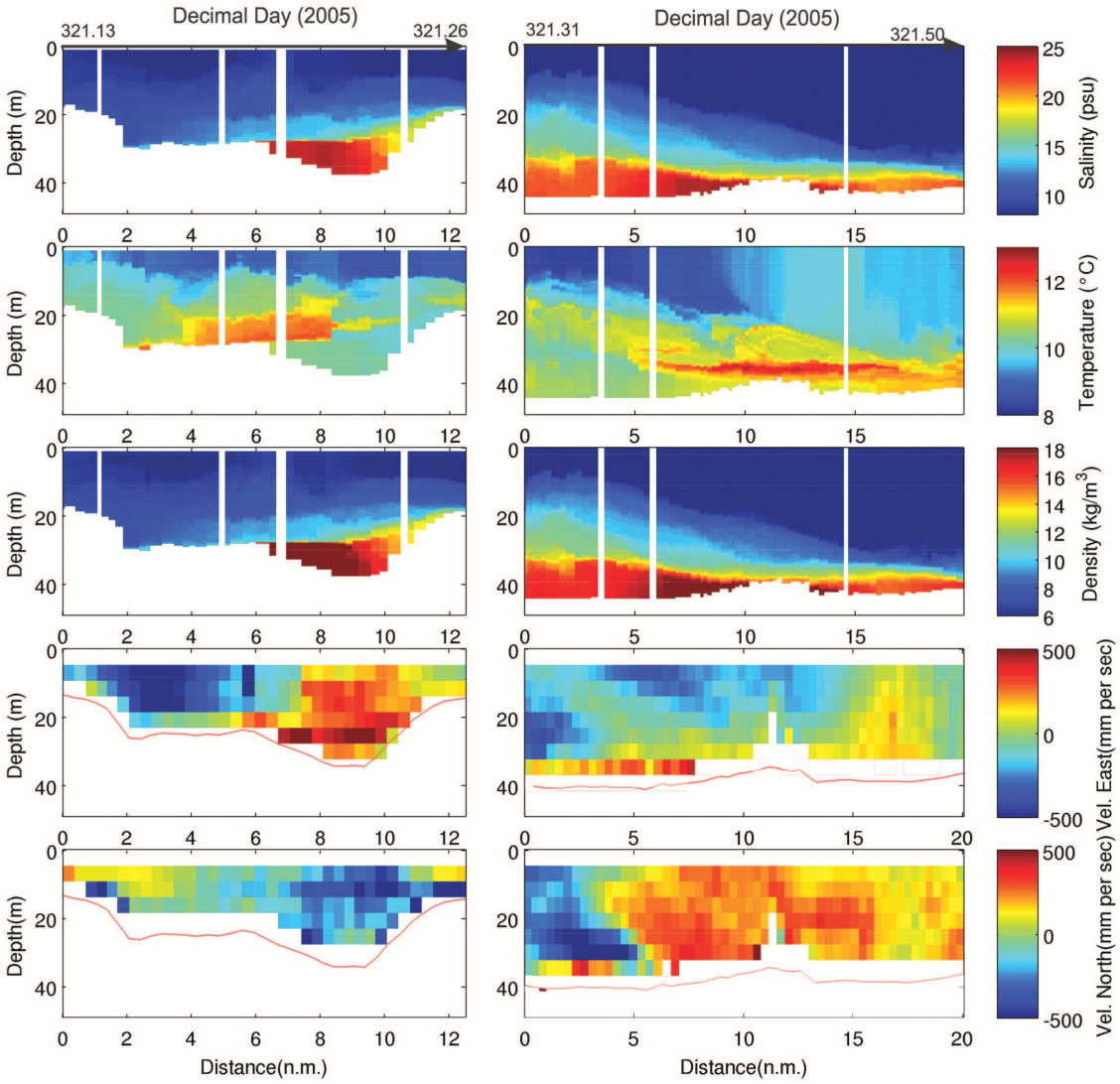

Figure 4.22: CTD and ADCP time series transects 13 and 14 made on 18th of November (see the map on fig. 3.6 on the page 30 for the location).

effects in the salinity data. The salinity decreases in the flow direction as as in equation 2.6:

$$\frac{\partial S}{\partial x} = \frac{(S - S_0)Bw_E}{Q} \tag{4.3}$$

Also on the fig. 4.23 the effect of the interfacial jet on the entrainment process is shown (compare with the fig. 2.7 on the page 17).

In this master thesis entrainment effect will be calculated for the area north of Kriegers Flak and in the Bornholm Channel. We need a steady current, so best what we can do is to compare transects 13 with 14 (see fig. 4.22) and 6 with 8 (see fig. 4.12). Transects 13 and 14 made north of the Kriegers Flak were taken about 30 km from each other, transect 14 was taken a few hours after transect 13. Transect 6 was made about 15 km east of transect 8, a few hours before transect 8. It can be assumed that for the transects 13 and 14 we see the same inflowing water, as the time gap between these two transect is similar to time necessary for the plume to propagate between these transects. The situation is different with transects 6 and 8. Transect 6 was made more east than transect 8 and earlier, but regarding the small time and distance difference between the transects it can be said that we observed the same water masses (steady current between these days can be assumed). Salinity profiles for KFN and the Bornholm Channel are given on fig. 4.24.

There is no strong trend in the salinity data and there is quite a lot of variability both in the Bornholm Channel and in north of the Kriegers Flak. The most common bottom layer salinity seems to be about 24 PSU for the transect 13 (taken more west) dropping to about 22 PSU for the transect 14 (more west). With a flow path length of about 30 km it gives us a salinity gradient of about $\frac{\partial S}{\partial x} = 6.8 \cdot 10^{-5}$ m^{-1}. For the Bornholm Channel there is a tendency of the salinities to be concentrated around 16 PSU for transect 8 dropping to 15 PSU for transect 6, which with the the flow path length of 15 km gives us salinity gradient $\frac{\partial S}{\partial x} = 6.8 \cdot 10^{-5}$ m^{-1}. In the following calculations equations from sect. 2.3 starting on page 14 will be used.

Now w_E (vertical velocity with which ambient water is entrained into the gravity current) can be calculated using eq. 4.3 from page 16. For the KFN area with other parameters: S = 20 PSU, S_0 = 8 PSU, Q = 35000 m^3/s, B = 35 km, we obtain the observed entrainment rate in the order of $w_E = 6 \cdot 10^{-6}$m/s. With typical gravity current speed of 0.3 to 0.4 m/s, plume thickness of about 10 m and a reduced gravity g'= 0.12 m/s^2, a representative Froude number for the current using eq. 2.2 is Fr = 0.27 - 0.37. Using eq. 2.3 predicted entrainment rate is $w_E = 0.0085 - 0.14 \cdot 10^{-6}$

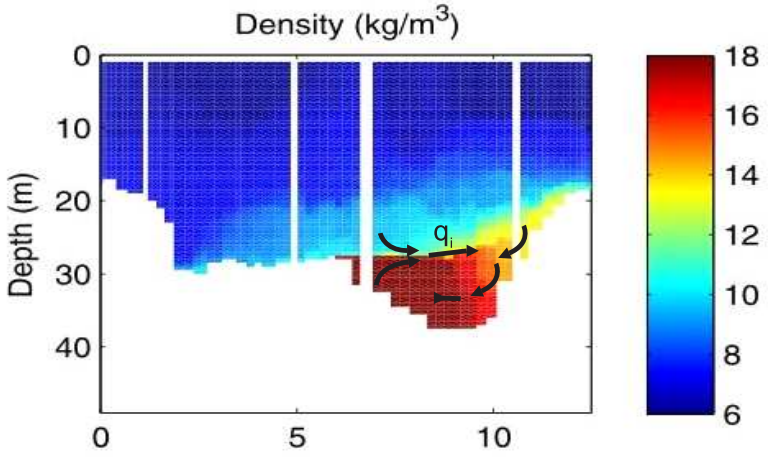

Figure 4.23: The entrainment process and the effect of the interfacial jet, shown with the black arrows, for the transect 13 taken north of the Kriegers Flak (see the map on fig. 3.6 on the page 30). Southern end of the transect is on the right hand side of the plot and the nothern on the left hand side. The down-channel direction is directed inside the page.

m/s, which is a wide range and tends to underestimate the observed value. Using eq. 2.4 predicted entrainment rate grows to $w_E = 1.2 - 4.9 \cdot 10^{-6}$ m/s which is closer to the observed value, but still to low. Finally, with the bottom slope between transects 13 and 14 s= $3.3 \cdot 10^{-4}$ and using eq. 2.5 we get $w_E = 6.9 - 9.2 \cdot 10^{-6}$ m/s, which is a little more then observed entrainment rate.

For the Bornholm Channel we use the parameters: S = 15 PSU, $S_0 = 8 PSU$, Q = 13000 m^3/s, B = 7 km, and obtain the entrainment rate in the order of $w_E = 18 \cdot 10^{-6}$ m/s. Using typical gravity current speed of 0.3 to 0.4m/s, plume thickness of about 5 m and a reduced gravity g'= 0.06, a representative Froude number for the current in the Bornholm Channel is Fr = 0.55 - 0.73. Then using eq. 2.3 predicted entrainment rate for the Bornholm Channel is $w_E = 2.5 - 32.2 \cdot 10^{-6}$ m/s, which is a wide range, but in good agreement with the observed entrainment rate. Using eq. 2.4 we get $w_E = 14.8 - 53 \cdot 10^{-6}$ m/s which is also in agreement with observed value. Finally with a slope between the transects $s = 10^{-3}$ and using eq. 2.5 we get $w_E = 21 - 28 \cdot 10^{-6}$ m/s, slightly bigger than the observed value.

Therefore, generally the strongest Froude number dependent entrainment parameterization (eq. 2.3) underestimate the entrainment rate for lower Froude numbers (i.e. KFN area), but is in good agreement for bigger Froude numbers (i.e. in the

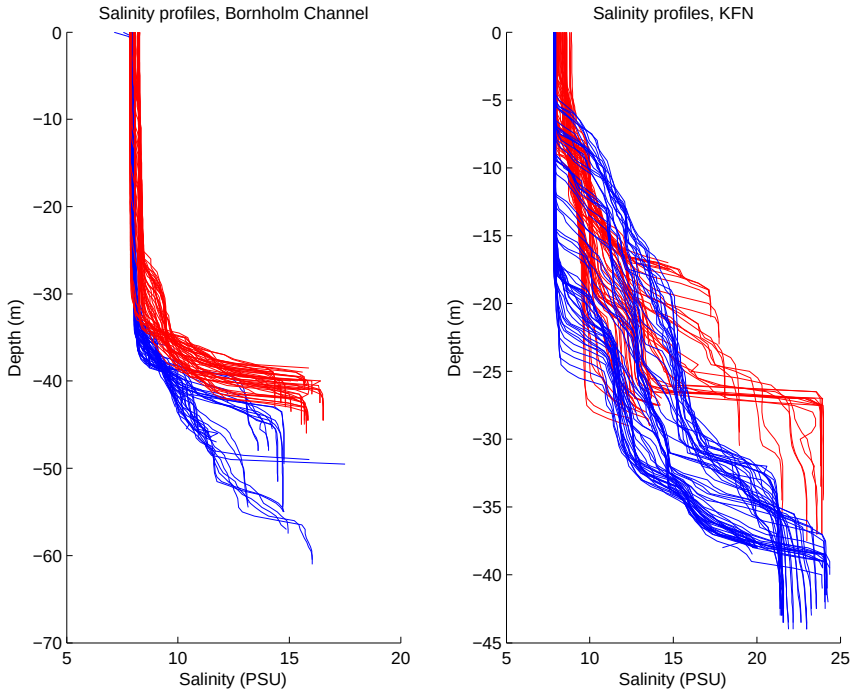

Figure 4.24: Salinity profiles for the transects 13 and 14 taken in the region north of the Kriegers Flak (left part) and for the transects 6 and 8 taken in the Bornholm Channel (right side). The blue profiles were taken for the transect made more to the west whereas the red ones - for the profiles taken more to the east (for maps see fig. 3.5 and 3.6 on page 29).

Bornholm Channel). The reason for this is that this empirical formula was based on observations with larger Froude numbers. For the KFN area eq. 2.4 also slightly tends to underestimate the entrainment rate, whereas eq. 2.5 tends to overestimate it. For the Bornholm Channel, which has a bigger Froude number, eq. 2.4 is in agreement with observed value, while eq. 2.5 overestimate the entrainment rate. In general, all expressions, but 2.3 for the KFN area, predict something within the correct order of magnitude, and further observations at similar Froude numbers are needed in order to distinguish between them.

Sellschopp et al. (2006) investigated entrainment rates in the KFN area for the inflow in January/February 2004 and come with observed entrainment rate $w_E = 3 \cdot 10^{-6}$ m/s and predicted entrainment rates using equations 2.3, 2.4 and 2.5 $w_E = 0.2 - 14 \cdot 10^{-6}$ m/s, which is in the same order of magnitude as the values observed and predicted in this thesis.

4.10 General discussion

In this chapter observational data obtained during the inflow was analyzed. First the general wind pattern over the transition area and its influence on the inflow was investigated (sect. 4.1). Later inflow through the Drogden Sill (sect. 4.2) and the propagation of the inflow in the Arkona Basin, over the Bornholm Chanel and into the Bornholm Basin was described (sect. 4.3 and 4.4). Next the correlation coefficients between the Drogden Sill and the KFN station, as well as between the Drogden Sill and the Darss Sill stations were measured (sect. 4.6). TS diagrams were analyzed for interesting transects and moorings taken in the Arkona Basin area (sect. 4.7). Finally a mesoscale eddy observed on one of the transect is described (sect. 4.8) and the inflow parameters are calculated (sect. 4.9).

During the period proceeding the inflow (from 5th to 20th of October) mainly easterly winds were observed over the transition area (fig. 4.1). This wind pattern caused an outflow from the Baltic Proper into the Kattegat and lowered the Baltic Sea mean elevation level. From 20th of October until 16th of November winds were generally southerly or westerly. This wind pattern caused sea level differences between the Kattegat and the Baltic Proper and indirectly a barotropic inflow. The correlation between the wind direction and the volume flux calculated from the Sea Surface Height stations in the north and south of the Drogden Sill is observed. The salinity increase in the Drogden Sill is delayed by a few days to the start of the inflow due to a brackish water front in the Kattegat area (see fig. 4.2).

A general plume propagation picture can be told using the transects made by R/V Oceania and the moorings' data. The inflow of the water with temperatures of about 12-13 degrees was propagating at the bottom through the Drogden Sill from 3rd to 14th of November, with salinities up to 25 PSU in the lower part of the strait (fig. 4.3). During the propagation through the Arkona Basin and further, entrainment processes will make the plume less saline but larger. This part of the inflow was observed at the KFS station from about 6th of November (fig. 4.5). At the Arkona Basin station bottom salinities on 8th of November were 13.5 PSU, raising to 14 PSU on the 9th of November, 15 PSU on the 10th and 16 PSU on 11th and temperatures for those days of about 13 degrees (fig. 4.6). The Arkona Basin station cannot observe plumes with thickness smaller then 5 meters, so it is hardly to predict when exactly the first part of the inflow arrived here. At the Darss Sill station warm part of the inflow arrived on 10th of November with salinities of 15 PSU raising later (fig. 4.7). Then, according to the transects taken by R/V Oceania (see sect. 4.4) first part of the inflow with salinities of 17 PSU reached mid part of the Bornholm Channel and was observed there from 10th to 12th of November,

spreading further on 13th of November. This part of the inflow was probably mixed with the waters in the dense water pool in the Arkona Basin (see sect. 2.2.5), which had similar salinity and temperature as the inflowing waters. There exists also a possibility that the saline water observed in the Bornholm Channel is not the described inflow, but just a leakage from the dense water pool in the Arkona Basin.

From 15th to 18th of November inflow through the Sound intensified. It was indirectly caused by the higher wind velocities over the transition area. The salinities observed during those days were up to 25 PSU in the whole water column passing through the Sound. Also temperatures of the inflowing water was lowered from 13 to 10 degrees (due to increased mixing of the inflow with the atmosphere). The cold inflow, with salinities of up to 15 PSU and temperature of about 10 degrees was observed by the R/V Oceania in the middle of Arkona Basin on 17th of November. This part of the inflow is not observed in the further areas of Arkona Basin before 19th of November. General inflow propagation picture is given on fig. 4.15. It can be seen that for the inflow it took about 3 days from its beginning to pass along the Kriegers Flak and enter the central Arkona Basin and probably 8 to 10 days to reach the Bornholm Channel.

The correlation of the bottom salinity between measuring stations at the Drogden Sill and KFN for the period from 20th of November 2005 until 10th of July 2006 was calculated (sect. 4.6). The bottom salinity correlation with 4 and 5 days shift between the stations is the biggest one and is equal to 0.63. The correlation for 3 and 6 days shift is also high and equal 0.58. So judging from the bottom correlation coefficient for the investigated period the typical delay of the inflow between the Drogden Sill and the KFN is about 3 to 6 days, which is in agreement to what was observed from observational data. The correlation of the inflows incoming through the Sound (observed at the Drogden Sill station) and through the Belt (the Darss Sill station) can be made, since both inflows are indirectly correlated by the wind patterns over the transition area. The calculated correlation for the bottom salinity data shifted by 9 and 10 days is the biggest one and is equal to 0.29.

In this thesis TS diagrams was used to compare water masses of transects made in different time periods, but in places nearby to each other (like transects 10 and 20), analyze water masses passing nearby moorings or discuss the inflow propagation. First water masses passing through the Drogden Sill and through the Darss Sill were compared (fig. 4.17). Water coming through the Sound is less entrained. Then transects taken in the same places were analyzed on TS diagrams to analyze the inflow propagation (fig. 4.18). The analyzes was in order with earlier considerations. Finally analyzes of the bottom part of TS diagrams for transects 10 and 20 lead

to a conclusion that the water masses hasn't change between 14th and 19th of November 2009 (fig. 4.19). The only difference is due to a cyclonic eddy observed for the transect 20. From this TS diagram it can be told that the described inflow hasn't arrived in the Bornholm Basin before 19th of November.

In the transect 20 a mesoscale eddy was observed (fig. 4.20). The eddy is a cyclonic one with volume of about 17 km^3. This is a lot comparing to typical Bornholm Basin eddies volume of 2 km^3 (Reissman et al., 2009). The velocities reaches 50 cm/s east in the south-western part of the eddy and 50 cm/s west in the north-eastern part. Southerly and westerly winds, which were prevailing on the eastern coast of the Bornholm Island a few days before the observation of the eddy, caused an upwelling, which could produce an cyclonic eddy. It later could move away from the shore to a place where the transect 20 was taken.

In the sect. 4.9 geostrophic eastward velocities were calculated by integrating thermal wind equation and compare them with observed velocities for two transects. For transect 13 taken in the trench north of the Kriegers Flak high agreement between observed and geostrophic velocities is observed, which means that the flow is in geostrophic balance in the cross-stream direction. For transect 17 taken in the Bornholm Channel the geostrophic balance is not visible, due to poor ADCP resolution or significant bottom friction.

In the same section the entrainment parameter in the area north of Kriegers Flak and in the Bornholm Channel was calculated. To do so first volume fluxes was estimated for these areas. For the area north of the Kriegers Flak (transect 13) the volume flux is approximately 35000 km^3/s, which compared with the flux in the Drogden Sill supports findings e.g. by Sellschopp et al. (2006) that the main part of the water entering through the Sound follows the path north of the Kriegers Flak. In the Bornholm Channel the volume fluxes for the transects 6, 7 and 8 made on 13th of November 2005 varies from 7000 to 18000 m^3/s.

For the KFN area we obtain the observed entrainment rate using formula 2.6 $w_E = 6 \cdot 10^{-6}$m/s. Calculated Froude number for the current is Fr = 0.27 - 0.37. Predicted entrainment rate varies from $w_E = 0.0085$ to $9.2 \cdot 10^{-6}$ m/s, depending on the used formula (2.3, 2.4 or 2.5). Formulas 2.3 and 2.4 tends to underestimate the observed value, while formula 2.5 gives a little higher result then expected. For the Bornholm Channel observed entrainment rate $w_E = 18 \cdot 10^{-6}$ m/s. A representative Froude number for the current is Fr = 0.55 - 0.73 and finally predicted entrainment rate varies from $w_E = 2.5$ to $53 \cdot 10^{-6}$ m/s. Formulas 2.3 and 2.4 gives a good result, whereas formula 2.5 tends to overestimate it slightly.

Generally the strongest Froude number dependent entrainment parameterization (eq. 2.3) underestimate the entrainment rate for lower Froude numbers (i.e. KFN area), but is in good agreement for bigger Froude numbers (i.e. in the Bornholm Channel). The reason for this is that this empirical formula was based on the observations with larger Froude numbers. For the KFN area eq. 2.4 also slightly underestimates the entrainment rate, whereas eq. 2.5 tends to overestimate it. For the Bornholm Channel eq. 2.4 is in agreement with the observed value, while eq. 2.5 overestimate the entrainment rate. In general, all expressions, but 2.3 for the KFN area, predict something within the correct order of magnitude, and further observations at similar Froude numbers are needed in order to distinguish between them.

Sellschopp et al. (2006) investigated entrainment rates in the KFN area for an inflow in January/February 2004 and come with observed entrainment rate $w_E = 3 \cdot 10^{-6}$ m/s and predicted entrainment rates using equations 2.3, 2.4 and 2.5 $w_E = 0.2 - 14 \cdot 10^{-6}$ m/s, which is in the same order of magnitude as the values observed and predicted in this thesis.

Chapter 5

Observation-simulation comparison

In this chapter, comparison between observational data and model data obtained from GETM model (see sect. 2.8) are made. First observational data from 5 moorings discussed in sect. 4.2 and 4.3 are compared with the model results with a temporal resolution of one day. Next two transects taken during the cruise of R/V Oceania are compared (see sect. 4.4 for observational data analysis). Finally propagation of the bottom current obtained from the model data is discussed and compared with the observations.

5.1 Moorings' comparison

Observational data for 5 moorings are available for the November 2005 (for some of the moorings, only the data from part of the month are available - compare sect. 4.3).

As discussed in sect. 2.8.1, the bathymetry adjustment procedure has been carried out in such a way, that the flow through the Sound has been optimized. Fig. 5.1 shows that the simulated salinities (red plots) in the Drogden Sill agree well with the observational data (blue plots). The vertical structure of the inflow events is reproduced by the model simulations. Occasional strong deviations of the order of up to 10 PSU may be explained by the low resolution of the model data. For the period from the beginning of the month up to 14th strong oscillations of the salinity for every depth occurs in the observational data. This period is roughly reproduced by the model, with better accuracies impossible to obtain due to low resolution. After 14th of November a strong inflow lasting a few days is in good agreement with the model.

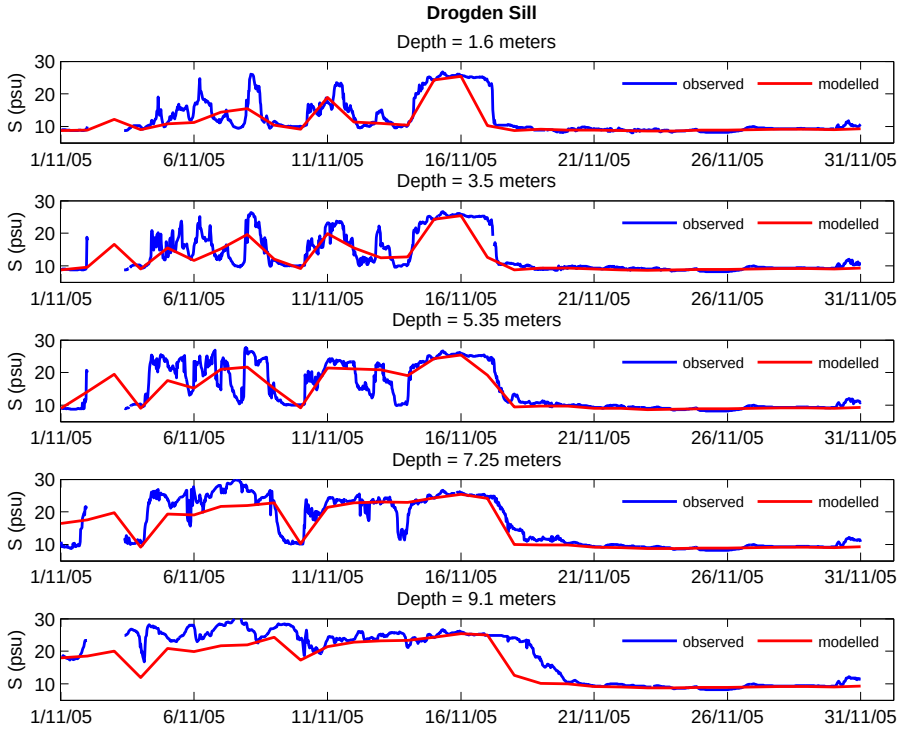

Figure 5.1: Time series of salinity at the Drogden Sill station for November 2005. Blue: observations, red: model results. Data at 1.6, 3.5, 5.35, 7.25 and 9.1 m below the mean sea level are shown. The mean water level at this station is 9.5 m. For the beginning of the month some observational data are missing.

For the KFN area (fig. 5.2) the observational data are available only for the second part of the inflow passing nearby KFN station and this part of the inflow is fairly well reproduced by the model. Strong deviations of the order of up to 10 PSU may be explained by the low resolution of the model data. The model results suggest that the inflow was observed at the KFN station from about 6th of November with salinities of about 17 PSU at the bottom.

Next buoy discussed here is the Kriegers Flak South buoy. Observational data are available only for the first part of the month. The salinity at depths 39 and 43 meters, so close to the bottom where the inflow is propagating, are reproduced well by the model. At depths 26 and 31 meters the modelled salinity is overestimated.

The last discussed buoy is the Arkona Buoy, placed the furthest from the entrance to the Baltic Sea. Data for only two depths, 25 and 40 m are compared on the fig. 5.4. At the depth of 40 m inflow is well reproduced by the model, with the deviations probably due to low resolution. At the depth of 25 m no inflow is shown for the observational data, which suggest that the inflow height is overestimated in the model.

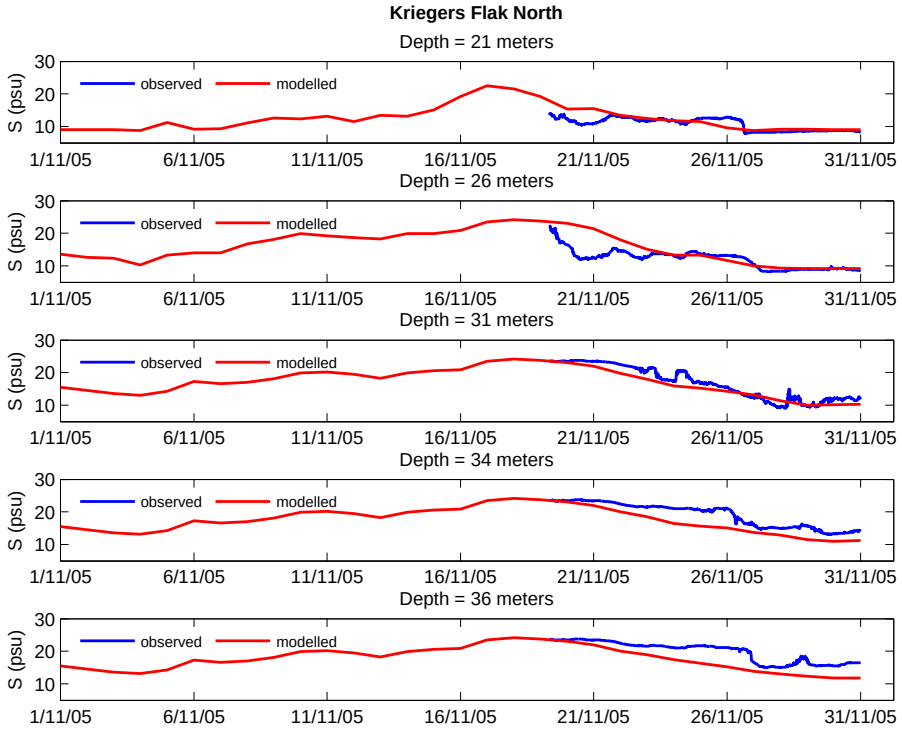

Figure 5.2: Time series of salinity at the Kriegers Flak North station for November 2005. Blue: observations, red: model results. Data at 21, 26, 31, 34 and 36 m below the mean sea level are shown. The mean water level at this station is 39 m. Observational data are available only for the second part of the month.

5.2 Transects' comparison

In this section observational data for two transects taken by R/V Oceania in the area north of the Kriegers Flak and in the Bornholm Channel are compared with the model results. First, transect 13 taken in the trench north of the Kriegers Flak on 17th of November 2005 is compared with the model results obtained for the same day and in the same place (fig. 5.5).

For transect 13 the observed general structure of the plume is in good agreement with the idealized model simulation. Salinity inside the plume in both cases is up to 22 PSU. Main feature on salinity plots is a strong stratification in the interface area, with salinity jump of more than 10 PSU within a few meters. Modelled plume's temperature is about 9 degrees, compared with observed temperature from 10 to 11 degrees. The waters above the observed highly saline plume are leftovers of the previous inflow pushed up by the incoming water and have temperature higher than the ambient water. This feature is also well reproduced by the model. The plume is geostrophically adjusted and leaning towards the northern slope of the Kriegers

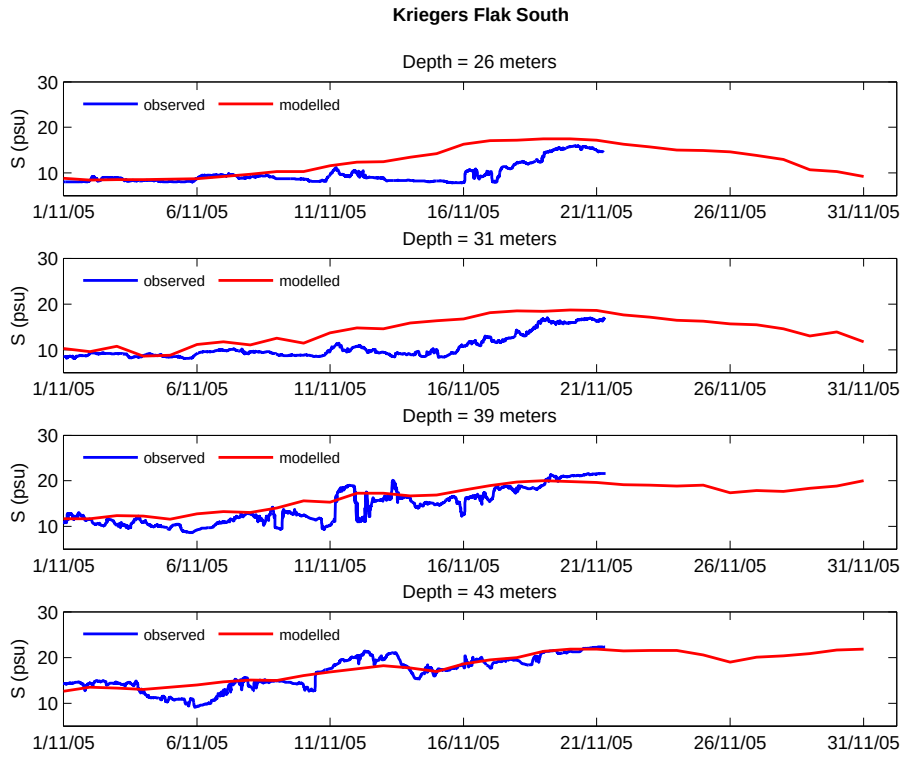

Figure 5.3: Time series of salinity at the KFS for November 2005. Blue: observations, red: model results. Data at 21, 26, 31, 39 and 43 m below the mean sea level are shown. The mean water level at this station is 44 m. Observational data are available only for the first part of the month.

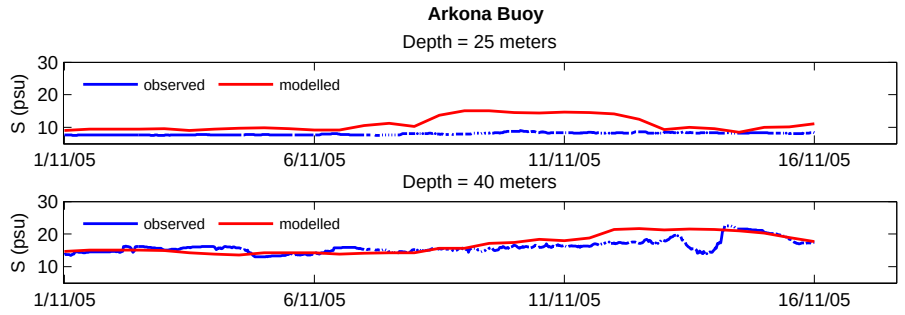

Figure 5.4: Time series of salinity at the Arkona Buoy station for November 2005. Blue: observations, red: model results. Data at 25 and 40 m below the mean sea level are shown. The mean water level at this station is 45 m.

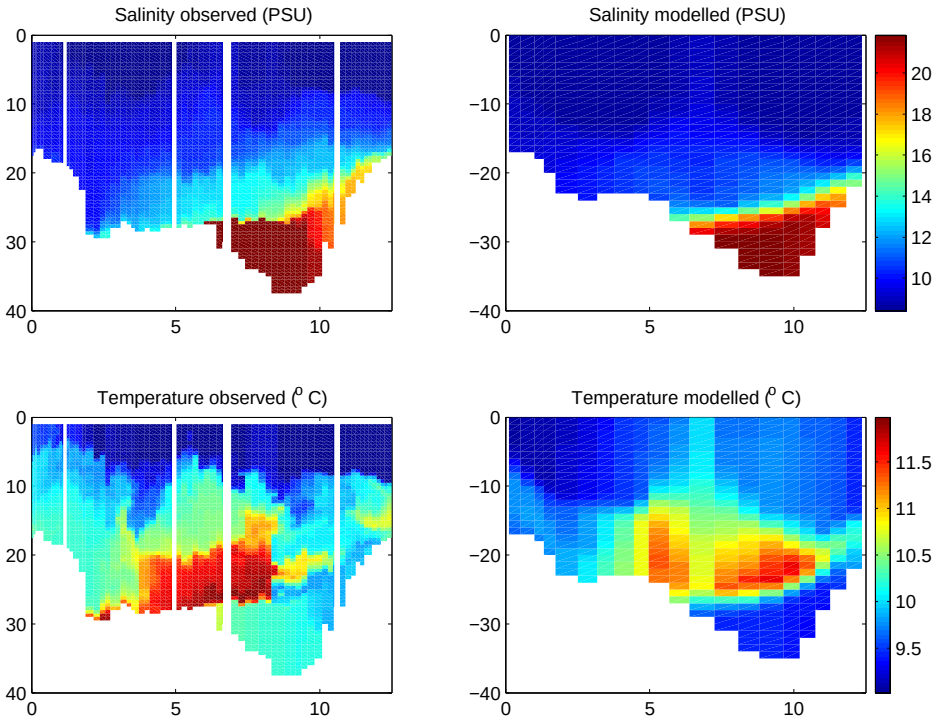

Figure 5.5: Observed (left panels) and modelled (right panels) salinity and temperature for transect 13 taken in the area north of Kriegers Flak (for map see fig. 3.6 on page 30) on 17th of November 2005.

Flak. The isopycnals spreading in the northern part of the trench is visible for the observed transect but not in the modelled one due to its low spatial resolution.

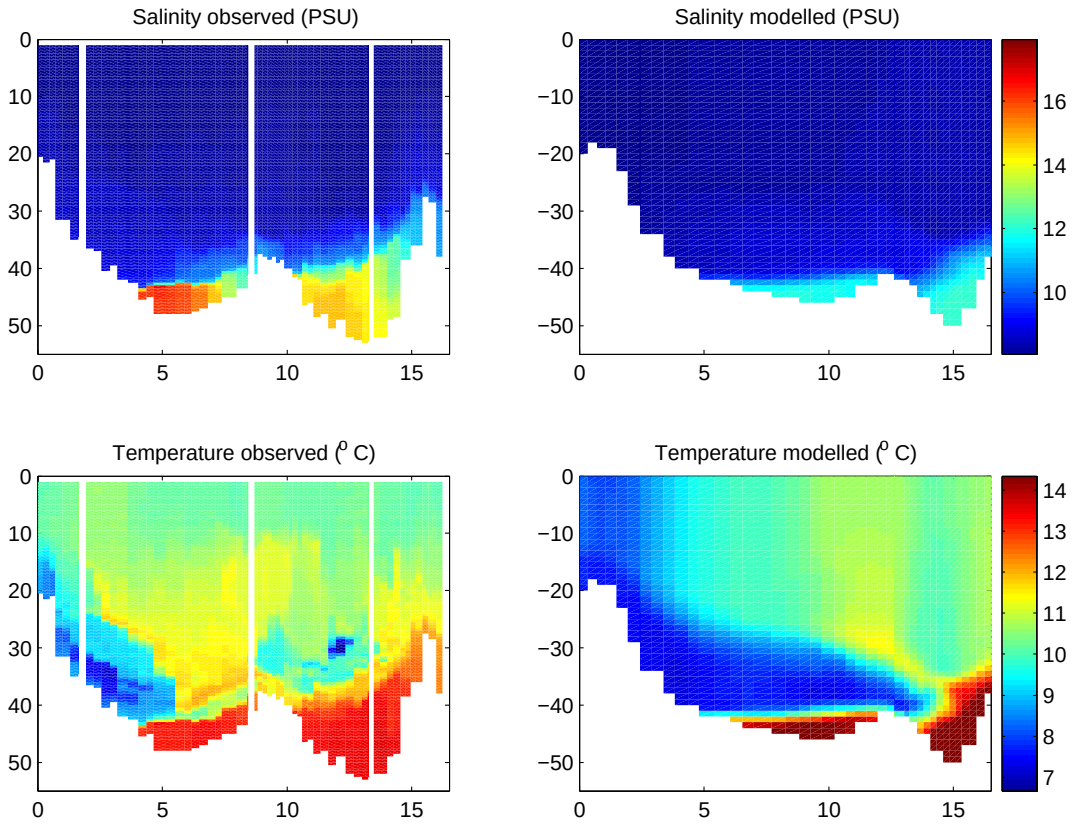

Figure 5.6: Observed (left panels) and modelled (right panels) salinity and temperature for transect 17 taken in the Bornholm Channel (for map see fig. 3.6) on 19th of November 2005.

On transect 17 taken on 19th of November 2005 two trenches in the Bornholm Channel are shown. The bathymetry of the observed and modelled situation is slightly different, however the both transect are taken in nearly the same place. The modeled plume salinity is underestimated by a few PSU, whereas the temperature is overestimated by about 2 degrees. However, the characteristic details of the plume seem to be well reproduced by the model simulations. Geostrophic tilt is observed for both trenches and for the northern trench as well a slight spreading of the isopycnals in the northern part of the northern trench.

5.3 Bottom current propagation

In this section modelled bottom inflow propagation will be discussed and compared with observational data (see sect. 4.5). Also, using tracers, division between part of the inflow coming through the Sound and through the Belt will be discussed.

Fig. 5.7 gives a qualitative impression about the situation in the Arkona Basin during and after the inflow. Shown are simulated bottom salinities on November 6, 12, 18 and 30. Before November 6 the saline water moves forward and backward from the Kattegat several times causing a smaller saline water plumes. On November 6 high salinities of up to 25 PSU have just passed the top of the Drogden Sill and start to descend towards the western Arkona Basin. A smaller plume of saline water is already visible during this day in the Arkona Basin with salinity of about 18 PSU. This is in a good agreement with observational data. Eastern part of the Arkona Basin shows typical salinities for the Baltic Sea bottom waters. Red line on the inflow propagation picture shows the inflow propagation on 6th of November according to the observational data. It is in good agreement with the model results.

On November 12 the inflow propagates into the middle Arkona Basin through the paths north of Kriegers Flak and south of Kriegers Flak. At the south-eastern end of the shoal both currents connect again. It should be noted that pathway north of Kriegers Flak has a bigger bottom salinity and carries more water. Due to the entrainment front of the inflow has lowered the salinity to about 20 PSU. The inflow through the Darss Sill filled the south western part of the Arkona Basin. The inflows through the Darss Sill and through the Drogden Sill are short before a confluence. From the observational data it can be said that on 12th of November the first part of the inflow already reached the Bornholm Channel (red line on the inflow propagation picture), however model results doesn't support this assumption, the modelled inflow is still in the middle parts of the Arkona Basin. It can be due to a fact that what was considered an inflow visible in the transect taken in the Bornholm Channel is just a leakage from the Arkona Basin dense pool (see sect. 2.2.5) and not actual inflow. Also possibility exists that the actual inflow propagated faster than in the model.

On November 18 inflows through the Darss Sill and through the Drogden Sill connect. Almost whole Arkona Basin is filled with a highly saline inflowing water with salinities up to 25 PSU in the western part of the Basin, decreasing to the east. In the Bornholm Channel arrives first part of the inflow with salinities of about 16 PSU. The inflow through the Drogden Sill has stopped. On November 30 situation after inflow is shown. Water inflowing through the both sills has reversed. The

Arkona Basin is emptied into the Bornholm Basin through the Bornholm Channel. However the bottom salinity in the Arkona Basin is still over 20 PSU. The saline water from the Arkona Basin propagates as well south, east of Rügen Island. According to the observational data, propagation of the cold, more saline (about 25 PSU) part of the inflow on the 18th of November is well reproduced by the model.

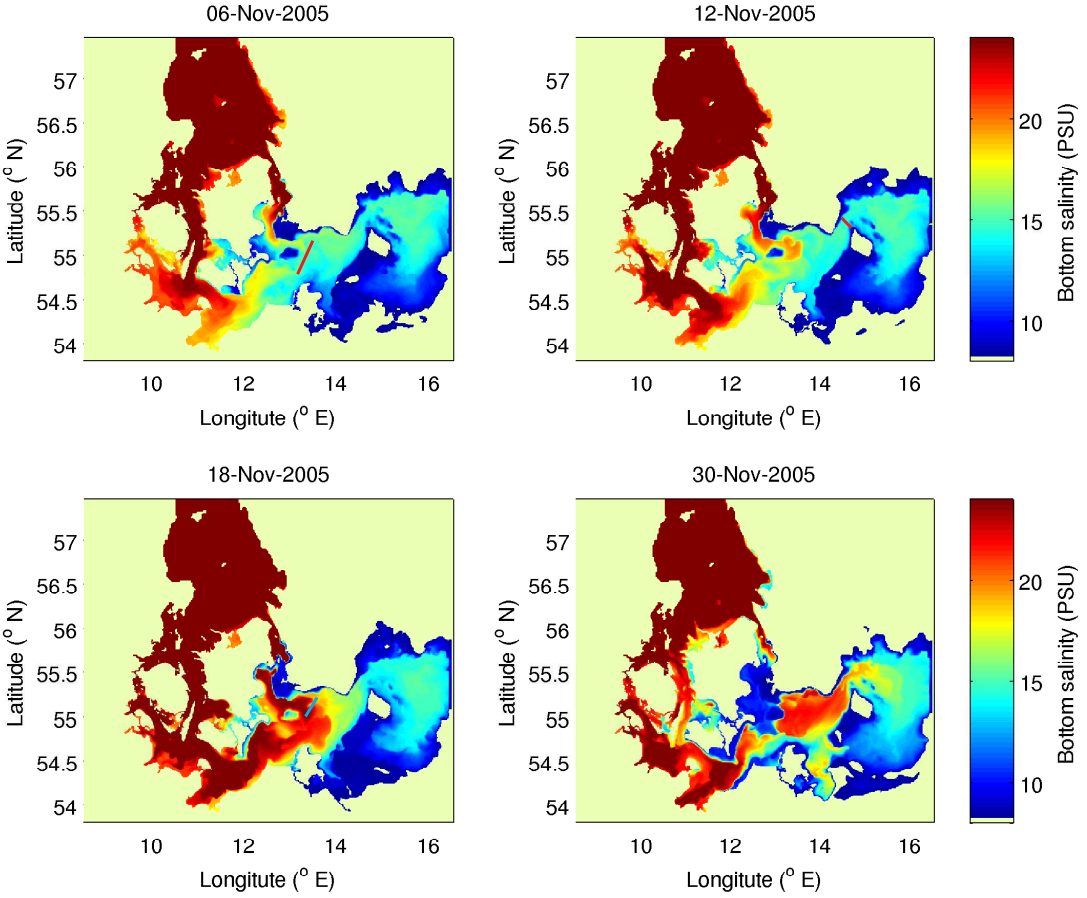

Figure 5.7: Simulated bottom salinity in the Arkona Basin during the medium intensity inflow in November 2005. Clockwise starting from the left-upper panel data from: 6th, 12th, 18th an 30th of November 2005 are displayed. The lines mark the inflow propagation as observed in the in-situ measurements. Red color marks the warmer part of the inflow with salinities up to 17 PSU, whereas the green one the following, colder part with salinities up to 25 PSU.

On the fig. 5.8 division of the inflowing water into the water coming through the Sound and through the Belt is visible. Tracer has the value of one if the salinity of the inflow exceeds a value given in the model. The figure shows the simulated bottom situation on 15th of November 2005, about 10 days after beginning of the

inflow. It can be told that water incoming through the Belt is propagating through the pathways north and south of Kriegers Flak and connects at the south-eastern end of the shoal. Clear division is visible between both inflowing waters, along 55th circle of latitude. This is due to the fact that the water inflowing through the Drogden Sill is heavier (less entrained because of its shorter way to the Arkona Basin) and is interleaving under water inflowing through the Darss Sill.

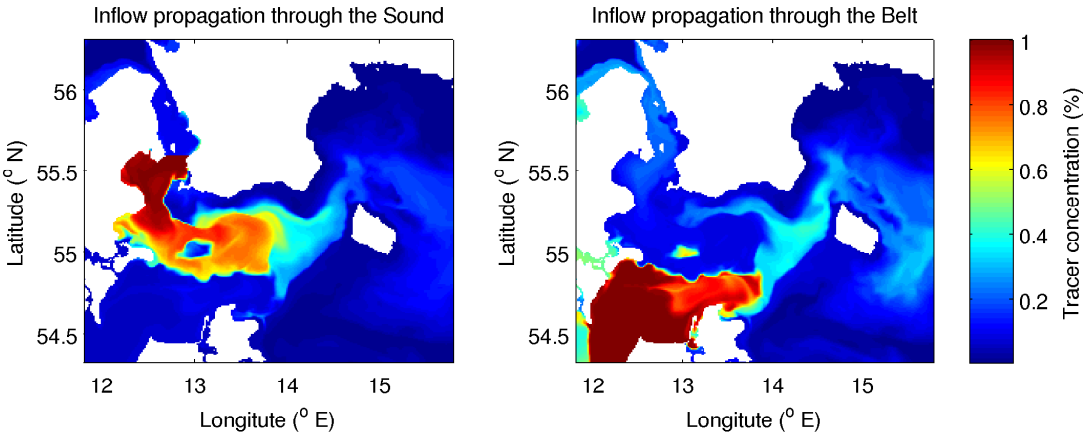

Figure 5.8: Simulated inflow propagation as on 15th of November 2005: the part of the inflow coming through the Sound(left panel) and through the Belt(right panel).

5.4 General discussion

In this chapter first the comparison of the observational data obtained from the moorings taken in the Arkona Basin and the Drogden Sill with the model data was made. The vertical structure of inflow events is reproduced well by the model simulations. Occasional strong deviations of the order of up to 10 PSU may be explained by the low resolution of the model data. For the Kriegers Flak South buoy and Arkona Buoy upper layer salinities are overestimated in the model, but in general the inflow event is well reproduced.

Then two transect taken in the area north of the Kriegers Flak and in the Bornholm Channel were compared with the model results. The observed general structure of the plume is in good agreement with the idealized model simulation for both transects. Main features are strong stratification at the interface between plume and ambient water and a geostrophic tilt of the interface.

The propagation of the current was discussed in the terms of observational data in sect. 4.5. In the Arkona Basin the model seems to reproduce the inflow propagation quite well, whereas in the Bornholm Channel the delay is observed between the observed situation and the model data (see fig. 5.7). The model study, as well as observations suggests that the major pathway of medium-intensity saline plumes over Drogden Sill passes Kriegers Flak northwards, whereas only a smaller amount of salt is transported around its southern edge.

From the observation of the pathways of the inflow coming through the Darss Sill and through the Drogden Sill a clear division is visible between both inflowing waters, along 55th circle of latitude. This is due to the fact that the water inflowing through the Drogden Sill is denser and is interleaving under water inflowing through the Darss Sill.

The presented simulation results which have been compared to selected field observations show that the numerical model has a reasonable degree of predictive capacity, especially in the vicinity of the sills (ie. in the Kriegers Flak area).

Chapter 6

Conclusions

This study on medium-intensity inflow in November 2005 investigates its dynamics, parameters, pathways and compares it with the model results. It particularly focus on the inflow over the Sound and its propagation through the Arkona Basin and over the Bornholm Channel. In the frame of this master thesis the mesoscale eddy observed during the cruise in the Bornholm Channel is described as well.

First, the general wind pattern over the transition area and its influence on the inflow through the Sound was investigated. The clear correlation between the westerly winds and the increase of the volume flux to the Baltic Proper can be seen. From the salinity observations inside of the Drogden Sill the typical delay of a few days is seen, between the inflow start and the salinity increase there. This is caused by the brackish water front in the Kattegat. From the observations of the temperature in the Drogden Sill a clear distinction between first, warmer part of the inflow and the second, colder one, was made. Because of this, both salinity and temperature can be used as tracer of inflow propagation.

From the data obtained from R/V Oceania, the moorings, the GETM model, as well as from the bottom salinity correlation coefficient, inflow propagation can be told. According to observational data the first warmer part of the inflow propagated from the Drogden Sill to the entrance of the Arkona Basin about 3 days. This is in agreement with the model data. The bottom salinity coefficient was calculated between the Drogden Sill buoy and the Kriegers Flak North buoy for the period from 20th of November 2005 until 10th of July 2006. From these calculation it can be told that the typical delay between these two stations is from 3 to 6 days, which is also in agreement with the observations and the model data. The warmer part of the inflow is observed at the Bornholm Channel about 7 to 9 days after being observed at the Drogden Sill. According to model, inflow propagates slower and it takes about 12 to 14 days to arrive at the Bornholm Channel.

The second, warmer part of the inflow propagated from the Drogden Sill to the entrance of the Arkona Basin in 2 to 3 days. This also in agreement with the model data as well as with the correlation coefficient. The second part of the inflow propagates slightly faster than the first one as it is denser and thicker. This part of the inflow haven't arrived at the Bornholm Channel between the end of the cruise.

The geostrophic and observed velocities were compared in the trench north of Kriegers Flak as well as in the Bornholm Channel. The correspondence between these velocities is seen north of the Kriegers Flak, which means that the flow there is in geostrophic balance in the cross-stream direction. This can not be told for the inflow observed in the Bornholm Channel, either due to low resolved ADCP data or bigger friction there. One clear feature of the geostrophic velocities, which was also seen in the trench north of the Kriegers Flak is a decrease in velocity with depth below the interface. This is caused by the transverse density gradient within the current, as already observed by Sellschopp et al. (2006) and Umlauf and Arneborg (2009).

The volume flux was calculated in the trench north of Kriegers Flak and compared with the volume flux in the Drogden Sill from 3 to 6 days earlier (the typical delay between these places calculated from the bottom salinity correlation coefficient). From this comparison it can be told that the dense water plumes from the Drogden Sill propagate mainly through the pathway north of the Kriegers Flak. This feature of salinity plume was also described by Burchard et al. (2005) and Sellschopp et al. (2006). Next the entrainment coefficient in the trench north of Kriegers Flak and in the Bornholm Channel from the observational data was calculated and compared with empirical formulas. Two empirical formulas using Froude number were used. The first one was derived for the bigger Froude numbers by Wahlin and Cenedese (2006) and for our inflow is in agreement with the observational results obtained in the Bornholm Channel (where the Froude number was bigger). The next one (Cenedese et al., 2004) slightly underestimated the value for the Kriegers Flak and is in agreement with the value at the Bornholm Channel. Finally the last formula base on the along-flow slope (Pedersen, 1980; Arneborg et al., 2004) tends to overstimate the result in both cases. Nevertheless all expressions, but first one for the KFN area, predict something within the correct order of magnitude, and further observations at similar Froude numbers are needed in order to distinguish between them. Sellschopp et al. (2006) investigated entrainment rates in the KFN area for an inflow in January/February 2004 and come with observed entrainment and predicted entrainment rates in the same order as this thesis.

Besides the main research, a mesoscale eddy observed in the Bornholm Basin (fig. 4.20) was described and its origin was anticipated. The eddy is a cyclonic one with volume of about 17 km^3, which is a lot comparing to typical Bornholm Basin eddies volumes of 2 km^3 ((Reissman et al., 2009)). Southerly winds, which were prevailing on the eastern coast of the Bornholm Basin a few days before the observation of the eddy, caused an upwelling, which could produce an cyclonic eddy. It later could move away from the shore to a place where the transect 20 was taken.

In general the investigation made during the R/V Oceania cruise were well timed and had a good spatial coverage regarding the inflow propagation. Therefore, it was possible to investigate the inflow in high details. The only thing is that no MSS (Micro Structure Sound) was available during the cruise. It would help us to investigate the turbulent mixing of the saline water inflow along its way to the Baltic basins.

Chapter 7

Appendix

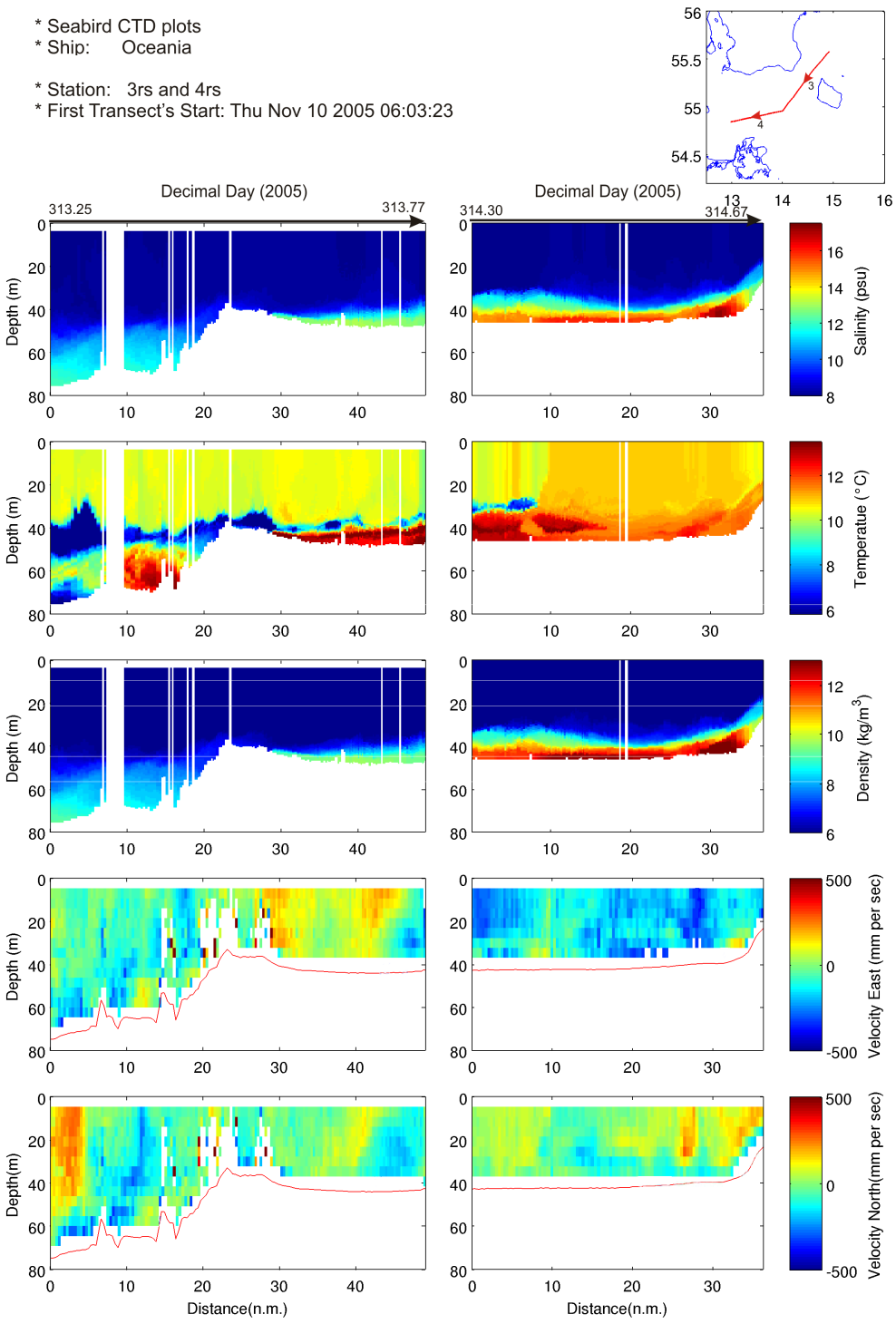

Figure 7.1: CTD and ADCP data for transects 3 and 4 taken in the Arkona Basin and Bornholm Channel (see the map in the upper right corner for location) on 10th and 11th of November 2005. Time gap between two transects occur. The arrows above the salinity plots show the direction in which the measurements were taken with the numbers being day of the year 2005 for starting and ending of each transect. White fields on the plots show the area below the seabed or corrupted data.

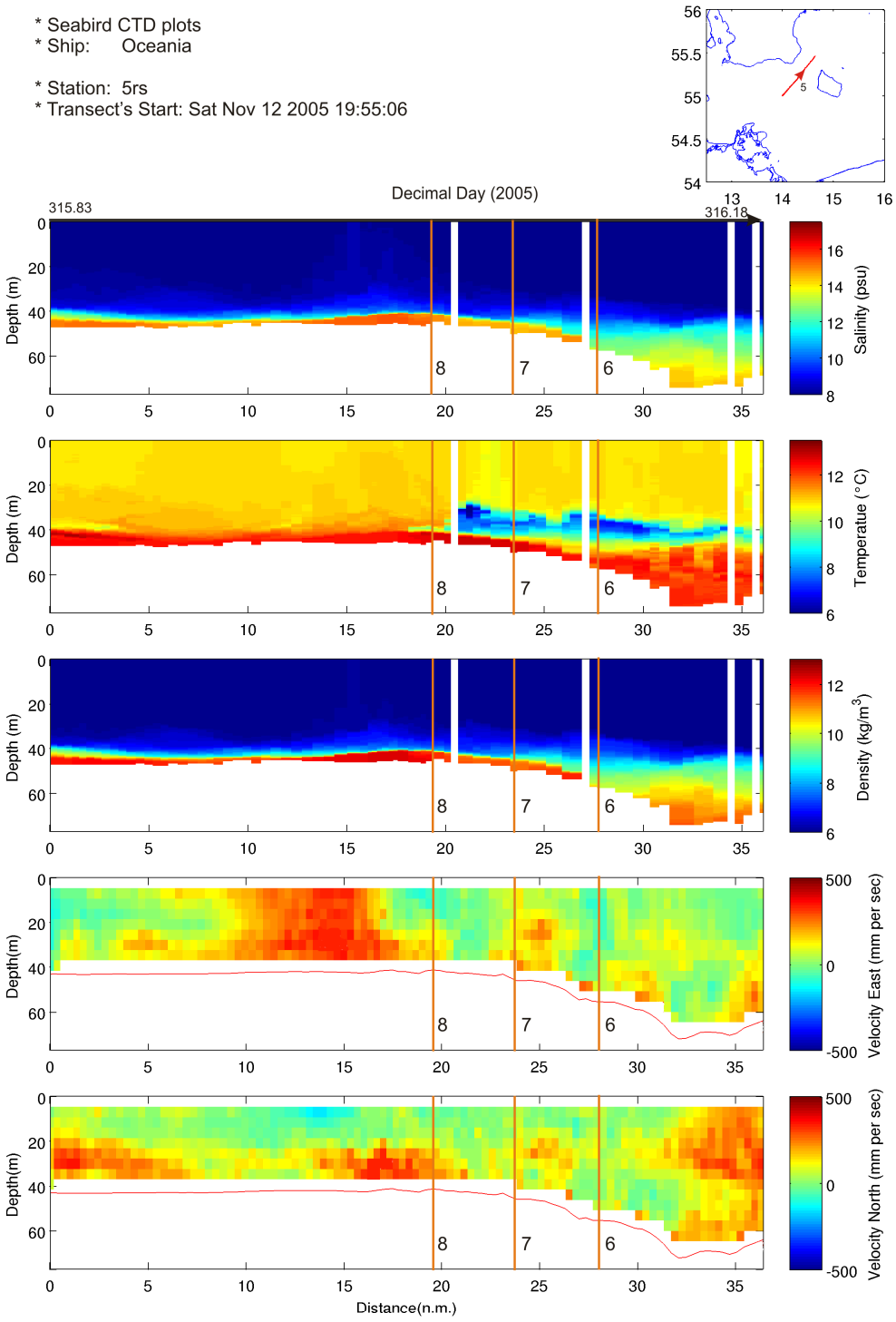

Figure 7.2: CTD and ADCP data for transect 5 taken in the Bornholm Channel (see the map in the upper right corner for location) on 12th of November 2005. The orange lines mark the place where the transect crosses with transects 6, 7 and 8.

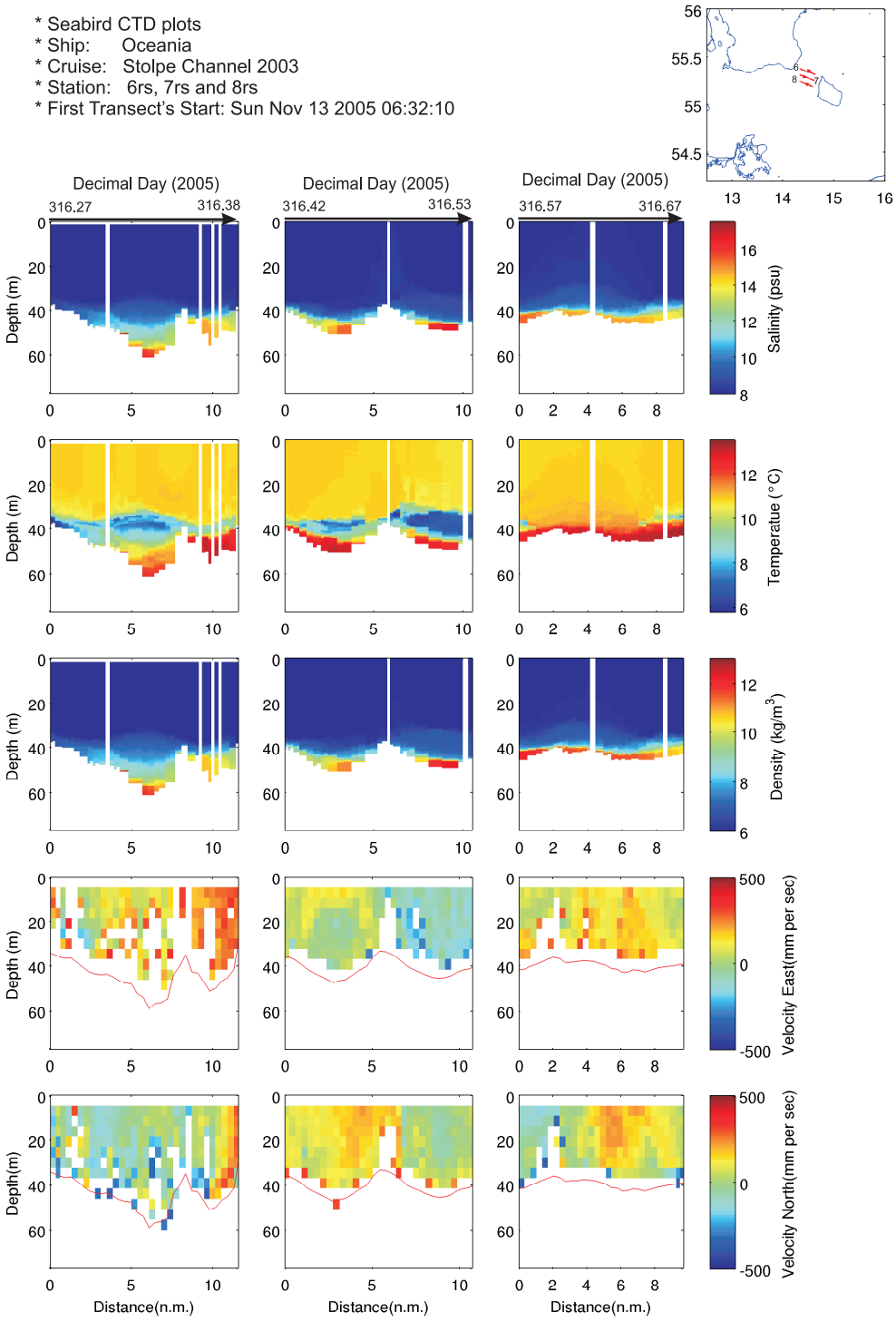

Figure 7.3: CTD and ADCP data for transects 6, 7 and 8 taken in the Bornholm Channel (see the map in the upper right corner for location) on 13th of November 2005. The orange lines mark the place where the transects crosses with transects 5 and 9. The transect 7 is shown in the opposite direction to the direction in which it was taken.

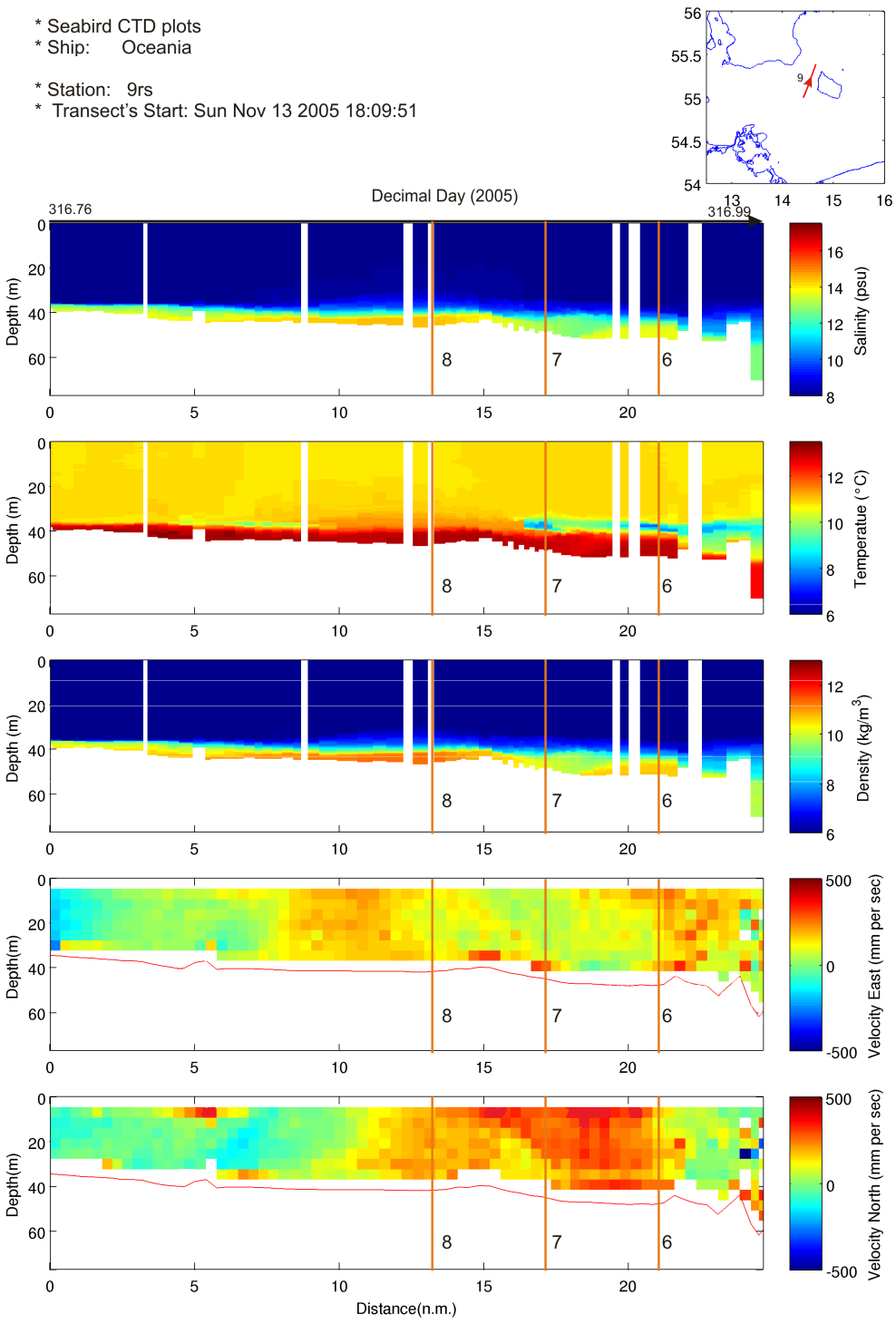

Figure 7.4: CTD and ADCP data for transect 9 taken in the Bornholm Channel (see the map in the upper roght corner for location) on 13th of November 2005. The orange lines mark the place where the transect crosses with transects 6, 7 and 8.

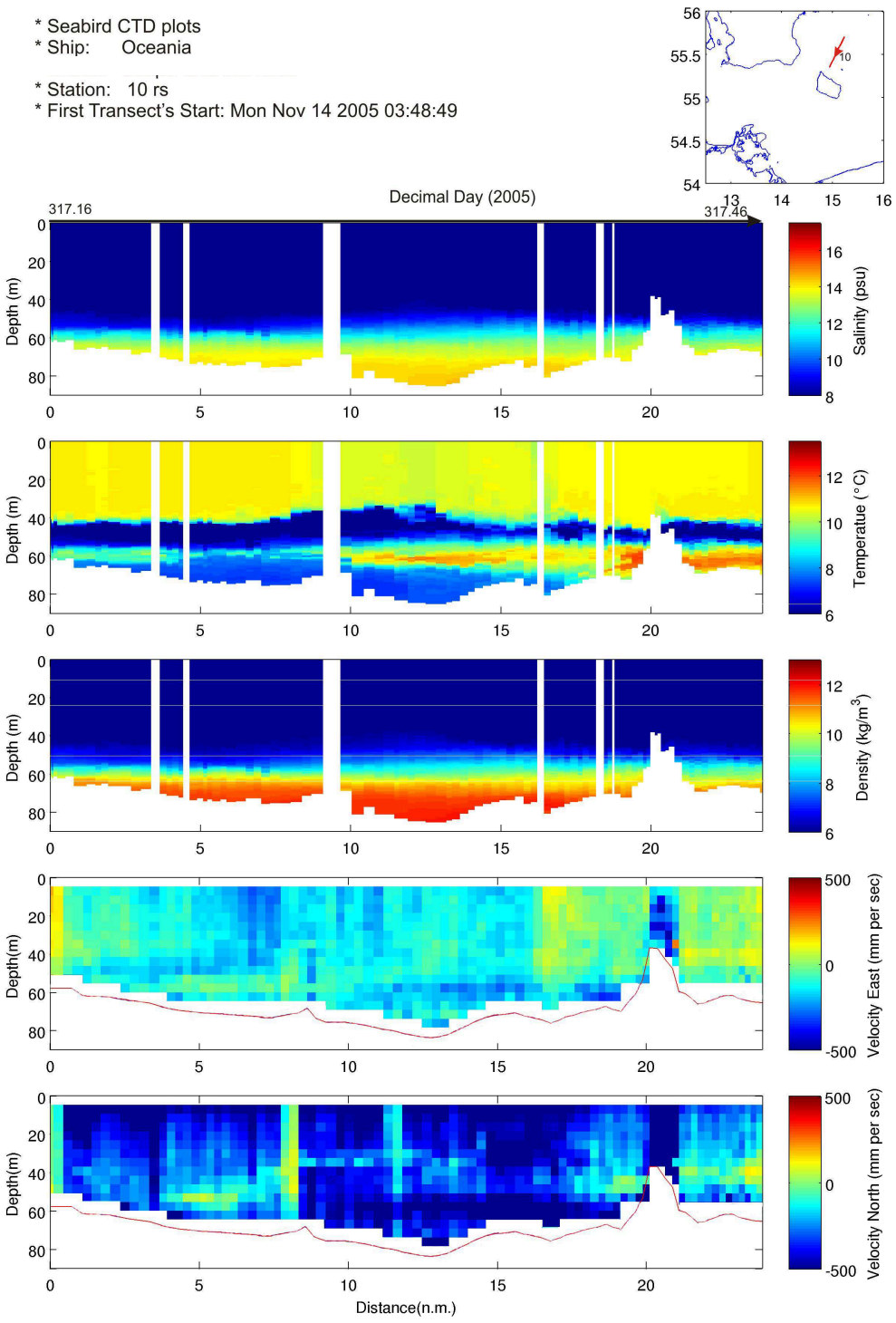

Figure 7.5: CTD and ADCP data for transect 10 taken in the Bornholm Basin (see the map in the upper right corner for location) on 14th of November 2005.

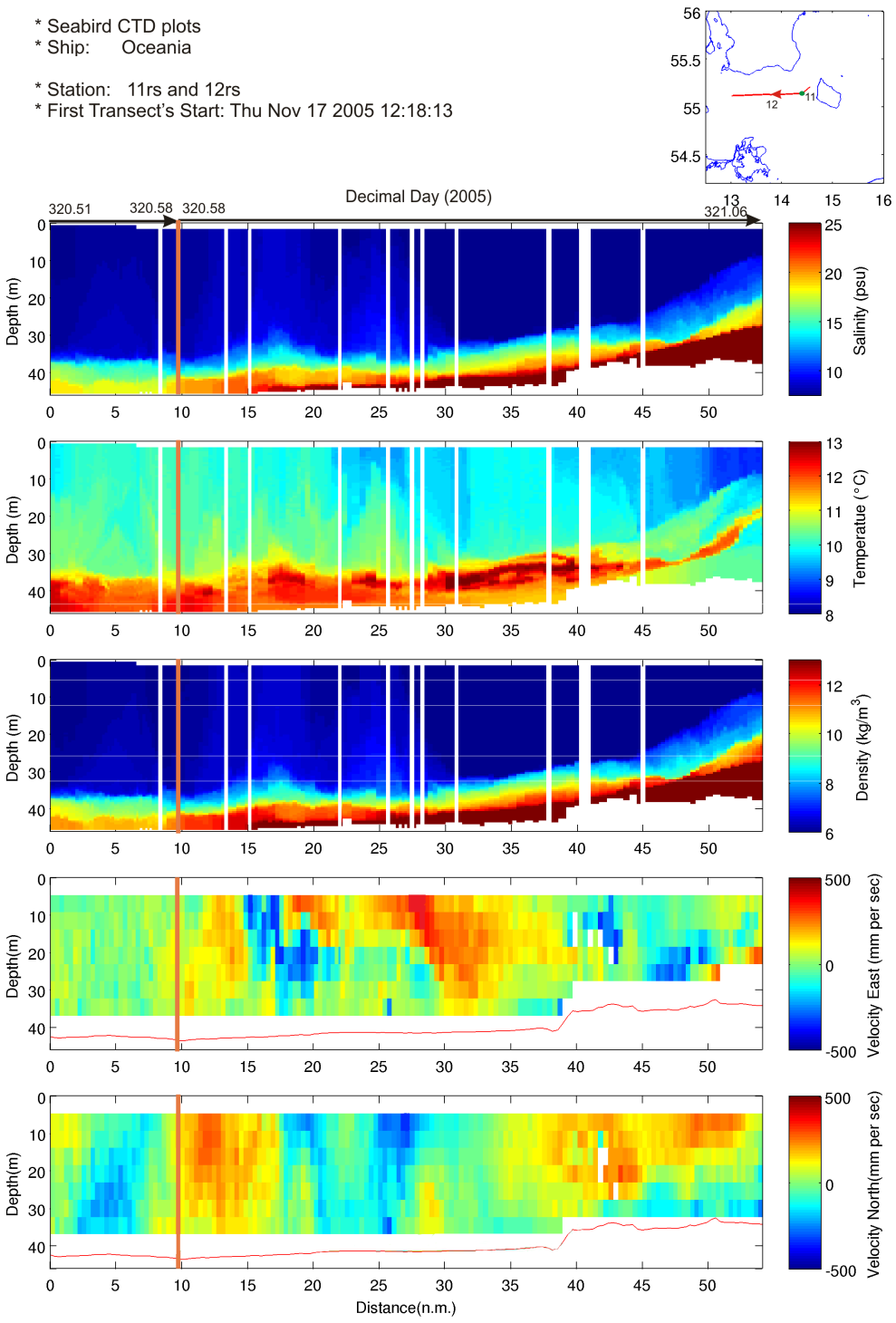

Figure 7.6: CTD and ADCP data for transects 11 and 12 taken in the Arkona Basin and Bornholm Channel (see the map in the upper right corner location) on 17th of November 2005. The orange line on the plots and the green point on the map mark the point where the first transect ends and the second one starts.

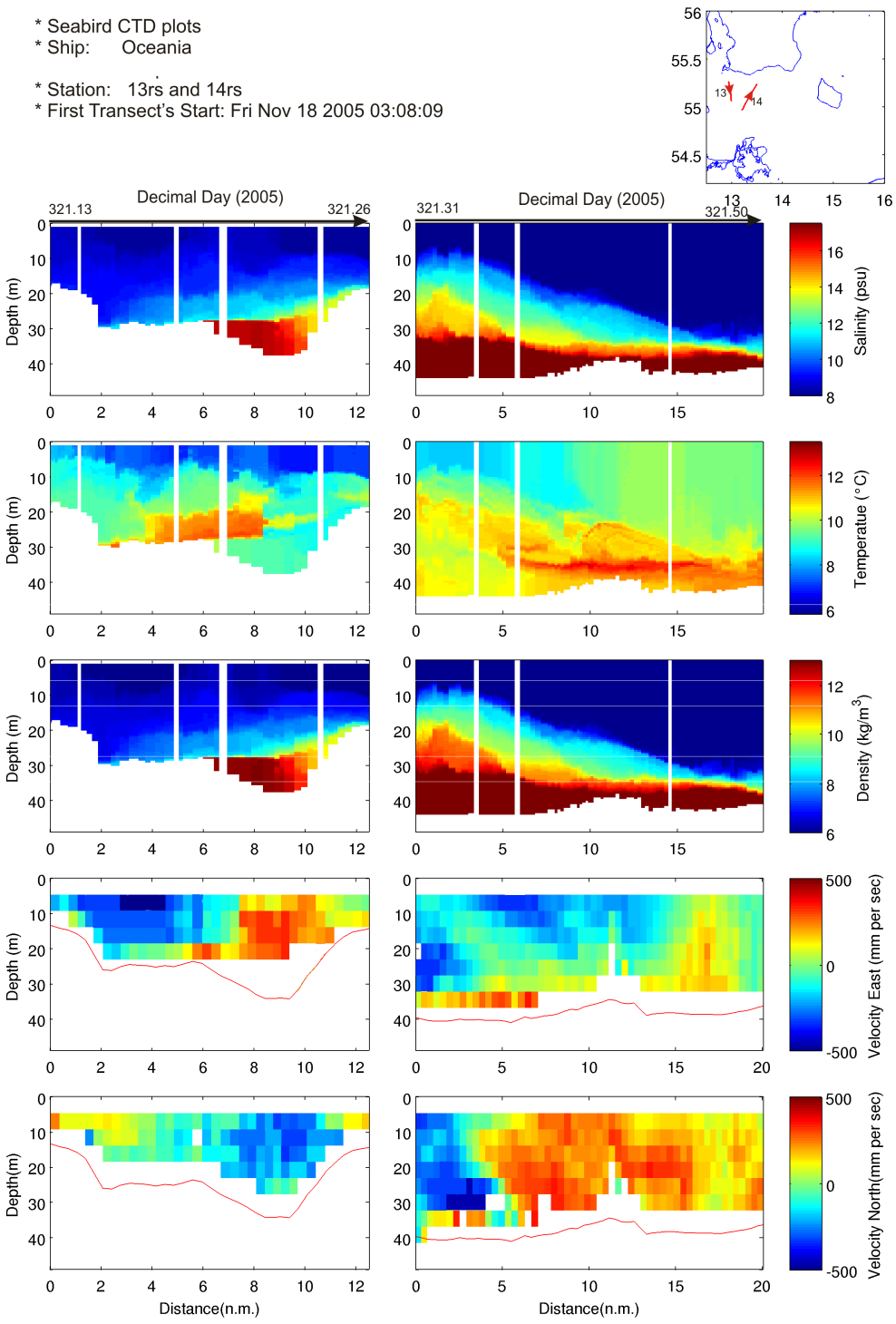

Figure 7.7: CTD and ADCP data for transects 13 and 14 taken in the Arkona Basin (see the map in the upper right corner for location) on 18th of November 2005.

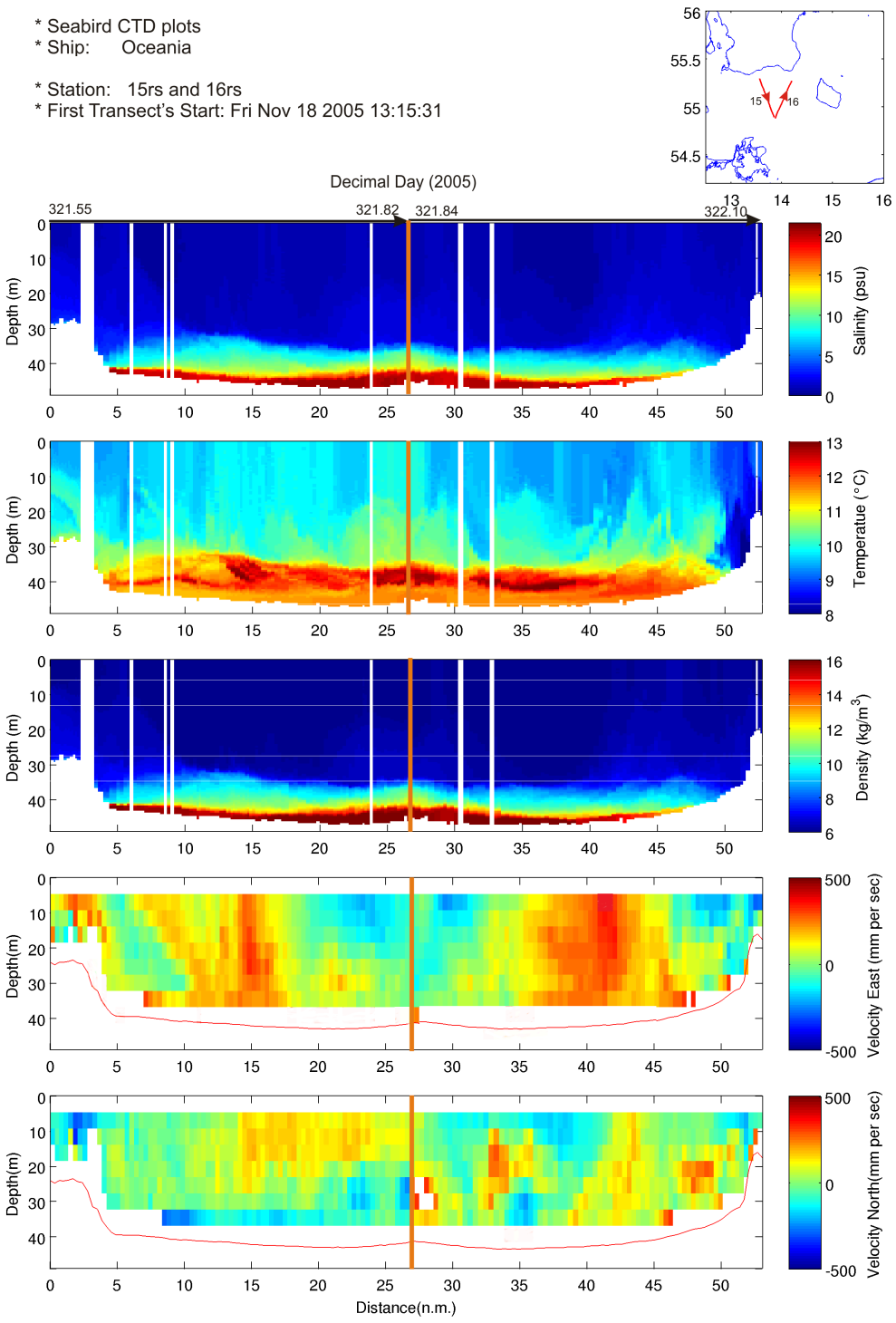

Figure 7.8: CTD and ADCP data for transects 15 and 16 taken in the Arkona Basin (see the map in the upper right corner for location) on 18th and 19th of November 2005. The orange line on the plots and the green dot on the map mark the end of first transect and the beginning of the second.

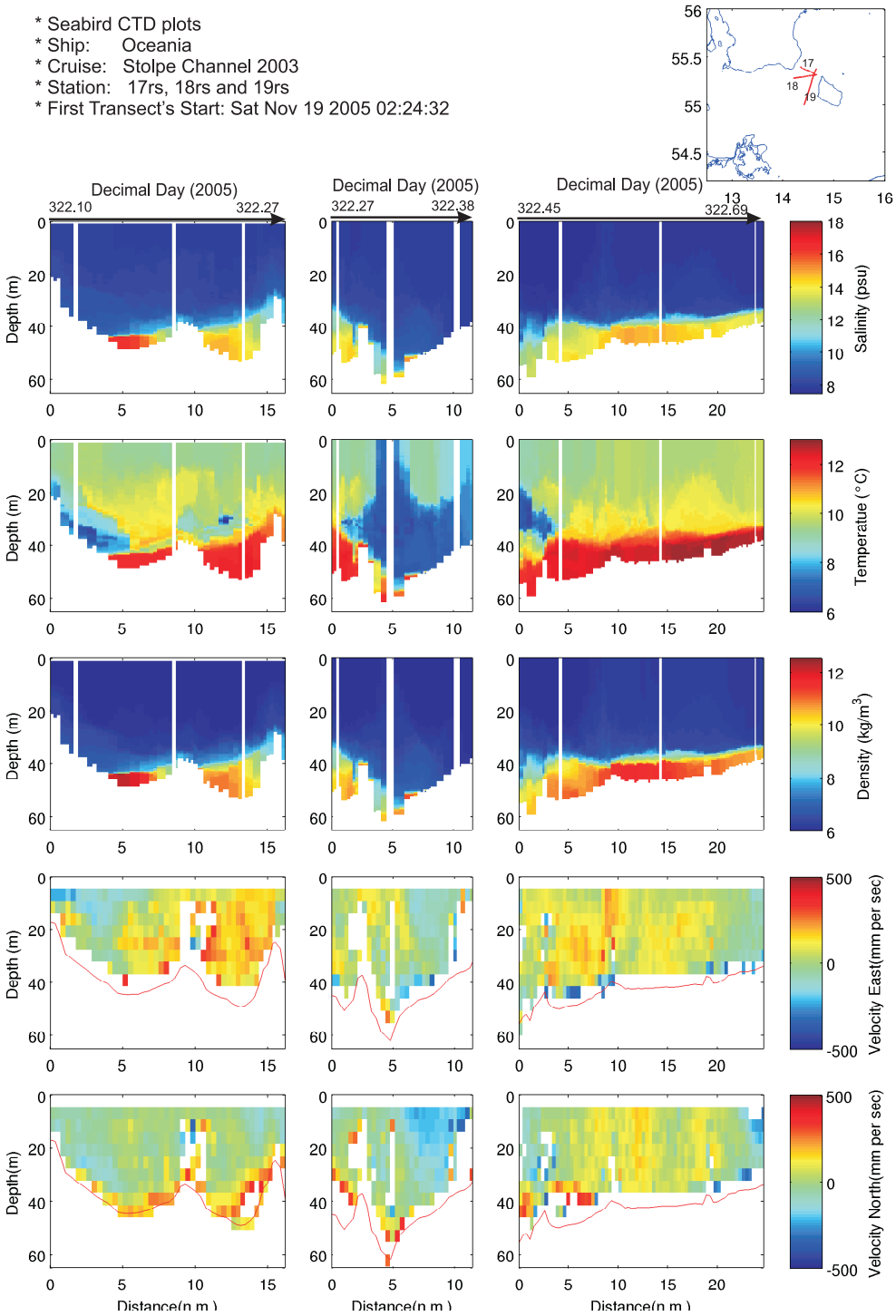

Figure 7.9: CTD and ADCP data for transects 17, 18 and 19 taken in the Bornholm Channel (see the map in the upper right corner for location) on 19th of November 2005. The orange lines mark the place where the transects crosses each other.

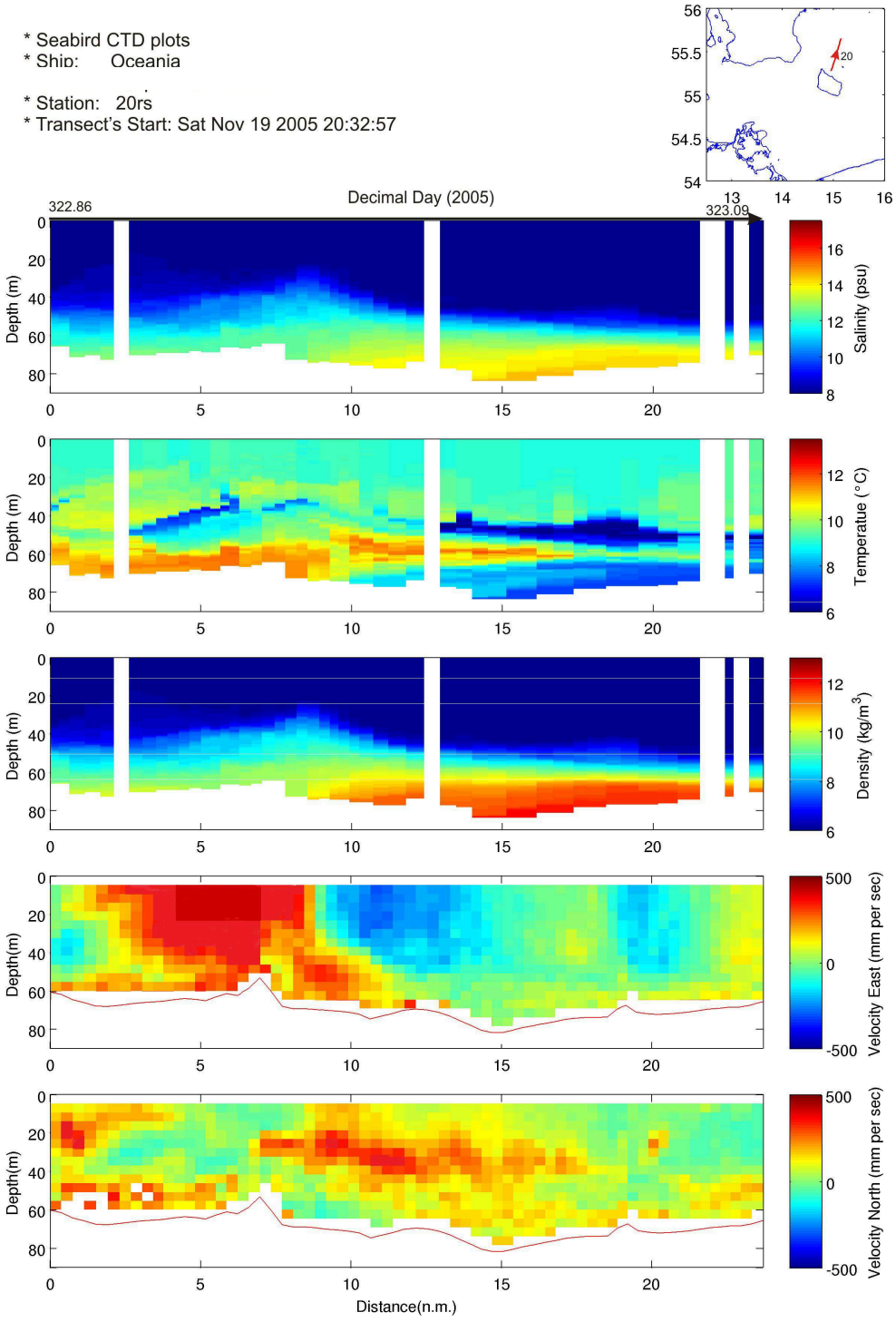

Figure 7.10: CTD and ADCP data for transect 20 taken in the Bornholm Basin (see the map in the upper right corner for location) on 19th and 20th of November 2005. On the ADCP data cyclonic eddy is visible.

Acknowledgement This work has been supported from the German Ministry for Environment, Nature Protection and Nuclear Safety Quantas-Off (Quantification of the Water Mass Transformation Processes in the Arkona Sea - Impact of the Offshore Wind Farms) project. The author is grateful to prof. Jan Piechura and Dr Waldemar Walczak from Polish Academy of Science for providing measurements data, as well as co-workers from the Institute for Baltic Sea Research in Warnemünde for help, especially prof. Hans Burchard, dr Lars Umlauf, Eefke van der Lee, Hannes Rennau and Johannes Becherer. I would like to express my special appreciation to Prof Hans Joachim Fitting, Dr Reinhard Mahnke, Dr Eberhard Hagen, Mrs Birgit Wünsch and Slawomir Skruszewicz for helping me during the whole period of my studies in Rostock. Last, but not least I would like to thank my parents.

Bibliography

L. Arneborg, C.P. Erlandsson, B. Liljebladh, and A. Stigebrandt. The rate of inflow and mixing during deep-water renewal in a sill fjord. *Limnology and Oceanography*, 1(49):768–777, 2004.

L. Arneborg, V. Fiekas, L. Umlauf, and H. Burchard. Gravity current dynamics and entrainment - a process study based on observations in the arkona basin. *J. Phys. Oceanogr.*, 37:2094–2113, 2007.

W. Brogmus. Eine revision des wasserhaushaltes der ostsee. *Kieler Meeresforchungen*, 9(1):15–42, 1952.

H. Burchard and K. Bolding. Getm - general estuarine transport model. *European Commission*, 2002.

H. Burchard, K. Bolding, and M.R. Villarreal. Three-dimensional modelling of estuarine turbidity maxima in a tidal estuary. *Ocean Dynamics*, 54:250–265, 2004.

H. Burchard, H.U Lass, V. Mohrholz, L. Umlauf, J. Sellschopp, V. Fiekas, K Bolding, and L. Arneborg. Dynamics of medium-intensity dense water plumes in the arkona basin, western baltic sea. *Ocean Dynamics*, 55:391–402, 2005.

H. Burchard, F. Janssen, K. Bolding, L. Umlauf, and H. Rennau. Model simulations of dense bottom currents in the western baltic sea. *Ontinental Shelf Research*, 29 (1):205–220, 2009.

C. Cenedese, J. A. Whitehead, T. A. Ascarelli, and M. Ohiwa. A dense current flowing down a sloping bottom in a rotating fluid. *J. Phys. Oceanogr.*, 34(1): 188–203, 2004.

E. Darelius. Topographic steering of dense overflows: Laboratory experiments with v-shaped ridges and canyons. *Deep Sea Res. I*, 55:1021–1034, 2008.

E. Darelius and A.K. Wahlin. Downward flow of dense water leaning on a submarine ridge. *Deep Sea Res.*, 54:1173–1188, 2007.

R.R. Dickson. The prediction of major baltic inflows. *Dt. Hydrogr. Z.*, 26:97–105, 1973.

J. Elken. Deep water overflow, circulation and vertical exchange in the baltic proper, eport series. Technical Report 6, Estonian Marine Institute, Tallin, 1996.

R. Feistel, G. Nausch, and E. Hagen. The baltic inflow of autumn 2001. *Meereswiss. Ber.*, 54:55–68, 2003a.

R. Feistel, G. Nausch, W. Matthäus, and E. Hagen. Temporal and spatial evolution of the baltic deep water renewal in spring 2003. *Oceanologia*, 45(4):623–642, 2003b.

R. Feistel, G. Nausch, and E. Hagen. Unsusual baltic inflow activity 2002/03 and varying deep water properties. *Oceanologia*, 48:21–35, 2006.

H. Fischer and W. Matthäus. The importance of the drogden sill in the sound for major baltic inflows. *Journal of Marine Systems*, 9:137–157, 1996.

H. Fisher and W. Matthäus. The importance of the drogden sill for major baltic inflows. *J. Mar. Sys.*, 9(3-4):137–157, 1996.

H. Franck, W. Matthäus, and R. Sammler. Major inflows of saline water into the baltic sea during the present century. *Gerlands Beitr. Geophys.*, 96:517–531, 1987.

M. Green and A. Stigebrandt. Instrument-induced linear flow resistance in oresund. *Continental Shelf Research*, 22:435–444, 2002.

B.G. Gustafsson and H.C. Andersson. Modeling the exchange of the baltic sea from the meridional atmospheric difference across the north sea. *Journal of Geophysical Research.*, 106:19731–19744, 2001.

E. Hagen and R. Feistel. Spreading of baltic deep water: A case study for the winter 19971998. *Meereswiss. Ber.*, 45:99–133, 2001.

HELCOM. First assessment of the state of the coastal waters of the baltic sea. volume 54. Baltic Marine Environment Protection Commission, 1993.

K. Huber, E. Kleine, H-U. Lass, and W. Matthäus. The major baltic inflow in january 1993 measurements and modelling results. *Ocean Dynamics*, 46(2), 1994.

F. Jakobsen, M.J. Lintrup, and J. Steen Møller. Observations of the specific resistance in oresund. *Nordic Hydrology*, 28:217–232, 1997.

T.S. Jakobsen. Sea water exchange of the baltic - measurements and methods. Technical report, The Belt Project, National agency of environment protection, Denmark, 1980.

G. C. Johnson and T.B. Sanford. Secondary circulation in the faroe bank channel outflow. *J. Phys. Oceanogr.*, 22:927–933, 1992.

T. Kouts and A. Omstedt. Deep water exchange in the baltic proper. *Tellus A*, 11 (45):311–324, 1993.

H.-U. Lass and V. Mohrholz. On dynamics and mixing of inflowing saltwater in the arkona sea. *J. Geophys. Res.*, 108(C2):3042, 2003a.

H.-U. Lass and V. Mohrholz. On dynamics and mixing of inflowing saltwater in the arkona sea. *J. Geophys. Res.*, 108(C2):3042, 2003b.

H.-U. Lass, V. Mohrholz, and T. Seifert. On pathways and residence time of saltwater plumes in the arkona sea. *J. Geophys. Res.*, 110(C11019), 2005.

H. U. Lass, V. Mohrholz, M. Knoll, , and H. Prandke. On the impact of a pile on a moving stratified flow. *Cont. Shelf Res*, 2006.

H.U. Lass and W. Matthäus. On the forcing of salt water inflows into the baltic sea. *Proceedings 19th Conference of Baltic Oceanography*, 1:192–211, 1994.

H.U. Lass and W. Matthäus. On temporal wind variation forcing salt water into the baltic sea. *Tellus*, 48 A, 1996.

B. Liljebladh and A. Stigebrandt. Observations of the deepwater flow into the baltic sea. *J. Geophys. Res.*, 101(C4):8895–8911, 1996.

W. Matthäus. The history of investigation of salt water inflows into the baltic sea from the early beginning to recent results. *Meereswissenschaftliche Berichte*, 65: 1–73, 2006.

W. Matthäus. Climatic and seasonal variability of oceanological parameters in the baltic sea. *Beitrge zur Meereskunde*, 51:29–49, 1984.

W. Matthäus and H. Franck. Characteristics of major baltic inflows - a statistical analysis. *Continental Shelf Research*, 12:1375–1400, 1992.

M. H. E. Meier, R. Feistel, J. Piechura, L. Arneborg, H. Burchard, V. Fiekas, N. Golenko, N. Kuzmina, V. Mohrholz, C. Nohr, Paka V.T., J. Sellschopp, A. Stips, and V. Zhurbas. Ventilation of the baltic sea deep water: A brief review of present knowledge from observations and models. *Oceanologia*, 48:133–164, 2006.

V. Mohrholz, J. Dutz, and G. Kraus. The impacts of exceptionally warm summer inflow event on the environmental conditions of the baltic sea. *J. Mar. Sys.*, 60: 285–301, 2006.

J. S Møller, N.-E.O. Hansen, , and F. Jakobsen. Mixing in stratified flow caused by obstacles. *Coastal Engineering*, 4:97–111, 1997.

R. Pacanowski and S. M. Griffies. Mom 3.0 manual. 1999.

F.B. Pedersen. *A monograph on turbulent entrainment and friction in two-layer stratified flow.* PhD thesis, IHHE, DTU, Lyngby, Denmark, 1980.

J. Piechura and A. Beszczyska-Möller. Inflow waters in the deep regions of the southern baltic sea transport and transformations. *Oceanologia*, 45(4):593–621, 2003.

J. H. Reissman. Integrale eigenschaften von mesoskaligen wirbelstrukturen in den tiefen becken der ostsee. *Meereswissenschaftliche Berichte*, 52:149, 2002.

J.H. Reissman, H. Burchard, R. Feistel, E. Hagen, H.U Lass, V. Mohrholz, N. Nausch, L. Umlauf, and G. Wieczorek. Vertical mixing in the baltic sea and consequences for eutrophication - a review. *Progress in Oceanography*, 82:47–80, 2009.

H. Rennau and H. Burchard. Quantitative analysis of numerically induced mixing in a coastal model application. *Ocean Dynamics*, 59:671–687, 2009.

J. Sellschopp, L. Arneborg, M. Knolla, V. Fiekasa, F. Gerdesa, H. Burchard, H.U. Lass, V. Mohrholz, and L. Umlauf. Direct observations of a medium-intensity inflow into the baltic sea. *Continental Shelf Research*, 26:2393–2414, 2006.

A. Stigebrandt. A moel for the vertical circulation of the baltic deep water. *J.Phys.Oceanography*, 17(10):1772–1785, 1987a.

A. Stigebrandt. A model for the vertical circulation of the baltic deep water. *J. Phys. Oceanogr.*, 17(10):1772–1785, 1987b.

A. Stigebrandt. Bridge-induced flow reduction in sea straits with reference to effects of a planned bridge across oeresund. *Ambio*, 21:130–134, 1992.

L. Umlauf and L. Arneborg. Dynamics of rotating shallow gravity currents passing through a channel. part i: Observation of transverse structure. *J. Phys. Oceanogr.*, 39:2385–2401, 2009.

L. Umlauf and U. Lemmin. Inter-basin exchange and mixing in the hypolimnion of a large lake: the role of long internal waves. *Limnology and Oceanography*, 50: 1601–1611, 2005.

A. K. Wahlin. Topographic steering of dense currents with application to submarine canyons. *Deep-Sea Res. I*, 49:305–320, 2002.

A. K. Wahlin. Downward channeling of dense water in topographic corrugations. *Deep-Sea Res. I*, 51:577–590, 2004.

A. K. Wahlin, E. Darelius, C. Cenedese, and G.F. Lane-Serff. Laboratory observations of enhanced entrainment in dense overflows in the presence of submarine canyons and ridges. *Deep-Sea Res. I*, 55:737–750, 2008.

A.K. Wahlin and C. Cenedese. How entraining density currents influence the ocean stratification. *Deep-Sea Research II*, 53:172–193, 2006.

G. Walin. On the deep water flow into the baltic. *Geophysica*, 17:75–93, 1981.

P. Welander. Two layer exchange in an estuary basin, with special reference to the baltic sea. *Journal of Physical Oceanography,*, 4(4):542–556, 1974.

K. Wyrtki. Die dynamik die wasserbewegungen in fehmarnbelt i. *Kieler Meeresforsch*, 9:155–190, 1954.